Brookhaven National Laboratory

Measurements of the Higgs boson mass.

Gaetano Αθανάσιος Barone

Brookhaven National Laboratory

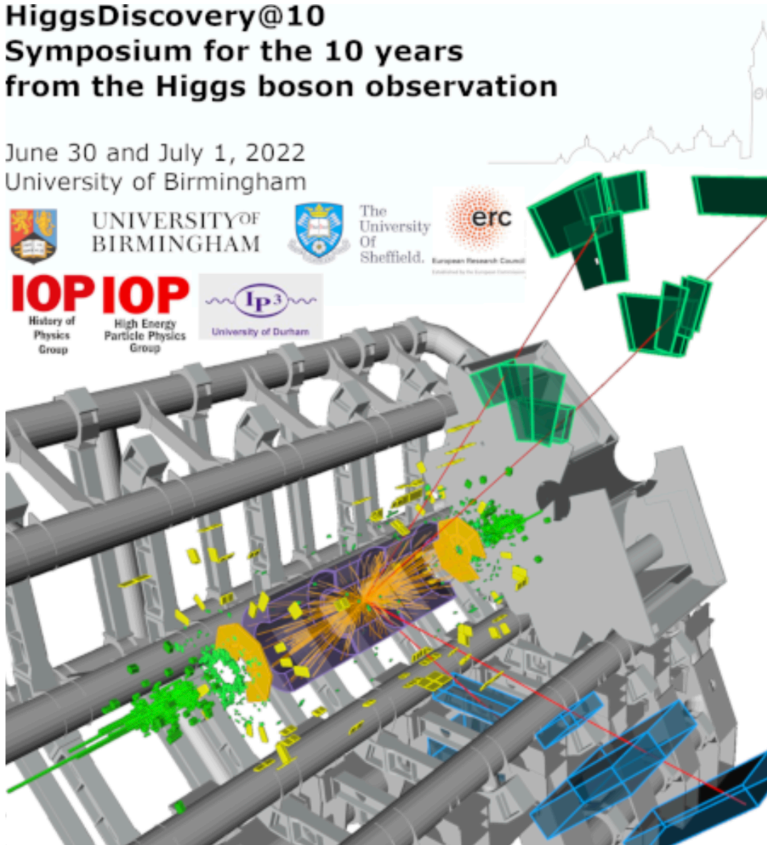

July 2022

Introduction

- Importance of m_H in several aspects of our understanding of fundamental physics.

Power law expansion of the potential

$$V(h) = \frac{1}{4}\lambda h^4 + \lambda v h^3 + \lambda v^2 h^2$$

$$\begin{aligned}\mathcal{L} = & -\frac{1}{4}F_{\mu\nu}F^{\mu\nu} \\ & + i\bar{\Psi}\not{D}\psi \\ & + D_\mu\Phi^\dagger D^\mu\Phi - V(\Phi) \\ & + \bar{\Psi}_L\hat{Y}\Phi\Psi_R + h.c.\end{aligned}$$

- Understanding the perturbative expansion of its potential ($\lambda v^2 h^2$).
- Precise higher order corrections to the theory predictions of the Higgs interactions depend on the value of m_H.
- Input to precision global fit of the Standard Model.
- Free parameter to be determined by the experiment.

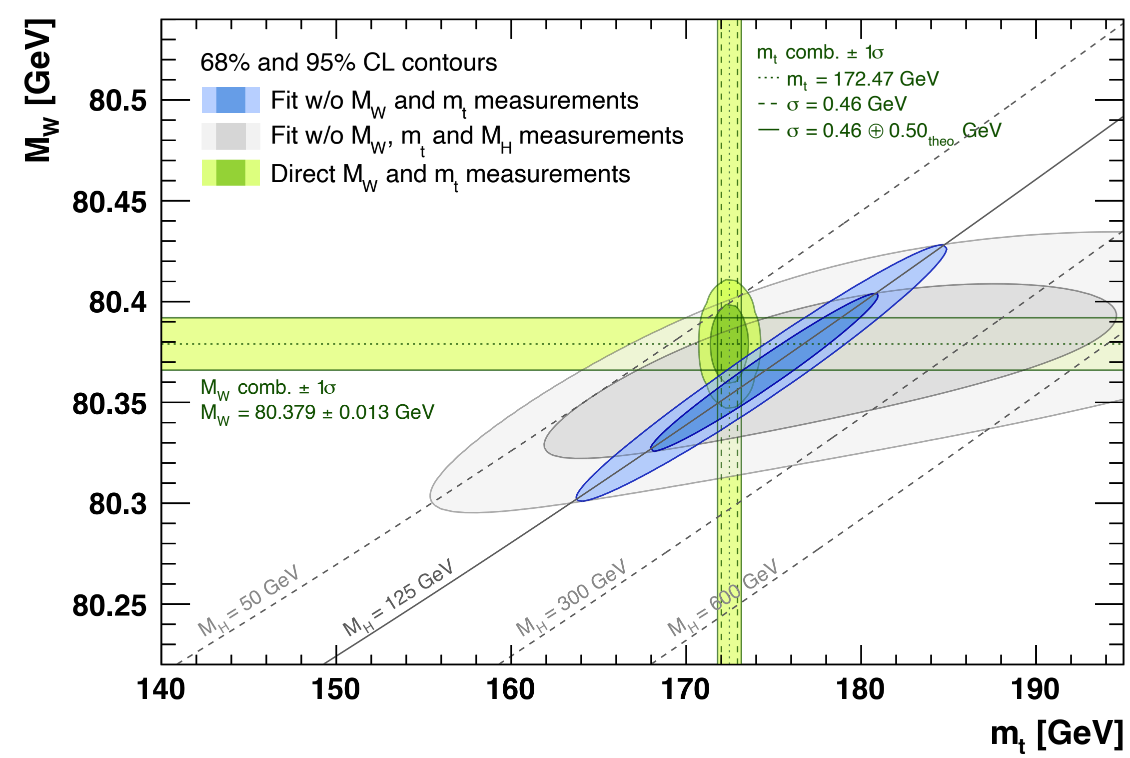

Global Electroweak fits from the Gfitter Collaboration

Introduction

- Importance of m_H in several aspects of our understanding of fundamental physics.

Power law expansion of the potential

$$V(h) = \frac{1}{4}\lambda h^4 + \lambda v h^3 + \lambda v^2 h^2$$

$$\begin{aligned}\mathcal{L} = &-\frac{1}{4}F_{\mu\nu}F^{\mu\nu} \\ &+ i\bar{\Psi}\not{D}\psi \\ &+ D_\mu\Phi^\dagger D^\mu\Phi - V(\Phi) \\ &+ \bar{\Psi}_L\hat{Y}\Phi\Psi_R + h.c.\end{aligned}$$

- Understanding the perturbative expansion of its potential ($\lambda v^2 h^2$).
- Precise higher order corrections to the theory predictions of the Higgs interactions depend on the value of m_H.
- Input to precision global fit of the Standard Model.
- Free parameter to be determined by the experiment

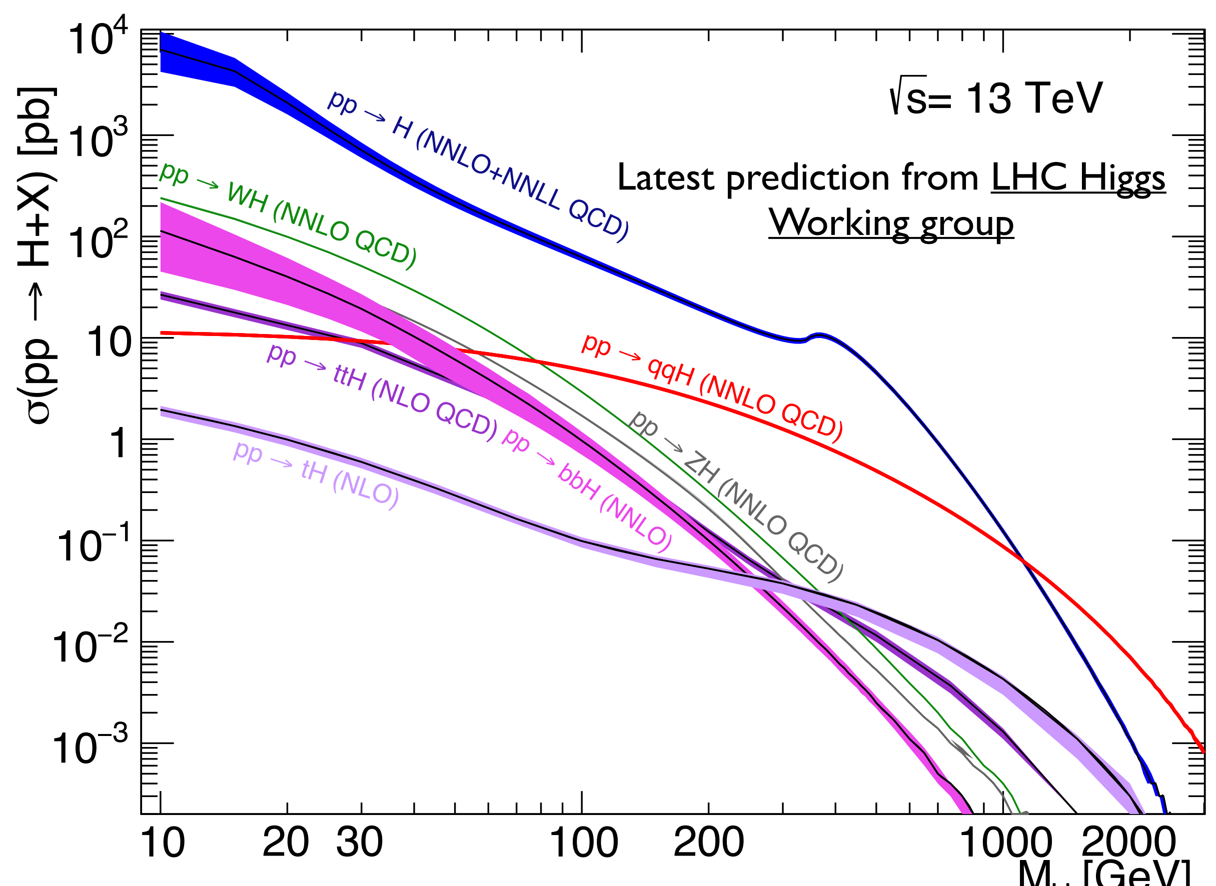

Prediction and uncertainties of Higgs production processes as a function of the m_H

Introduction

- Importance of m_H in several aspects of our understanding of fundamental physics.

Power law expansion of the potential

$$V(h) \;=\; \frac{1}{4}\lambda h^4 + \lambda v h^3 + \lambda v^2 h^2$$

- Understanding the perturbative expansion of its potential ($\lambda v^2 h^2$).
- Precise higher order corrections to the theory predictions of the Higgs interactions depend on the value of m_H.
- Input to precision global fit of the Standard Model.
- Free parameter to be determined by the experiment

Gfitter Collaboration

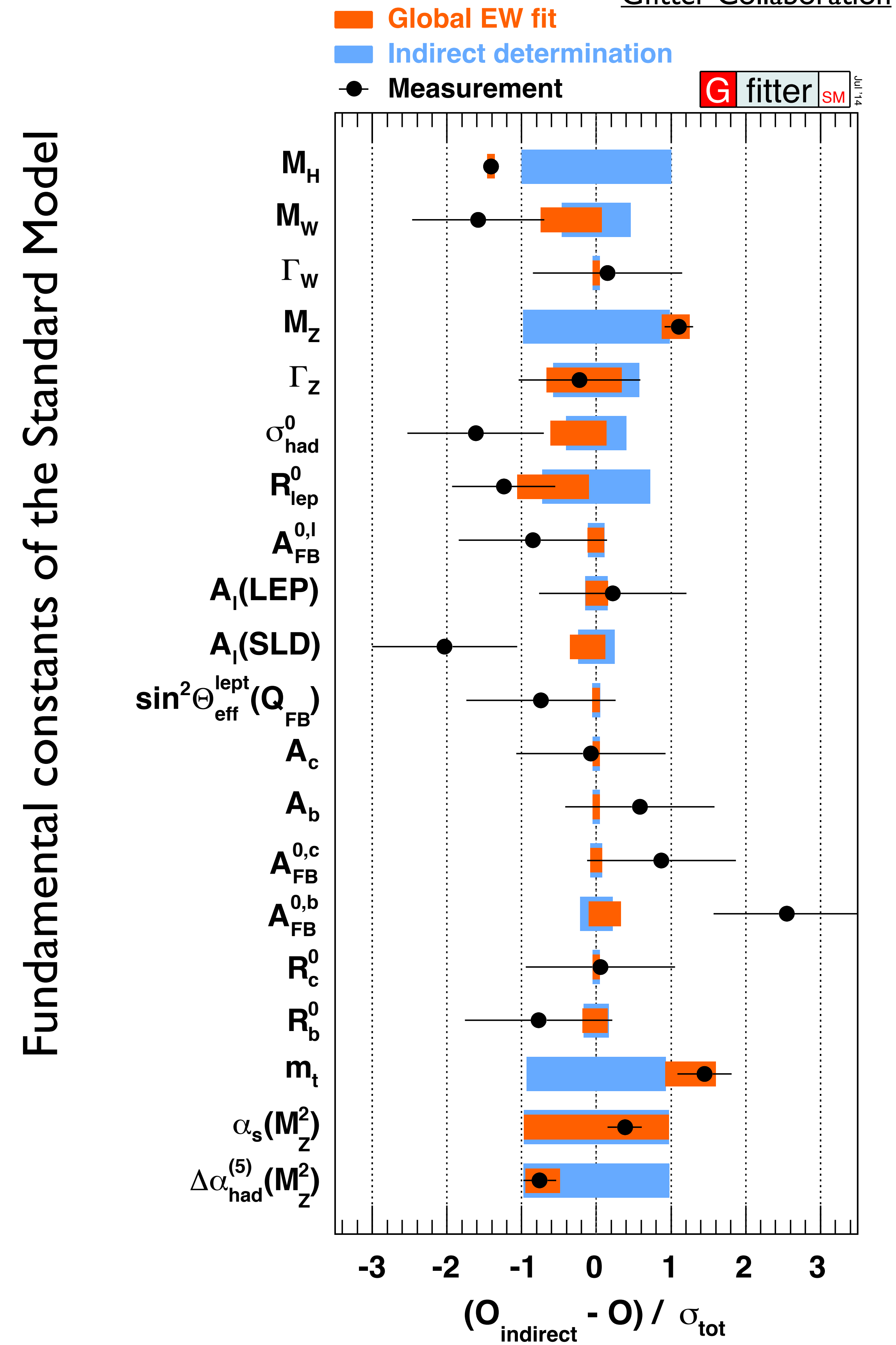

Introduction

- Importance of m_H in several aspects of our understanding of fundamental physics.
  - Point of performance benchmark for ATLAS and CMS.
  - Solenoid (4T) vs solenoid + toroid, lead tungstate scintillating crystals vs liquid argon sandwich, …
  - As C. Anastopoulos said yesterday, their names say it all.

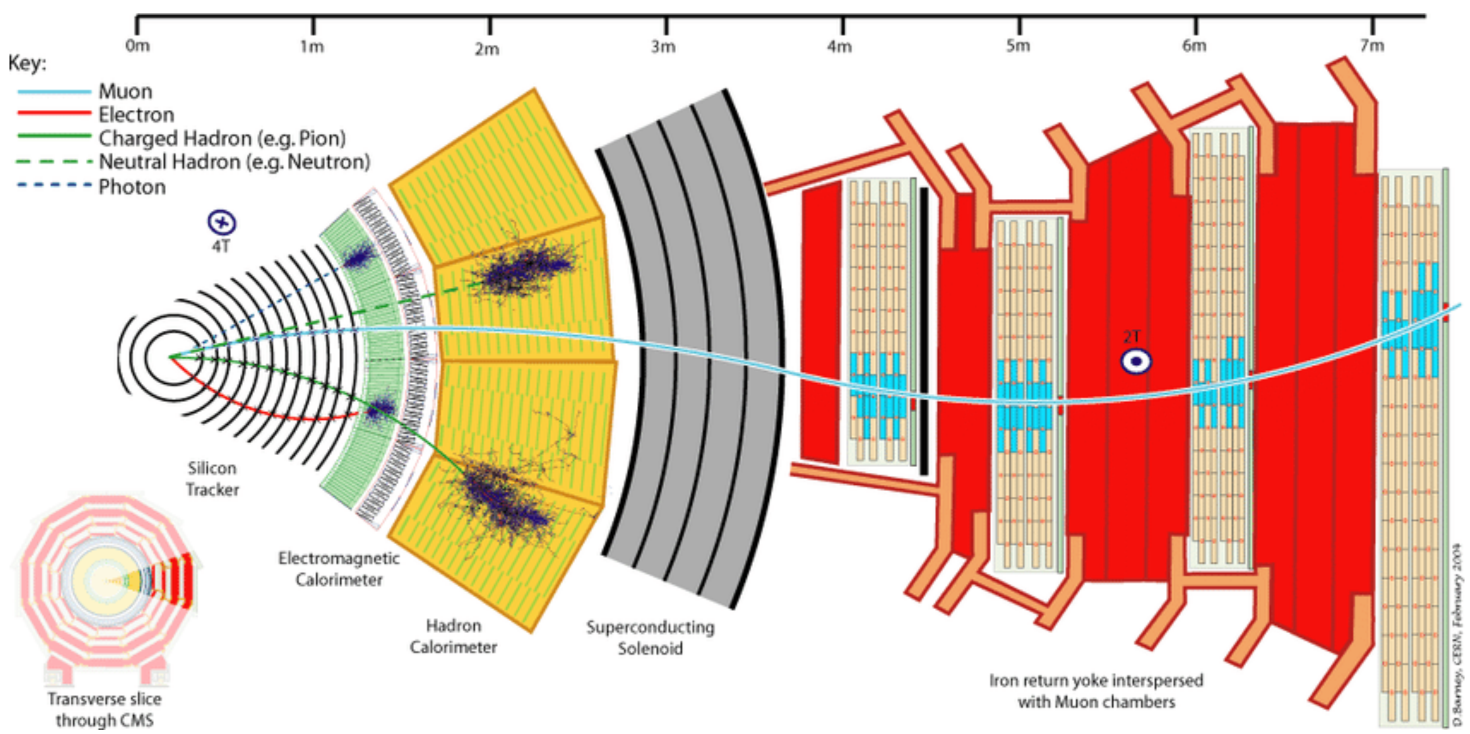

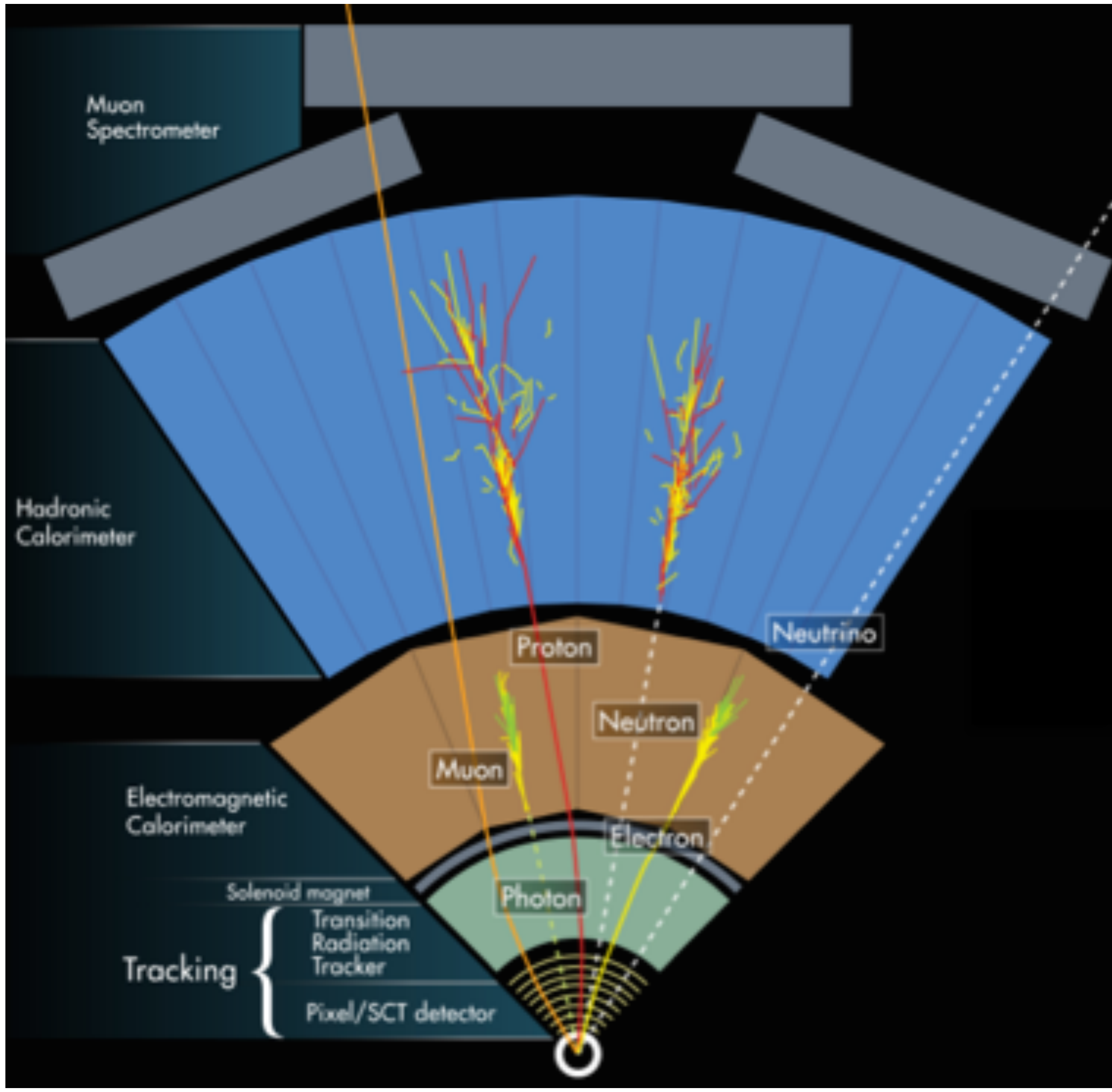

How to race ?

- In the $H \rightarrow ZZ \rightarrow 4\ell$ the signal is a narrow resonant peak above a background continuum.

ℓ = electron or muon

Higgs signal, resonant at the value of m_H

Non resonant background from other non H production

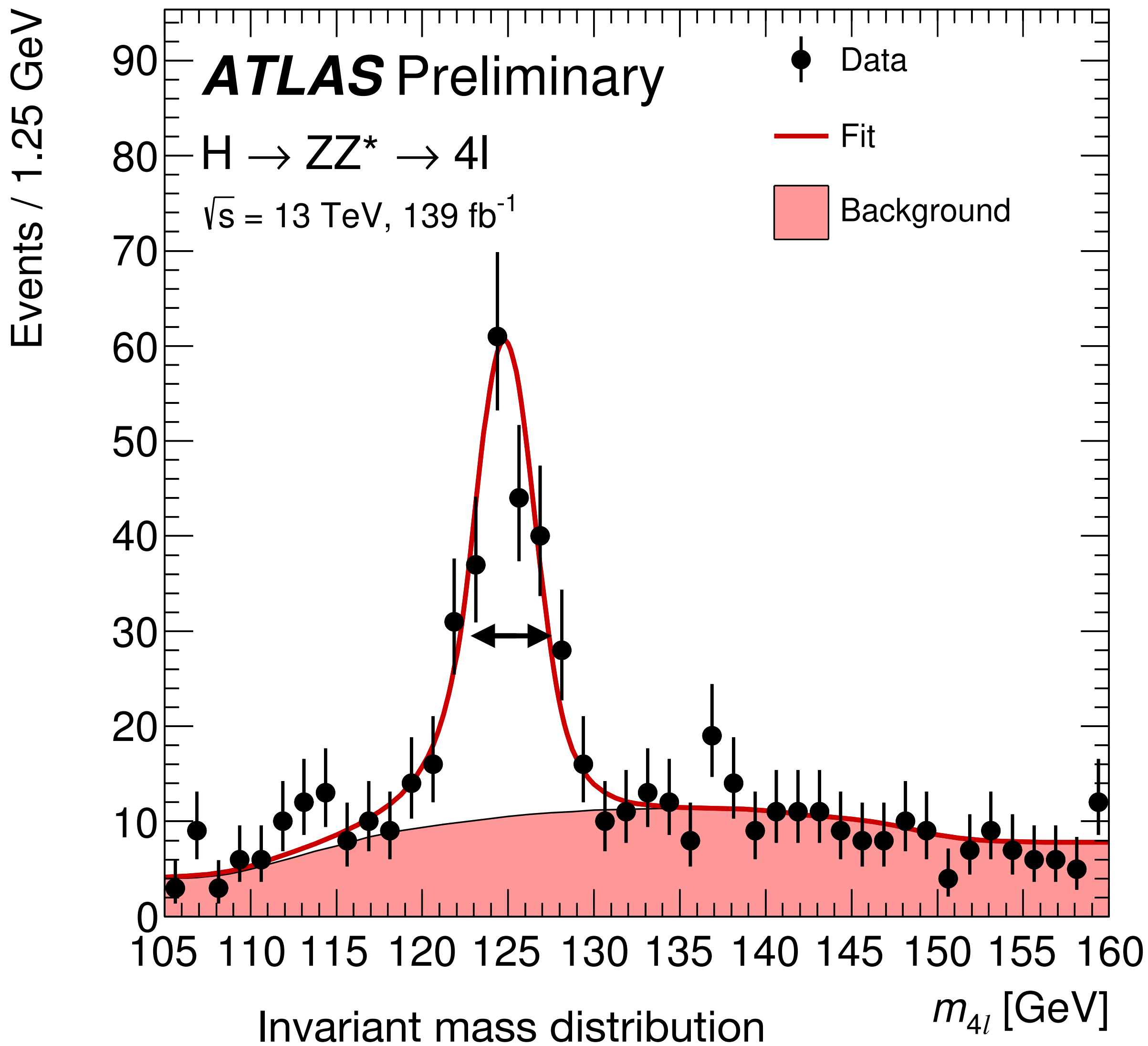

Invariant mass distribution

$$\delta m_H \simeq \frac{\sigma(m_{4\ell,\gamma\gamma})}{\sqrt{N - N_b}}$$

Uncertainty on m_H approximated by the uncertainty on the mean of the mass distribution

(I) Statistical precision precision depends upon: resolution of the reconstructed final state and number of signal events.

(II) Systematic uncertainty from understanding of detector performance:

Run 1 Discovery

- Run-1 featured *in primis* the discovery in July 2012
  - First properties measurements
  - How did the mass measurements evolve since the discovery.

  - Where do we stand with our understanding of the Higgs boson mass 10 years later and how did we get there ?

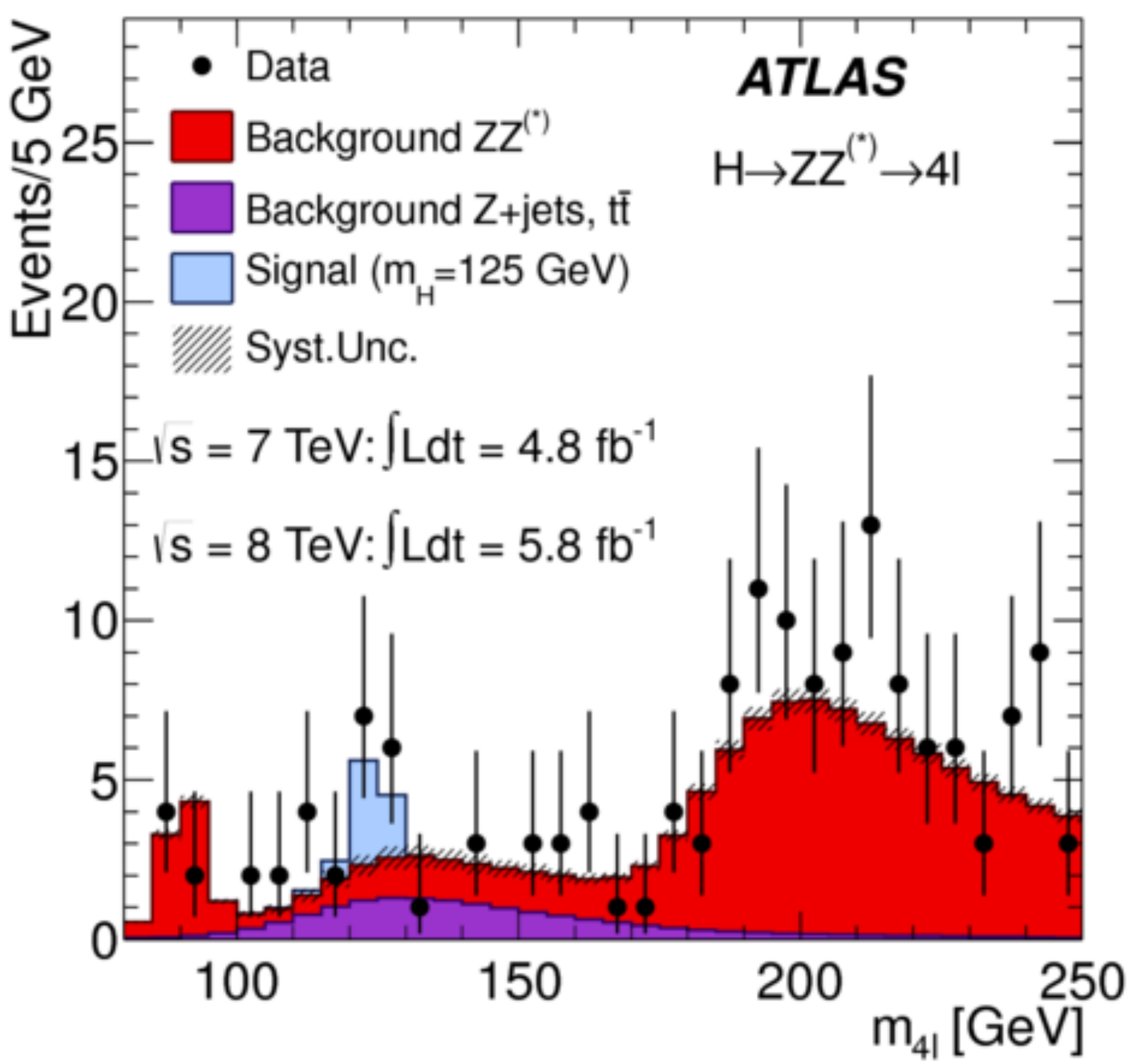

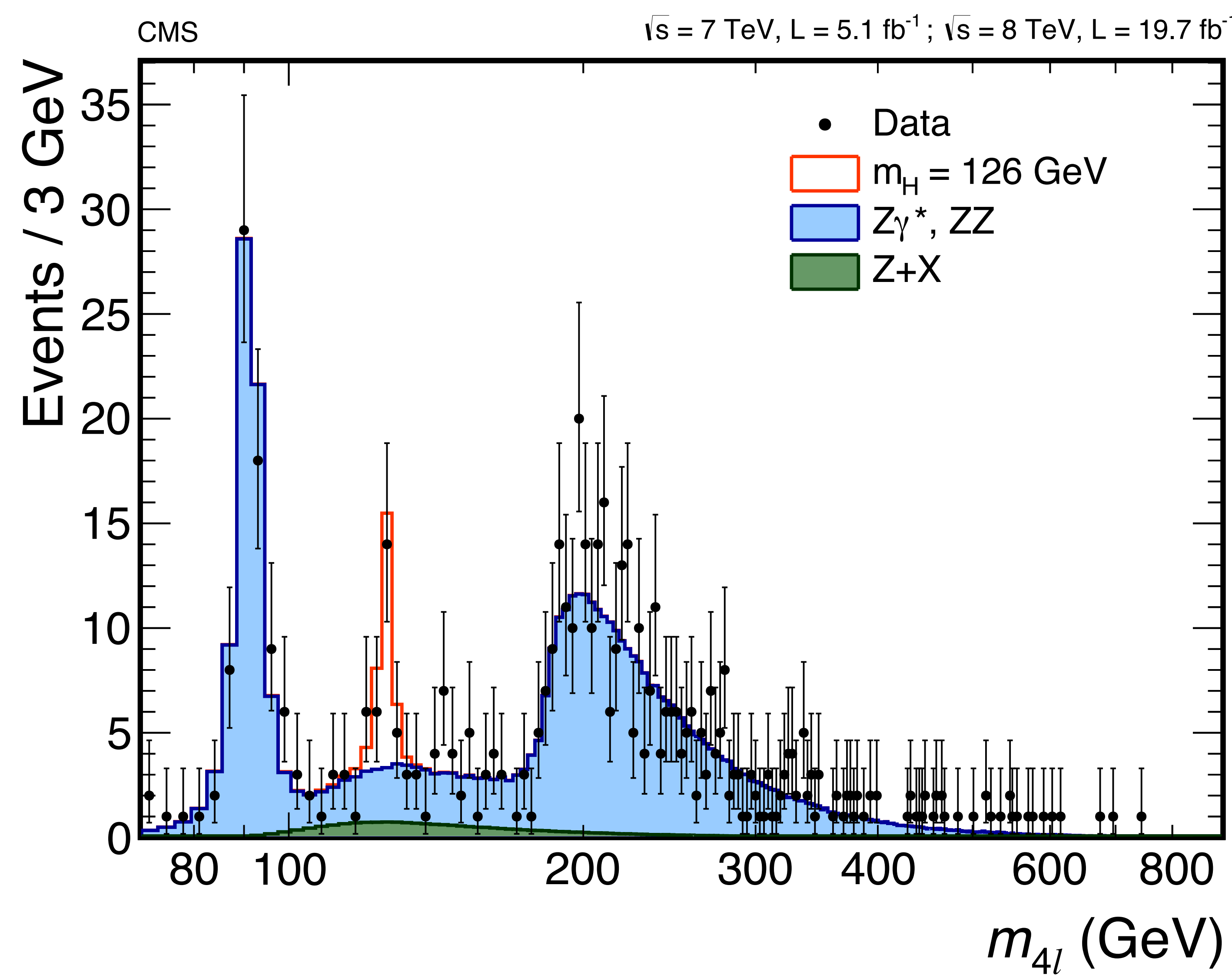

Run I status

- ATLAS+CMS Run I precision on m_H of 2 per mille.
  - combined measurement from $H\rightarrow\gamma\gamma$ and $H\rightarrow ZZ^*\rightarrow 4\ell$.

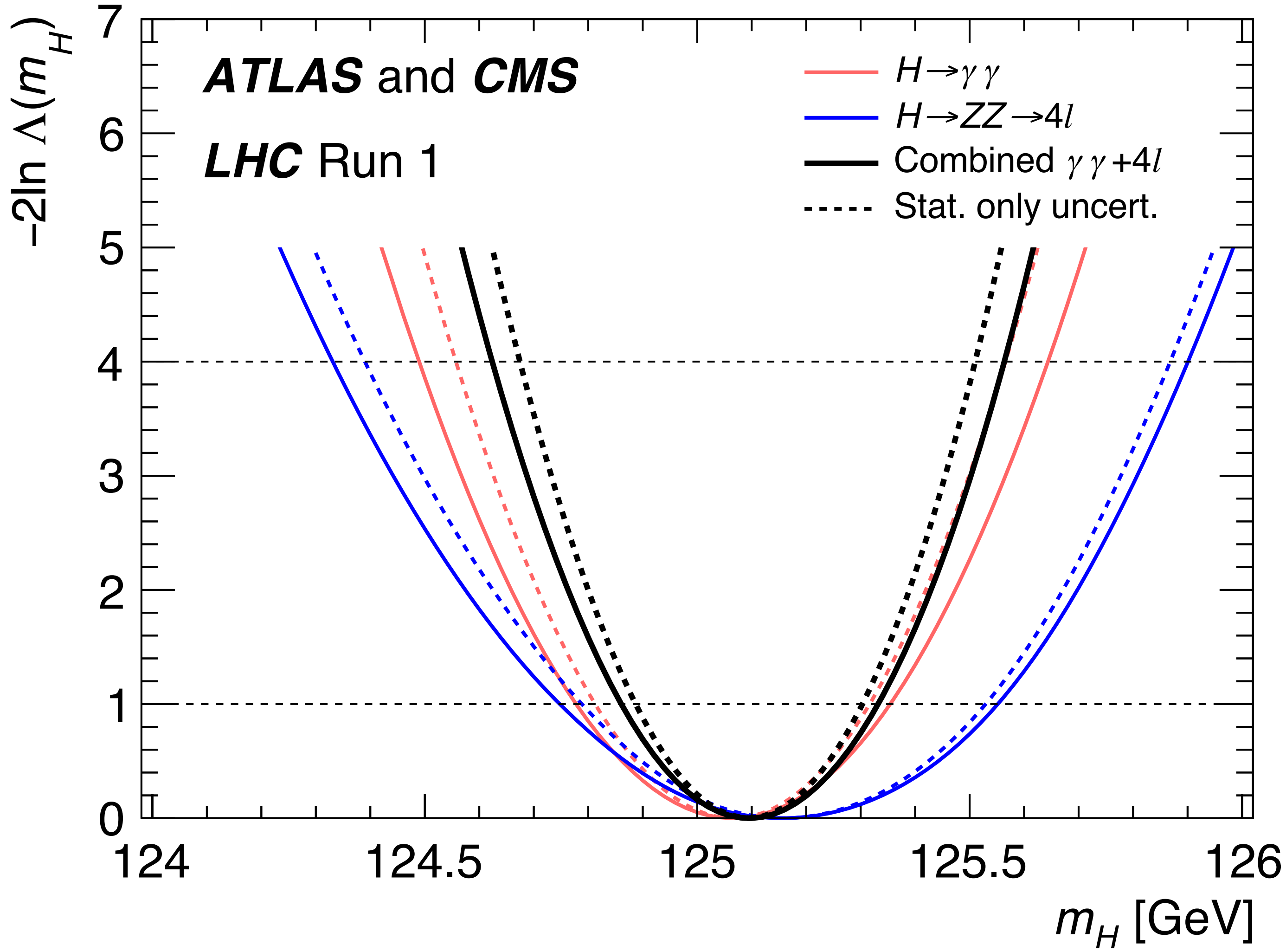

  - For both channels dominated by statistical uncertainty.

$$m_H = 125.09 \pm 0.21\,(\text{stat.}) \pm 0.11\,(\text{scale}) \pm 0.02\,(\text{other}) \pm 0.01\,(\text{theory})\text{ GeV}$$

Run I status

- ATLAS+CMS Run I precision on m_H of 2 per mille
  - For both channels dominated by statistical uncertainty.

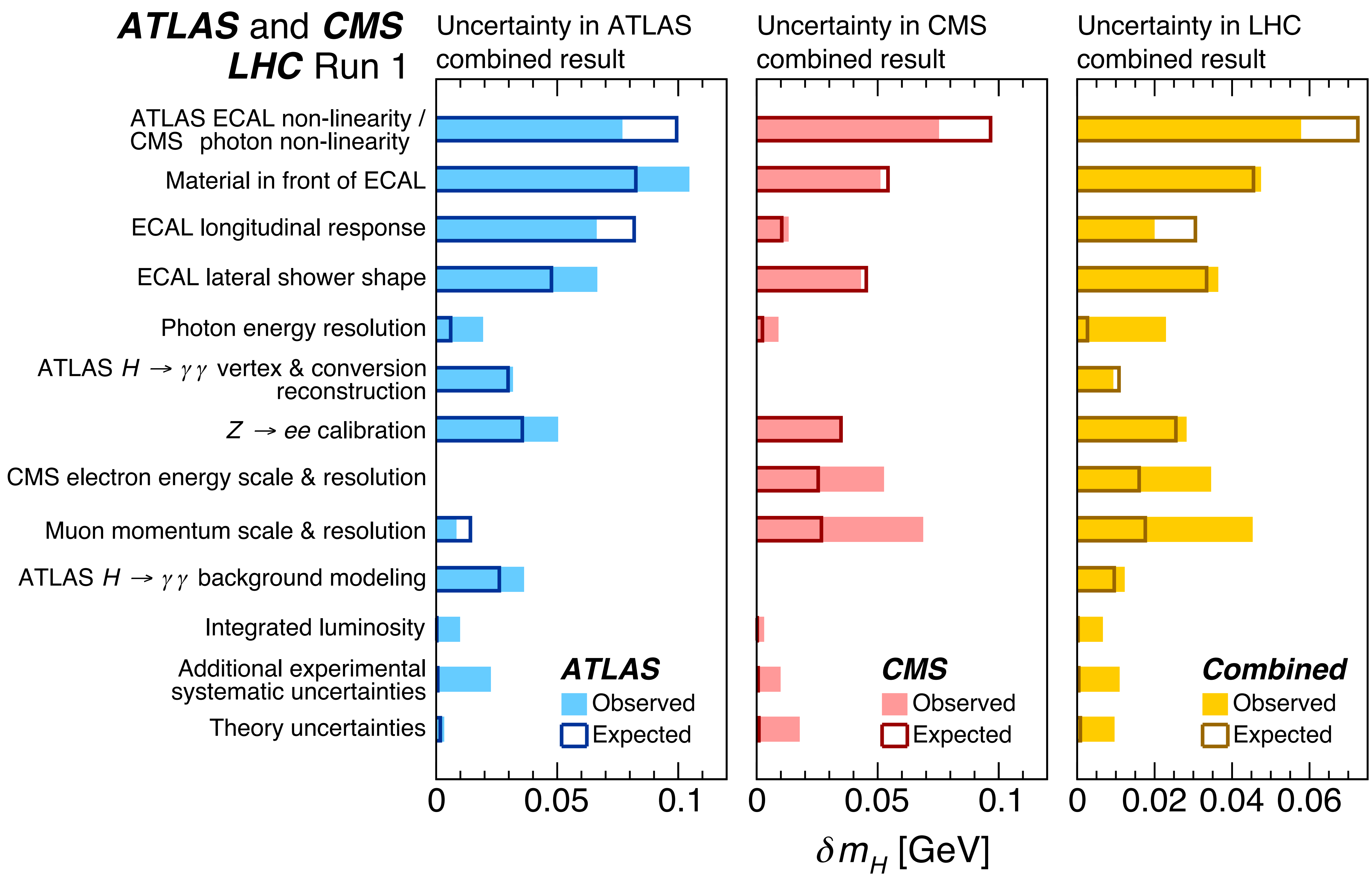

Run I status

- ATLAS+CMS Run I precision on m_H of 2 per mille
  - combined measurement from $H\to\gamma\gamma$ and $H\to ZZ^*\to 4\ell$.

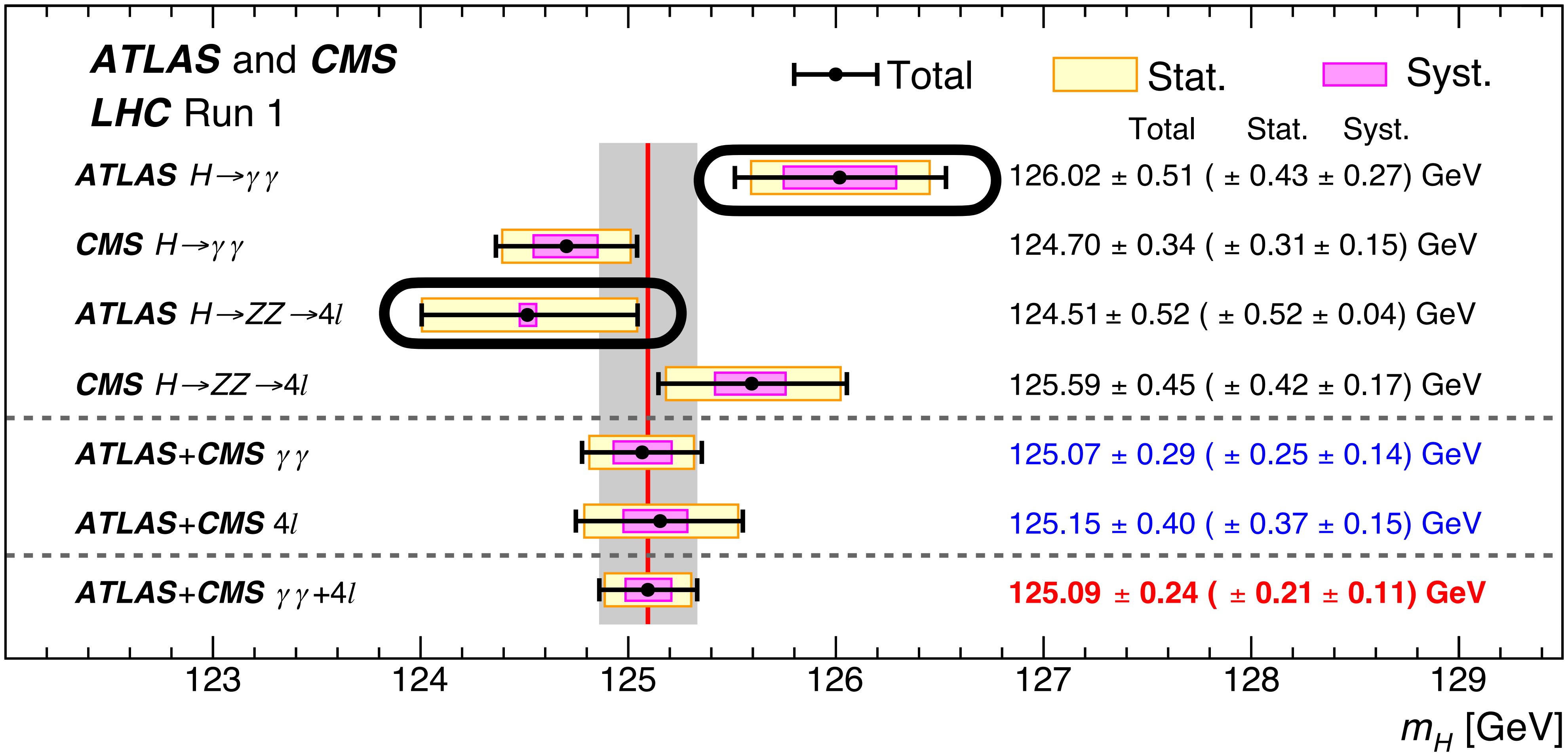

- In the mean time and within ATLAS,

Energy resolution

- We used well known processes to calibrate the detector response.
  - Resonant process of J/ψ, (Υ) and Z,
  - for modelling of calorimeters deposits, alignment precision, etc.

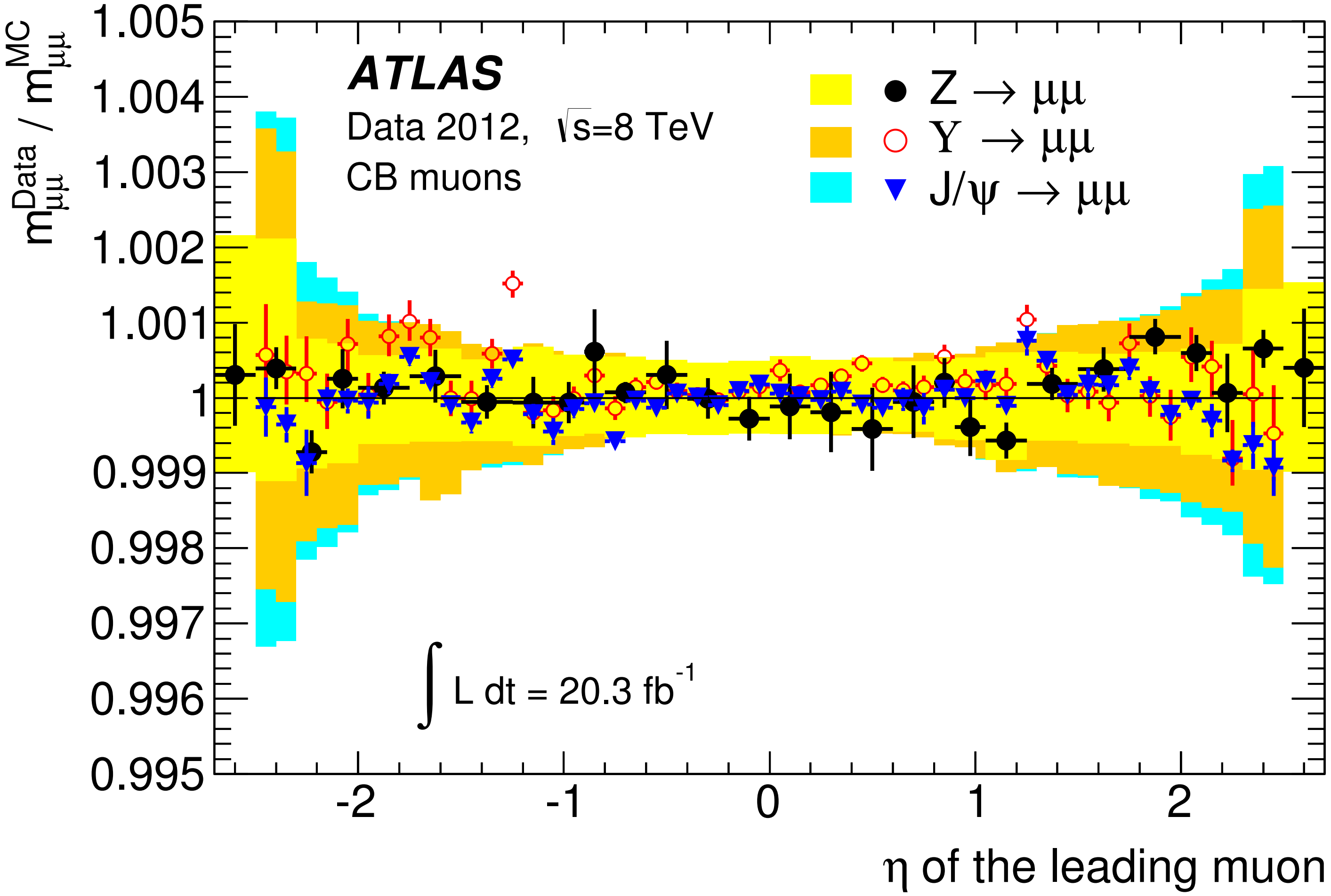

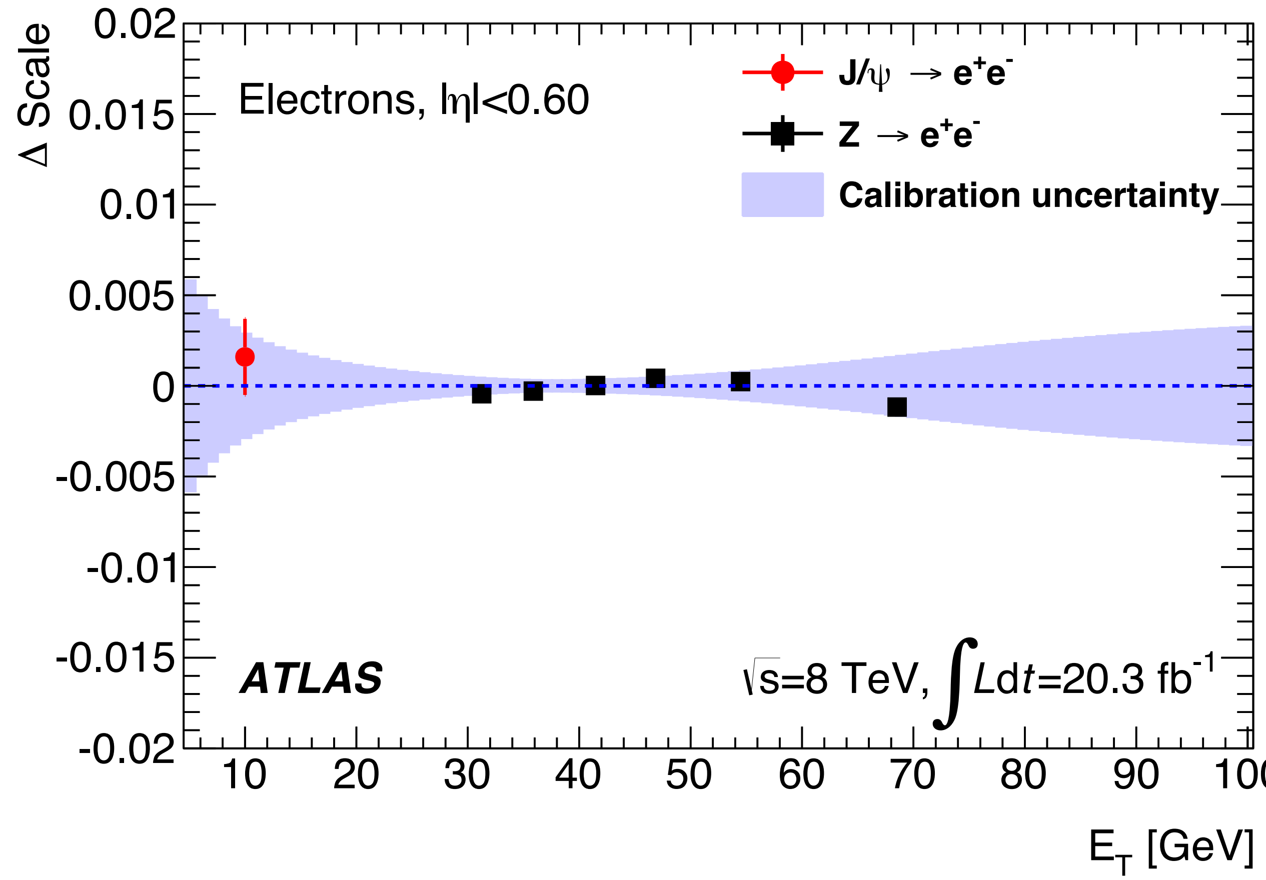

Run I status

- ATLAS+CMS Run I precision on m_H of 2 per mille.
  - combined measurement from $H \to \gamma\gamma$ and $H \to ZZ^* \to 4\ell$.

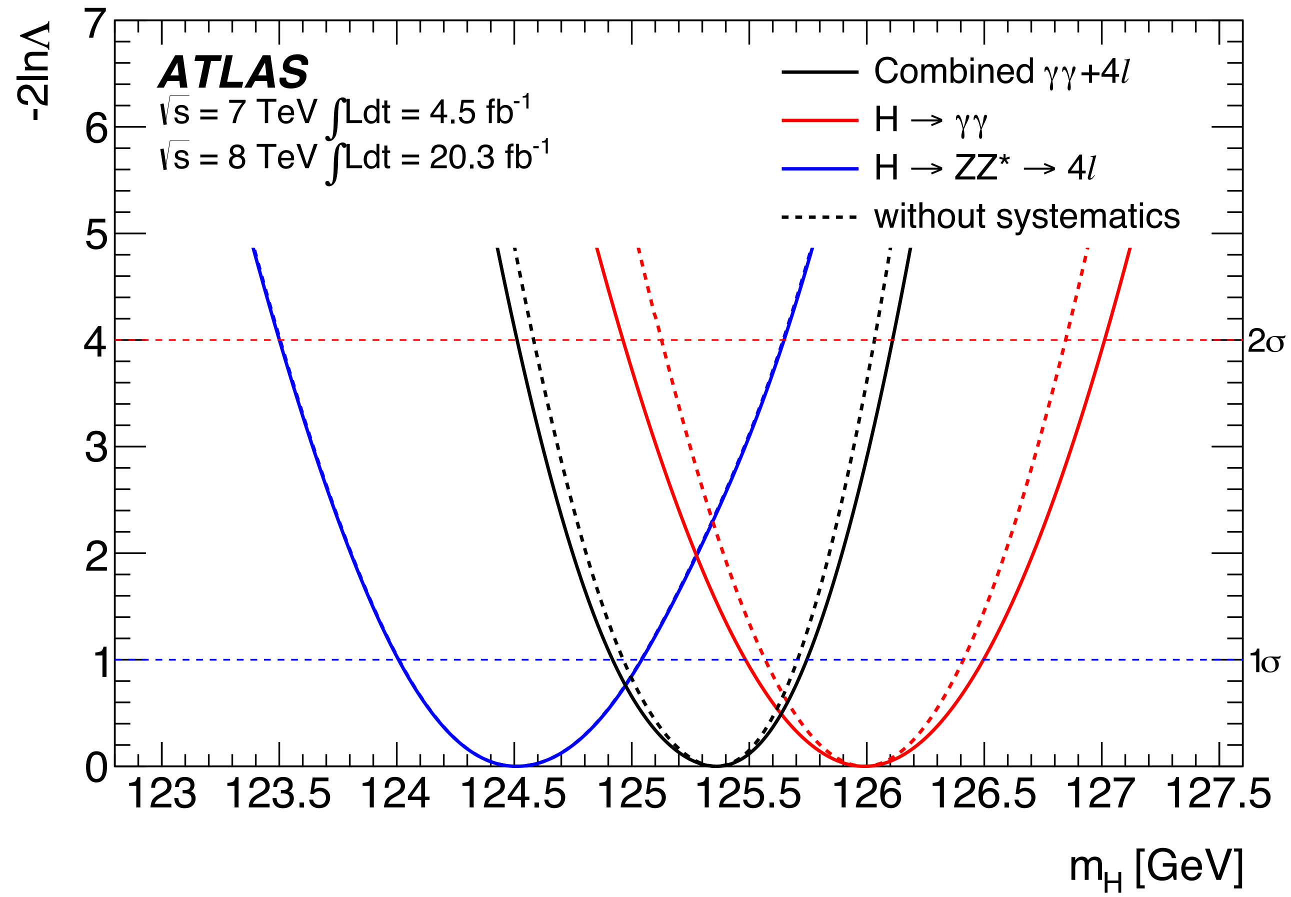

  - ATLAS compatibility between γγ and 4ℓ 4%

Channel	Mass measurement [GeV]
$H \to \gamma\gamma$	$125.98 \pm 0.42\,(\text{stat}) \pm 0.28\,(\text{syst}) = 125.98 \pm 0.50$
$H \to ZZ^* \to 4\ell$	$124.51 \pm 0.52\,(\text{stat}) \pm 0.06\,(\text{syst}) = 124.51 \pm 0.52$
Combined	$125.36 \pm 0.37\,(\text{stat}) \pm 0.18\,(\text{syst}) = 125.36 \pm 0.41$

Run I status

- ATLAS run I precision on m_H of 0.33%
  - combined measurement from $H\rightarrow\gamma\gamma$ and $H\rightarrow ZZ^{*}\rightarrow 4\ell$.

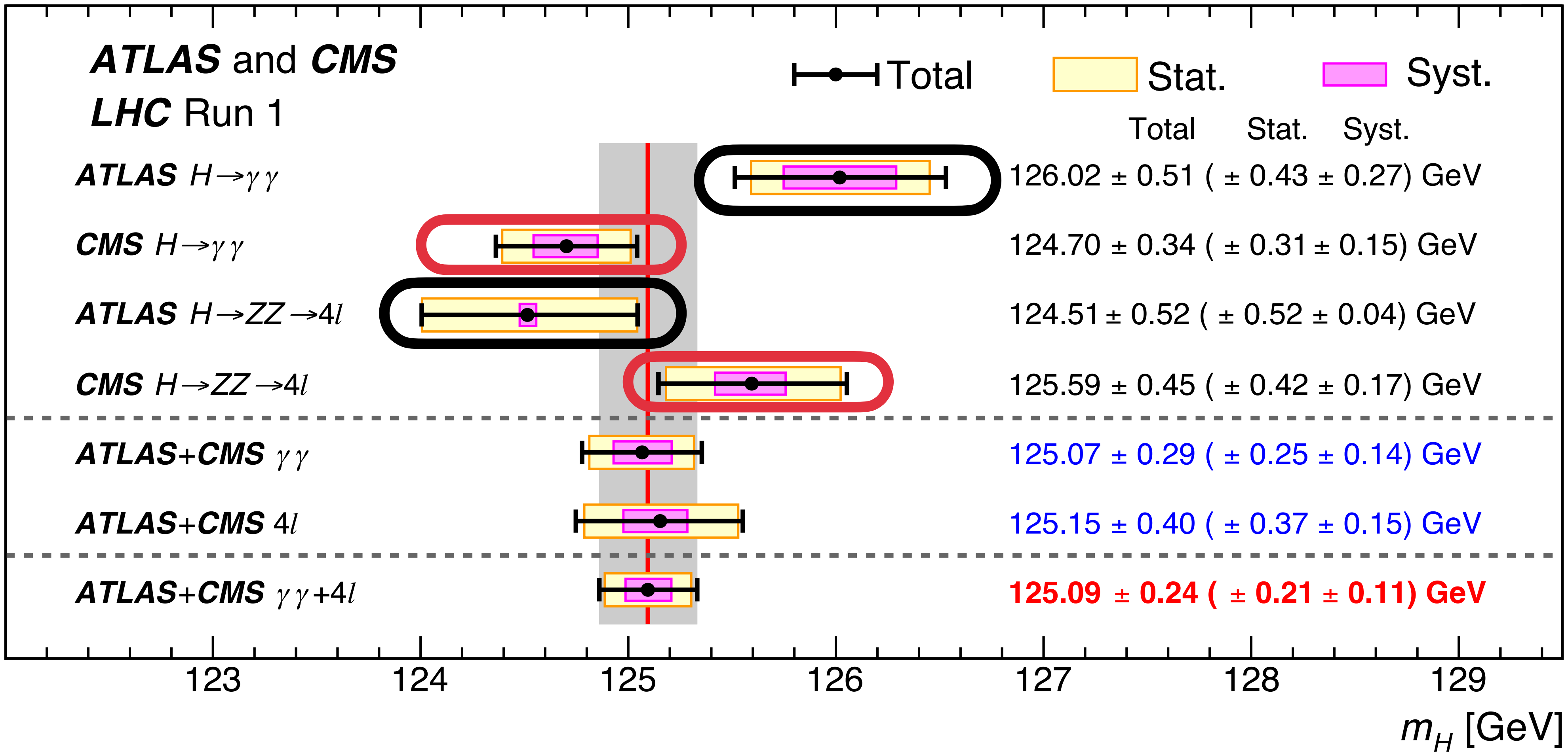

Energy resolution

- We used well known processes to calibrate the detector response.
  - Resonant process of J/ψ, (Υ) and Z,
  - for modelling of calorimeters deposits, alignment precision, etc.

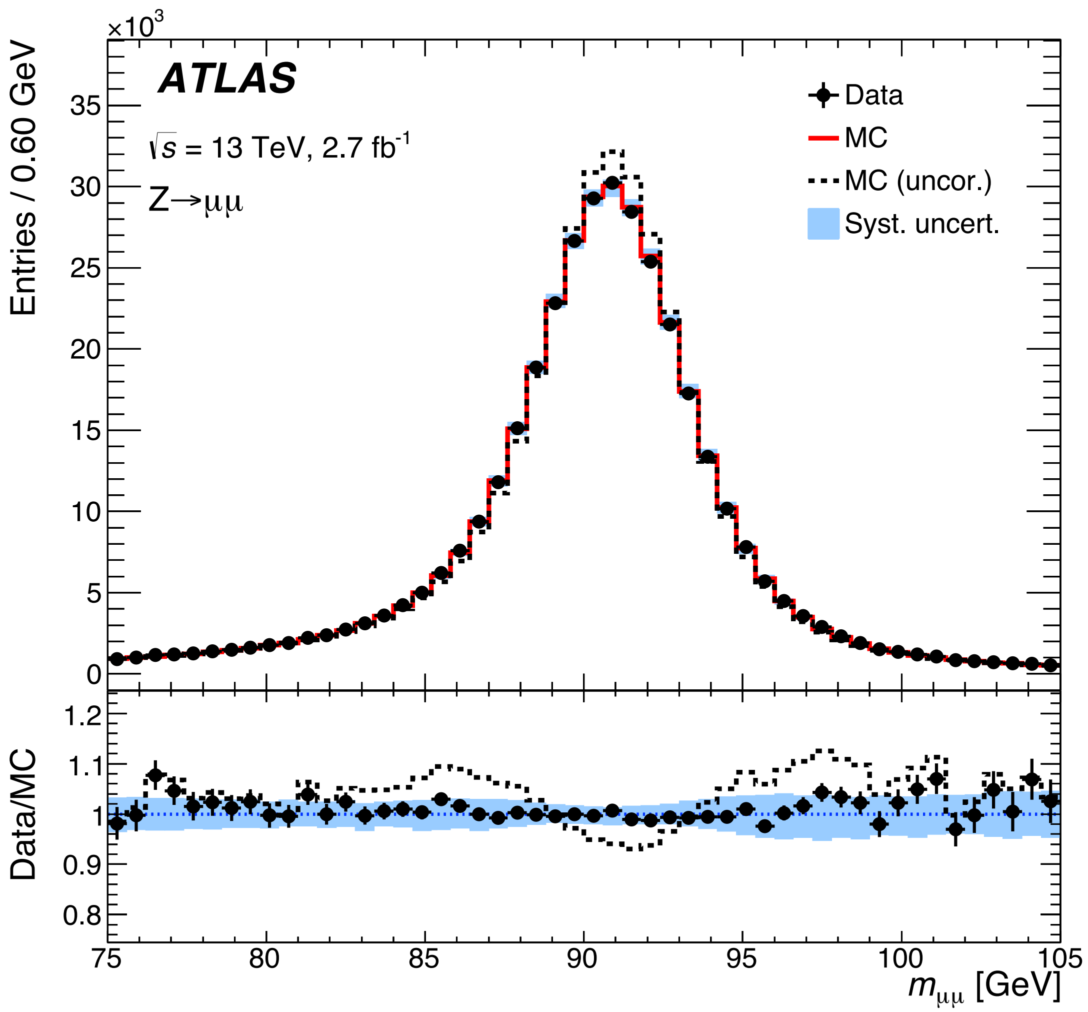

$Z\rightarrow\mu\mu$ resonant line shape for data and detector simulation

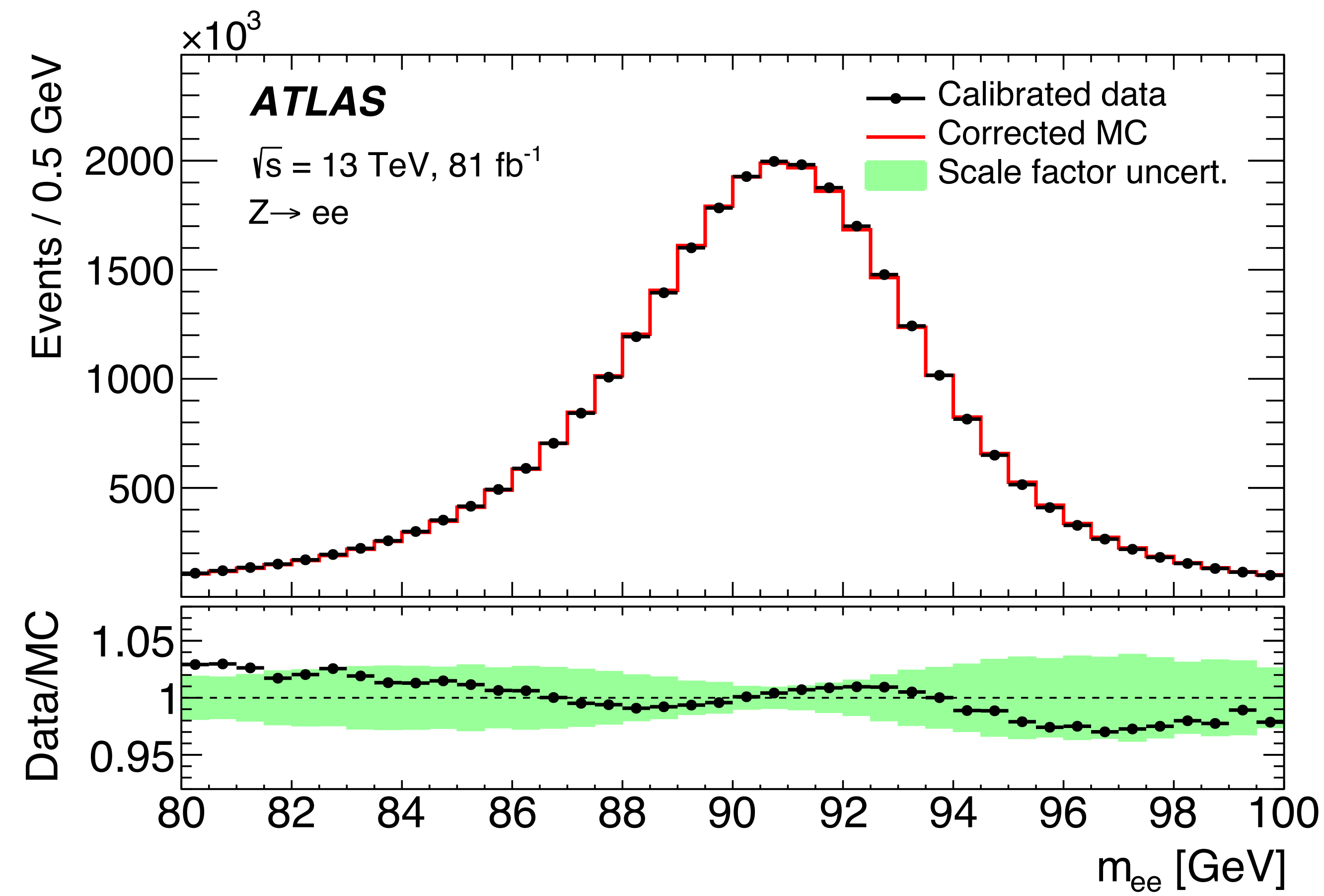

$Z\rightarrow ee$ resonant line shape for data and detector simulation

- Local misalignments: second or first order effects ?
  - Charge dependent sagitta bias, with net effect of worsening resolution and biasing the result.
  - Solution: Let's correct these *a posteriori*

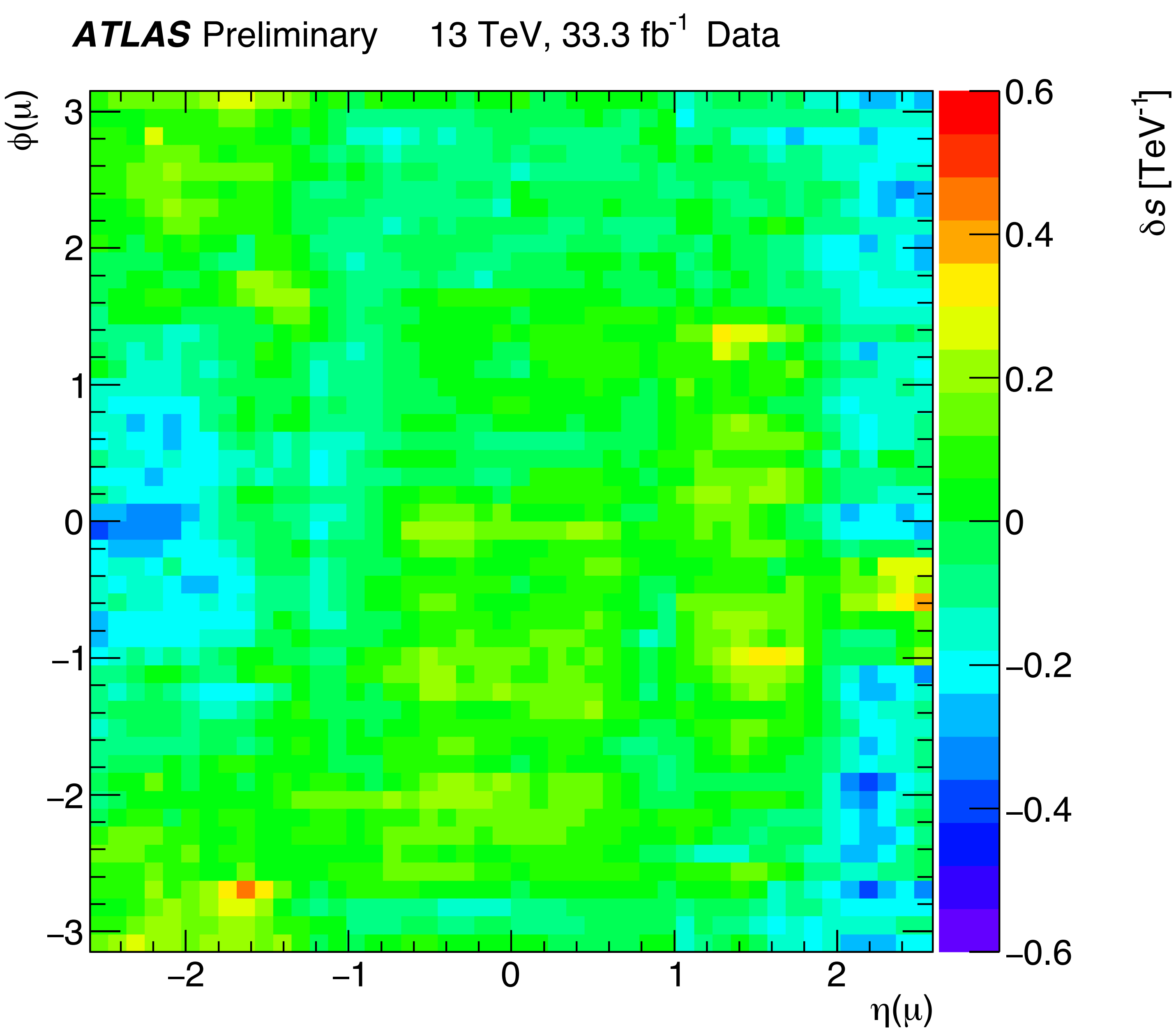

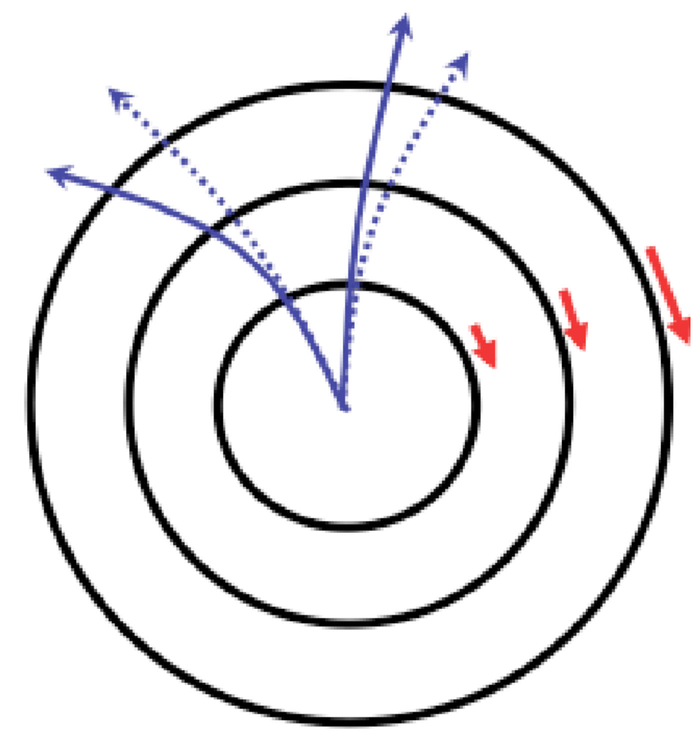

Detector layer movements biasing the measurement of the bending of the particle

Muon p_T resolution — Mass measurement

- Local misalignments: second or first

  - Charge dependent sagitta bias, with net effect of v
  - Solution: Let's correct these *a posteriori*

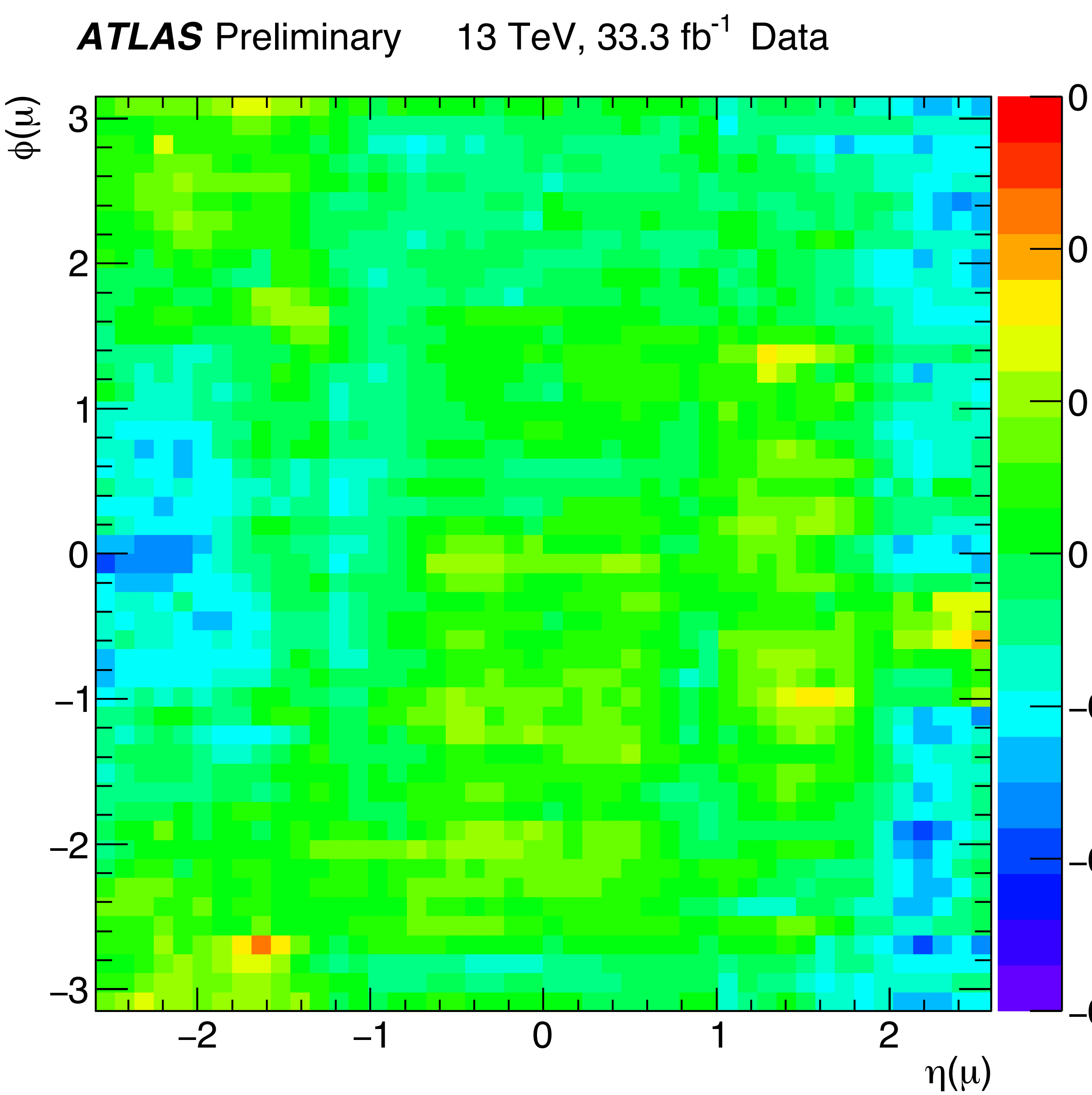

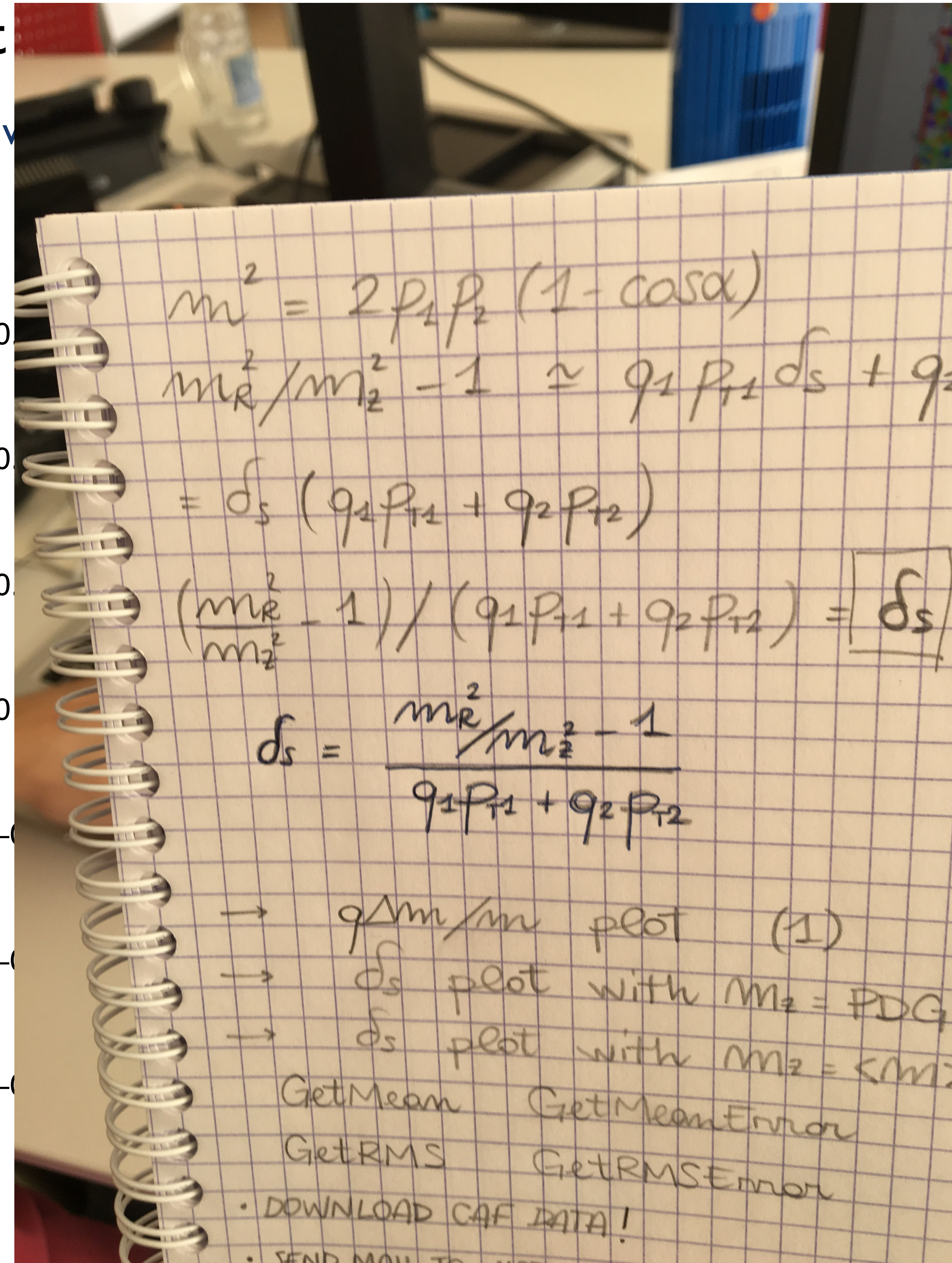

- Local misalignments: second or first order effects ?
  - Charge dependent sagitta bias, with net effect of wor
  - Solution: Let's correct these *a posteriori*

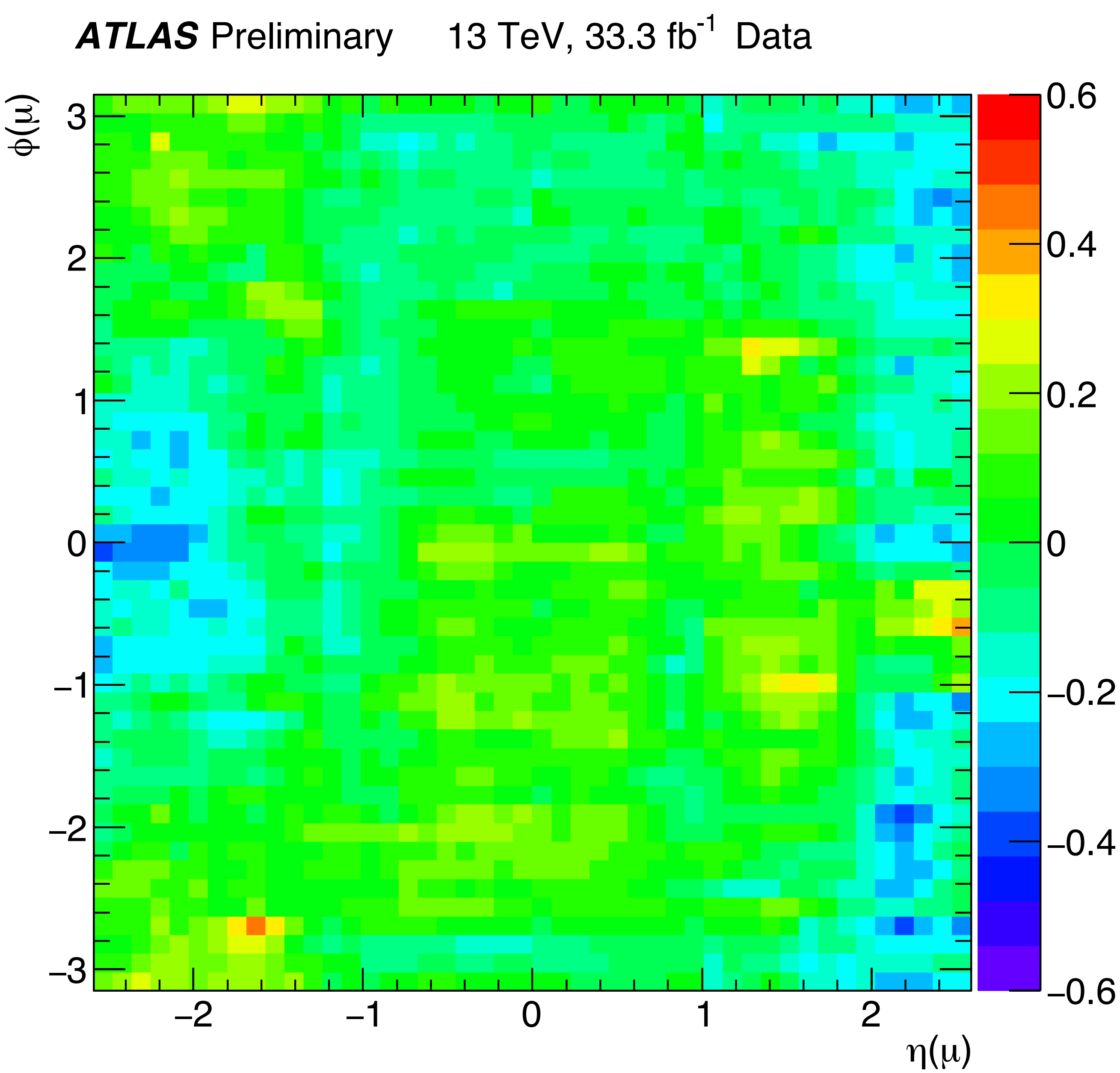

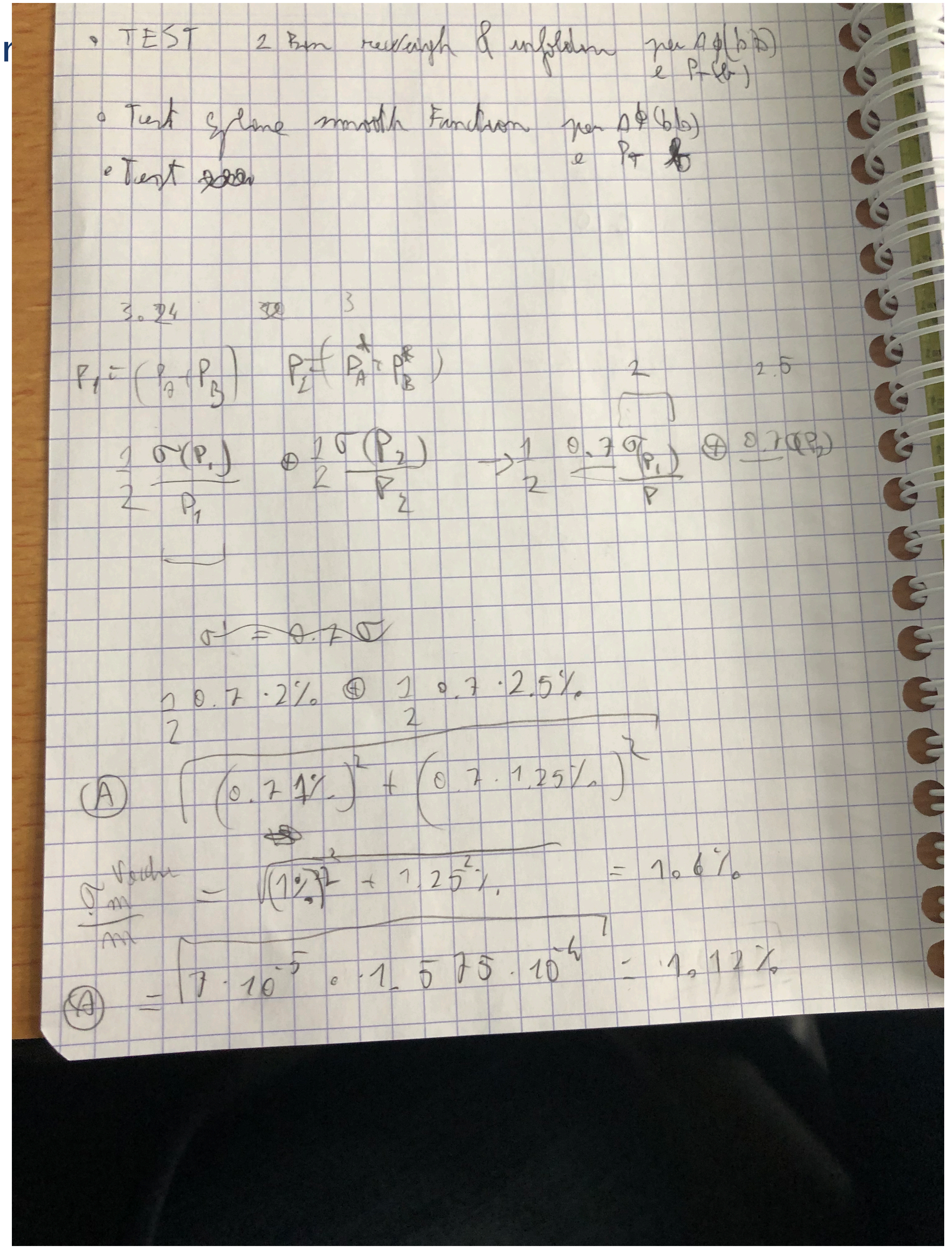

- **Local misalignments and second order effects:**
  - Charge dependent sagitta bias, with net effect of worsening resolution
  - *In-situ* correction based on Z→μμ data, recovers up to 5% in resolution.
- **Momentum scale understood down to the per mille level**
  - Precision down to 0.5 per mille for |η|<1.0

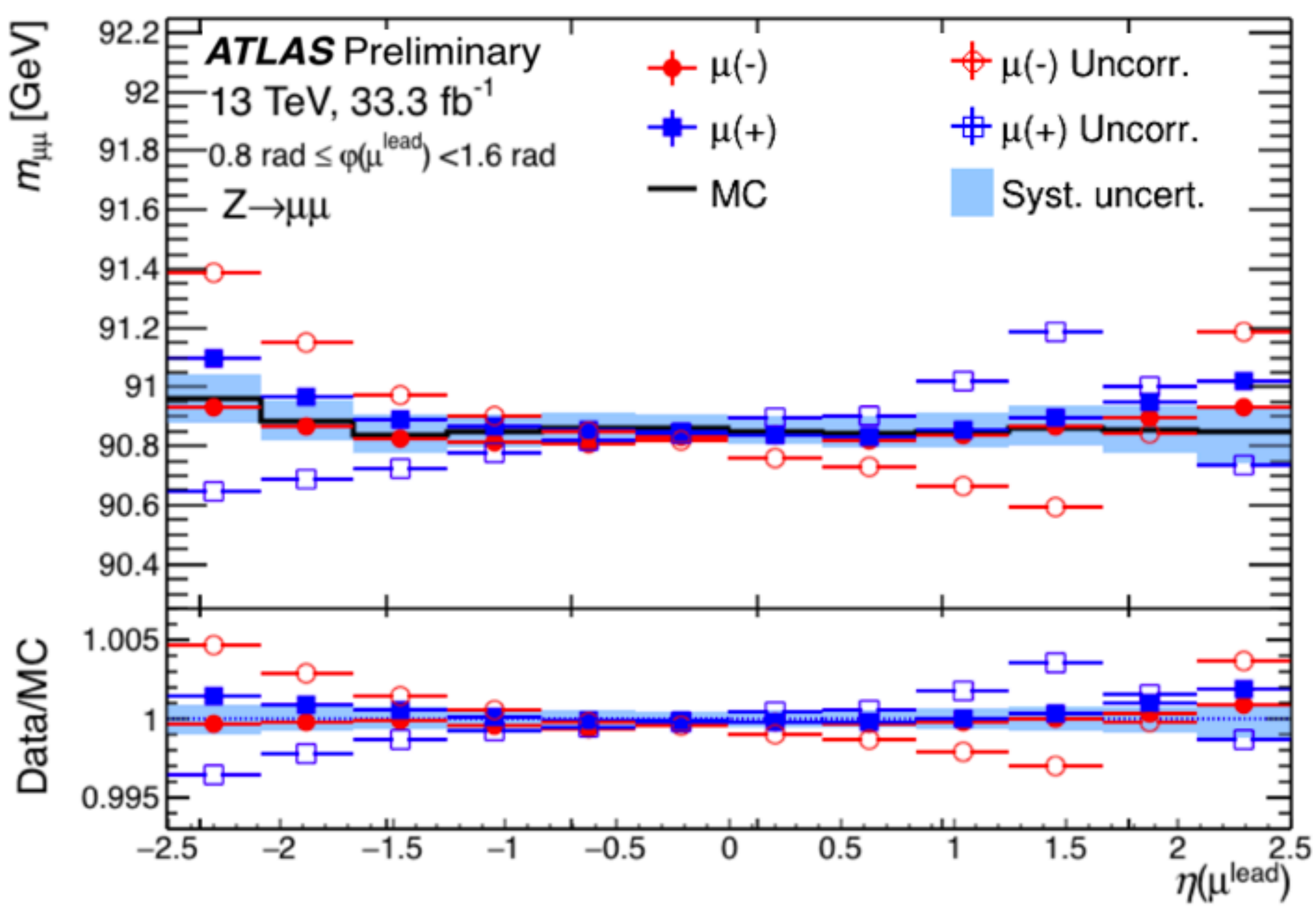

Biased positive and negative tracks
Corrected positive and negative tracks

$E_T(e/\gamma)$ resolution

- Good energy calibration necessary for increased precision on m_H
  - Two step approach: i) material energy loss and ii) global calorimetric scale from $Z\to ee$ data.
  - Also here: *crisis mode to avoid the crisis mode.*
- Total scale uncertainty of at 40 GeV at the per-mille level.

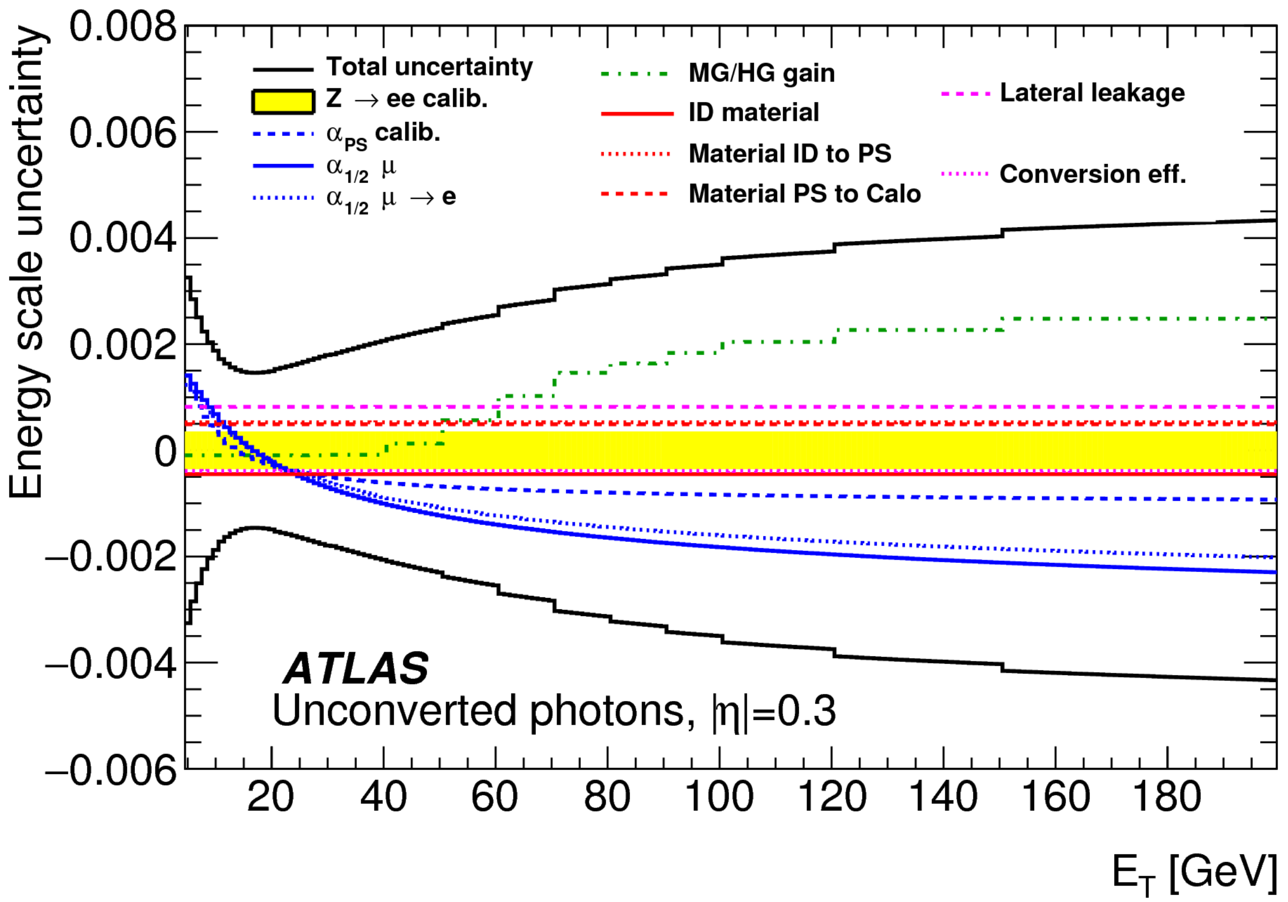

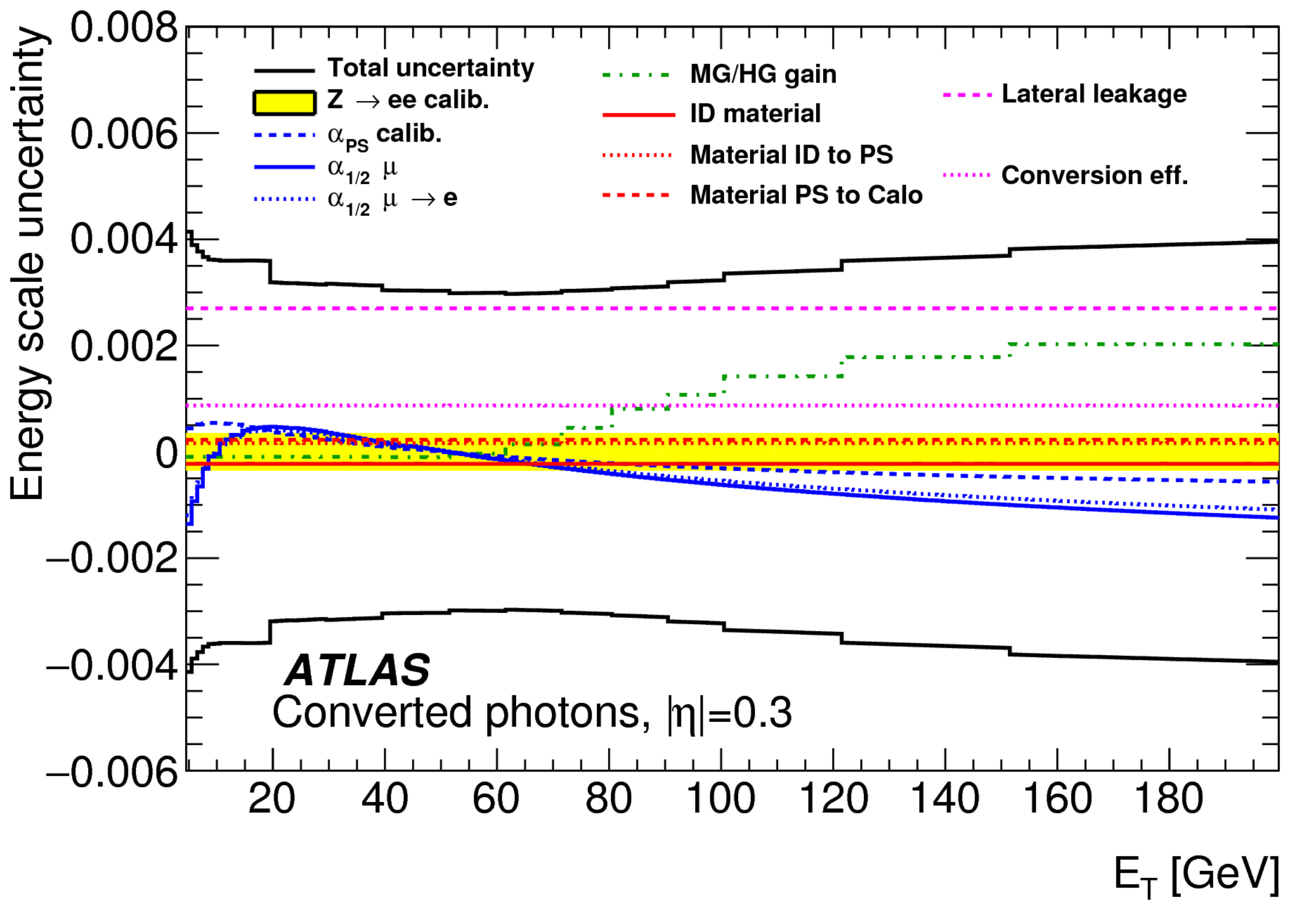

arXiv:1806.00242

- Final estimate from 4x4 simultaneous un-binned fit
  - Four kinematic categories and four final states
- Good agreement between channels.
- Systematic uncertainty of 50 MeV

Systematic effect	Uncertainty on $m_H^{ZZ^*}$ [MeV]
Muon momentum scale	40
Electron energy scale	26
Pile-up simulation	10
Simulation statistics	8

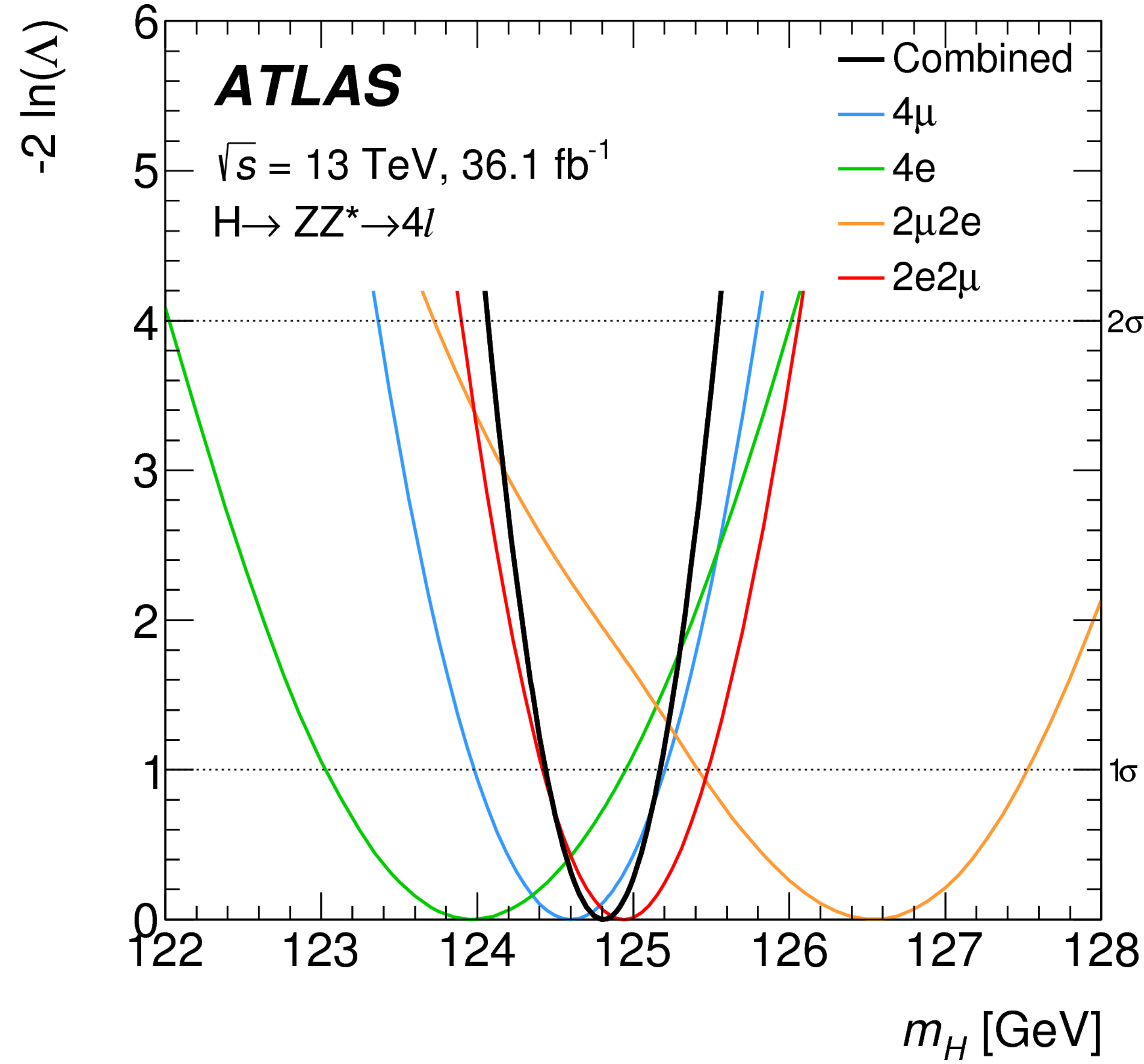

- Result:
  - 25% improved precision with respect to Run I ATLAS Combination.

$$m_H^{ZZ^*} = 124.79 \pm 0.36 \; (\pm 0.05 \text{ stat only}) \text{ GeV}$$

- 4ℓ and γγ measurements are combined with ATLAS Run 1 result

arXiv:1806.00242

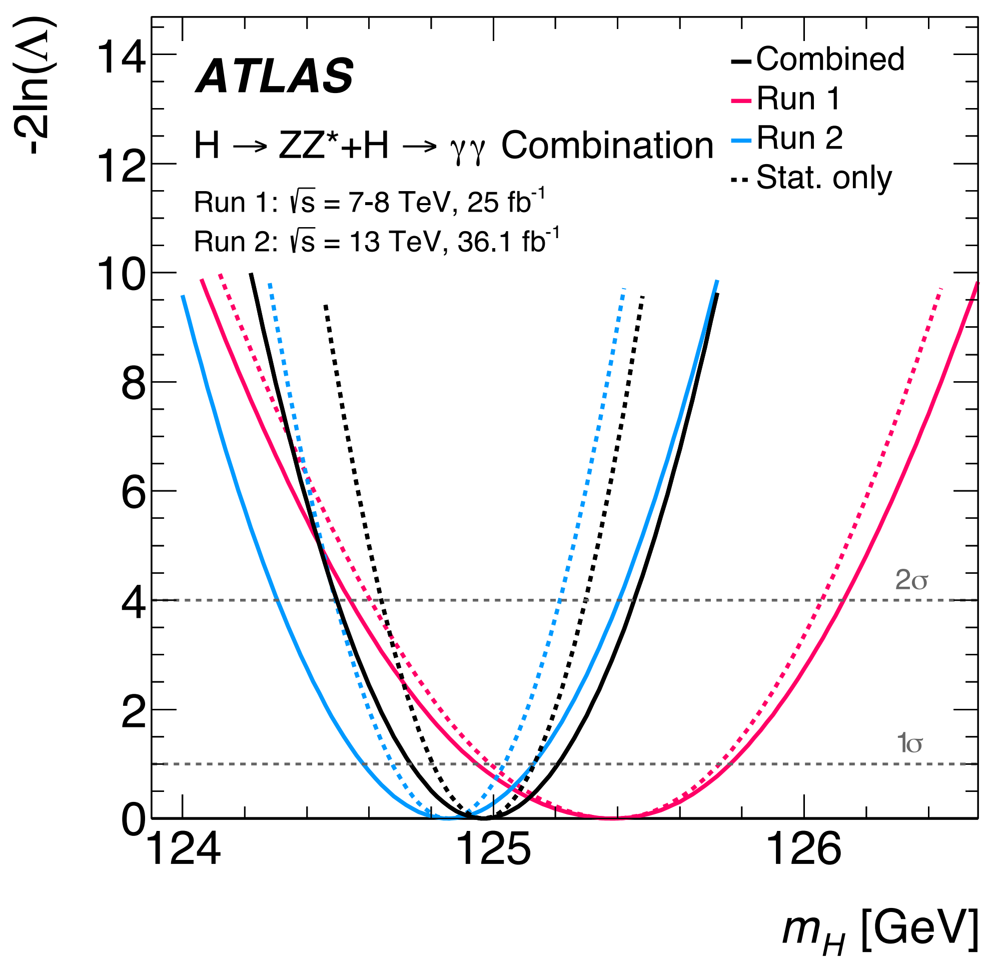

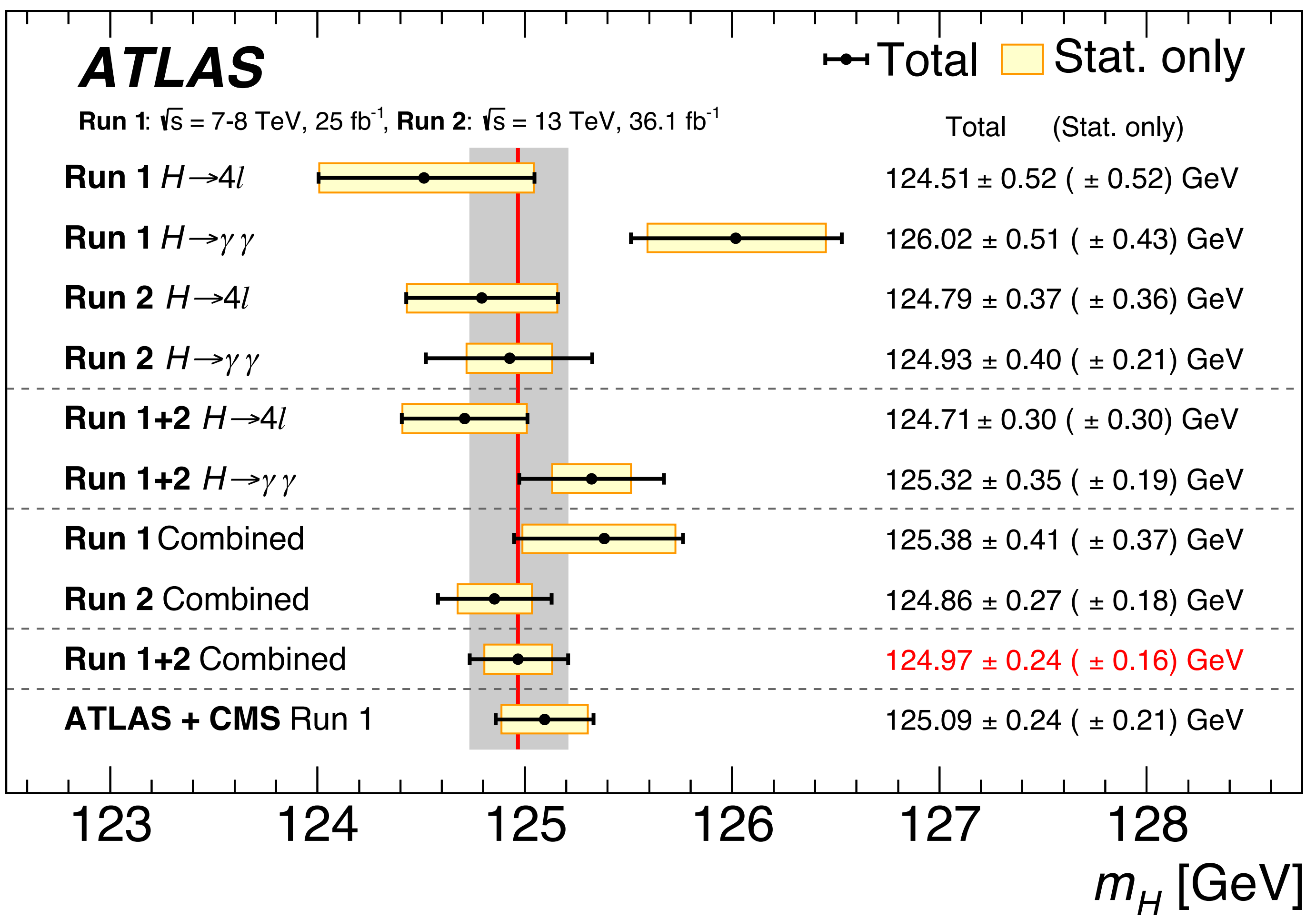

- ATLAS Run 1 + 2 (36.1) comparable precision to LHC Run 1 combination.

$$m_H = 124.97 \pm 0.24(\pm 0.16 \text{ stat only}) \text{ GeV}$$

- 4ℓ and γγ measurements are combined with ATLAS Run 1 result arXiv:1806.00242

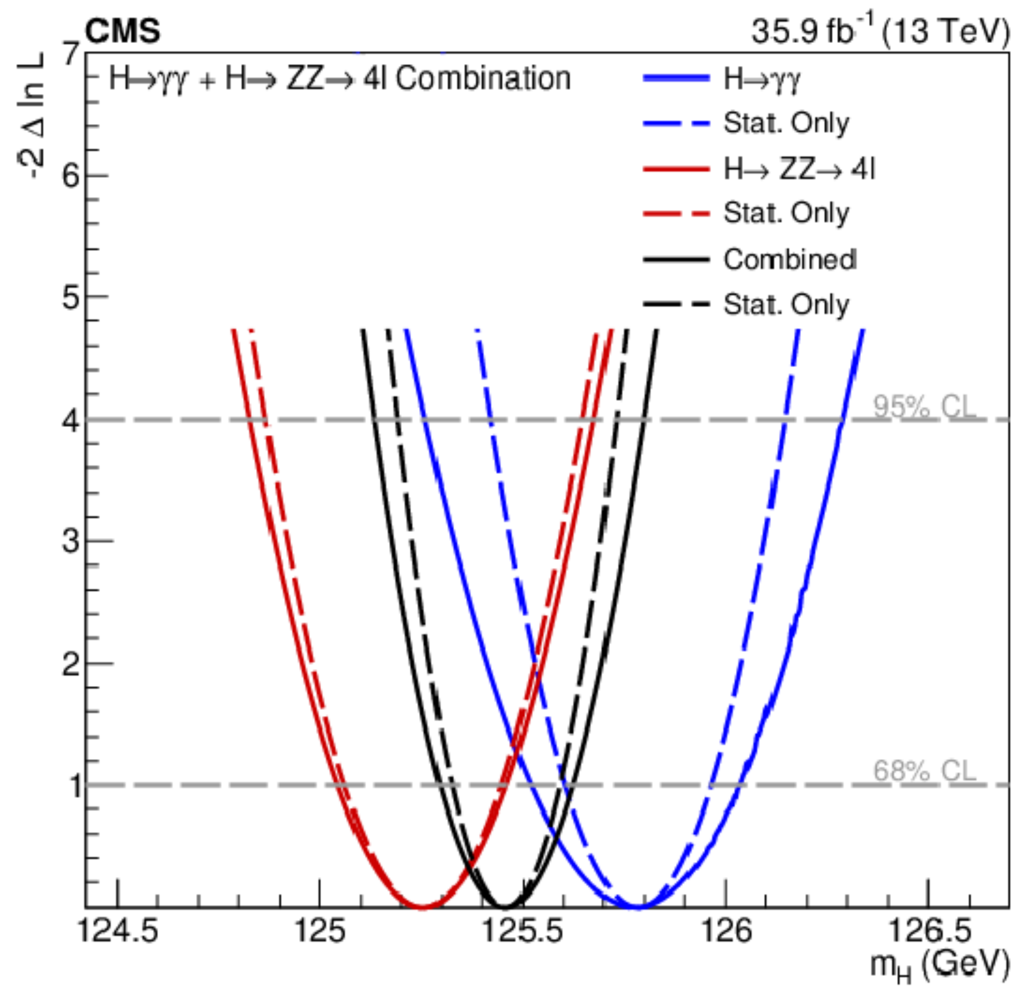

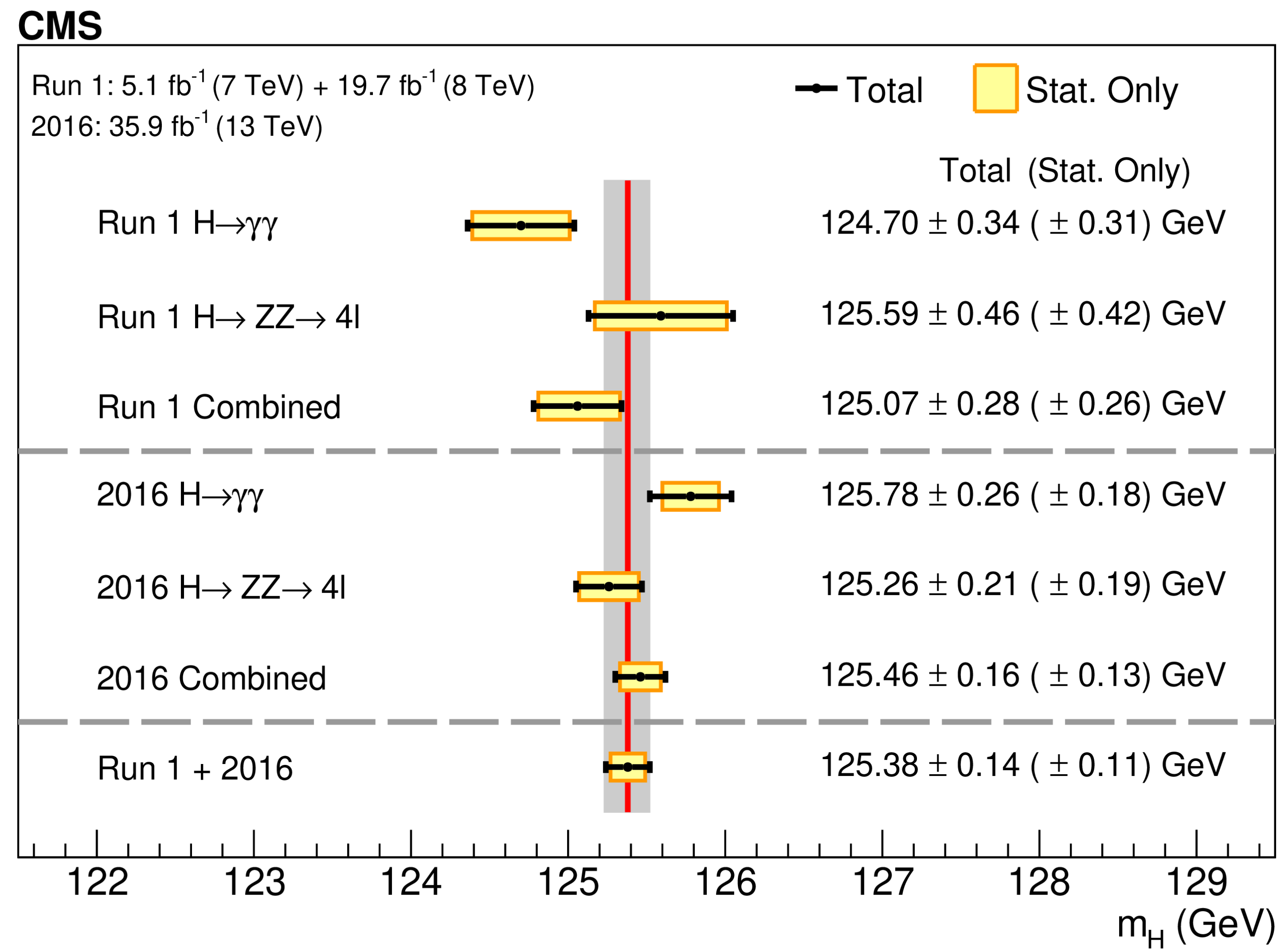

- CMS Run 1 + 2 (36.1) comparable precision to LHC Run 1 combination.

Towards full Run 2

- Three-prong approach to reduce uncertainty at analysis level:
  - (i) (~15%) from m_{12} constraint to m_Z with kinematic fit and m_Z constraints on alignment weak modes.
  - (i) (~2%) from kinematic discriminant selecting signal and background events
    - Boosted Decision Tree on $p_T(4\ell)$, $y(4\ell)$ (ATLAS) and $\log(|\mathscr{M}_H|^2/|\mathscr{M}_{ZZ*}|^2)$
  - (ii) (2-3% - 11%) from multivariate per-event resolution likelihood.
    - Neural network to solve uncertainty correlations induced by kinematic discriminant.

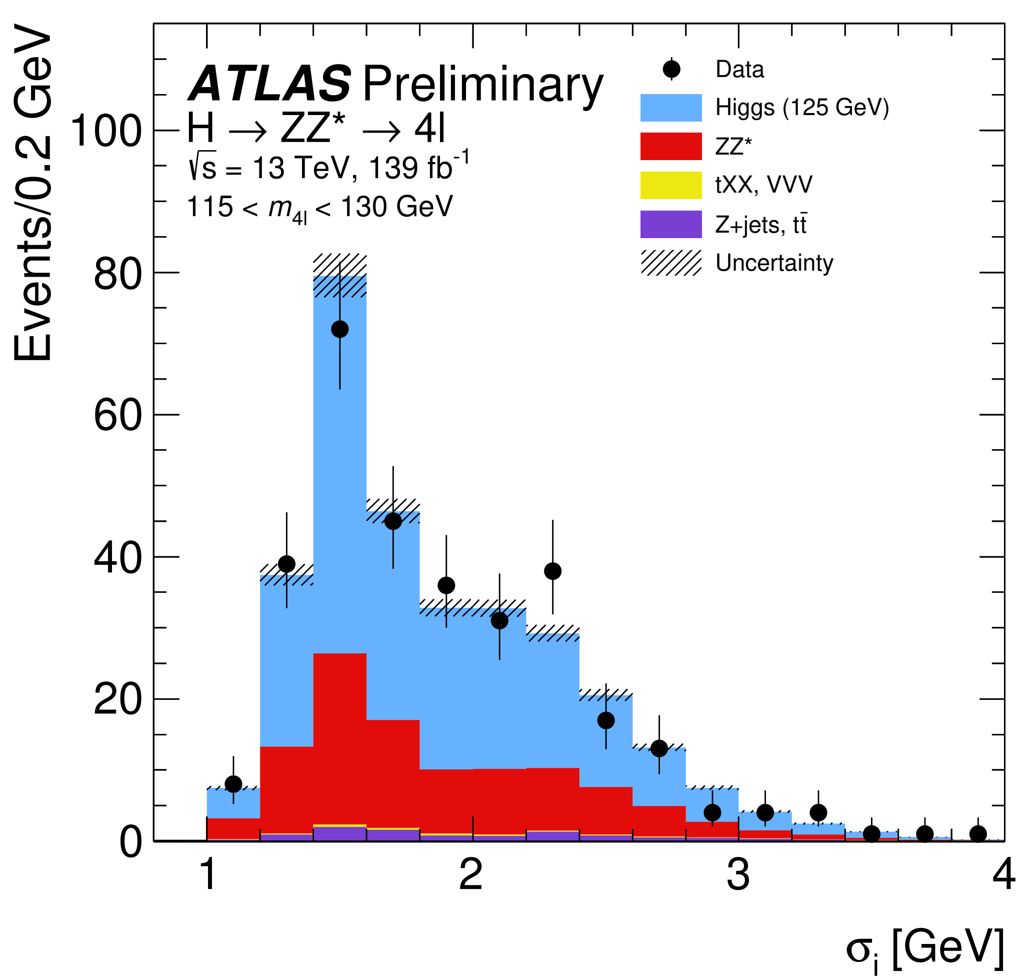

Neural network output of the event's uncertainty

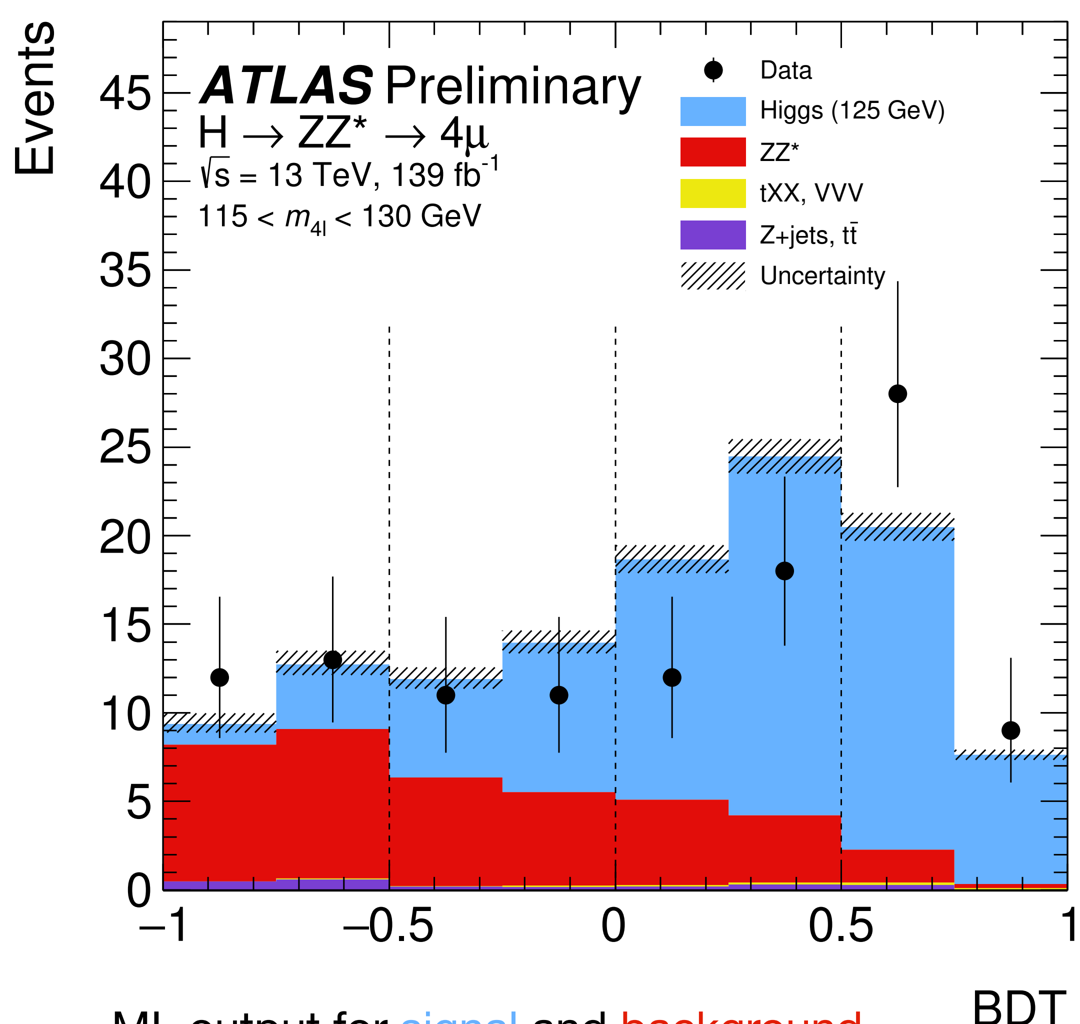

ML output for signal and background

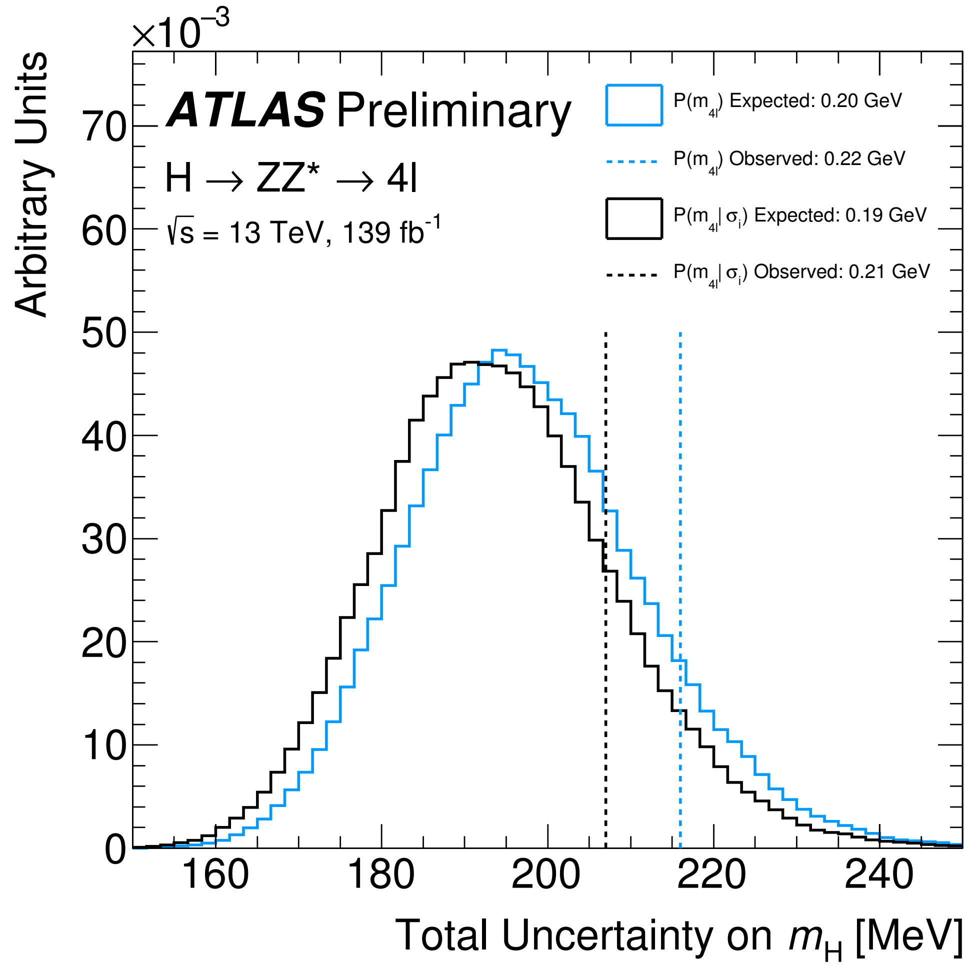

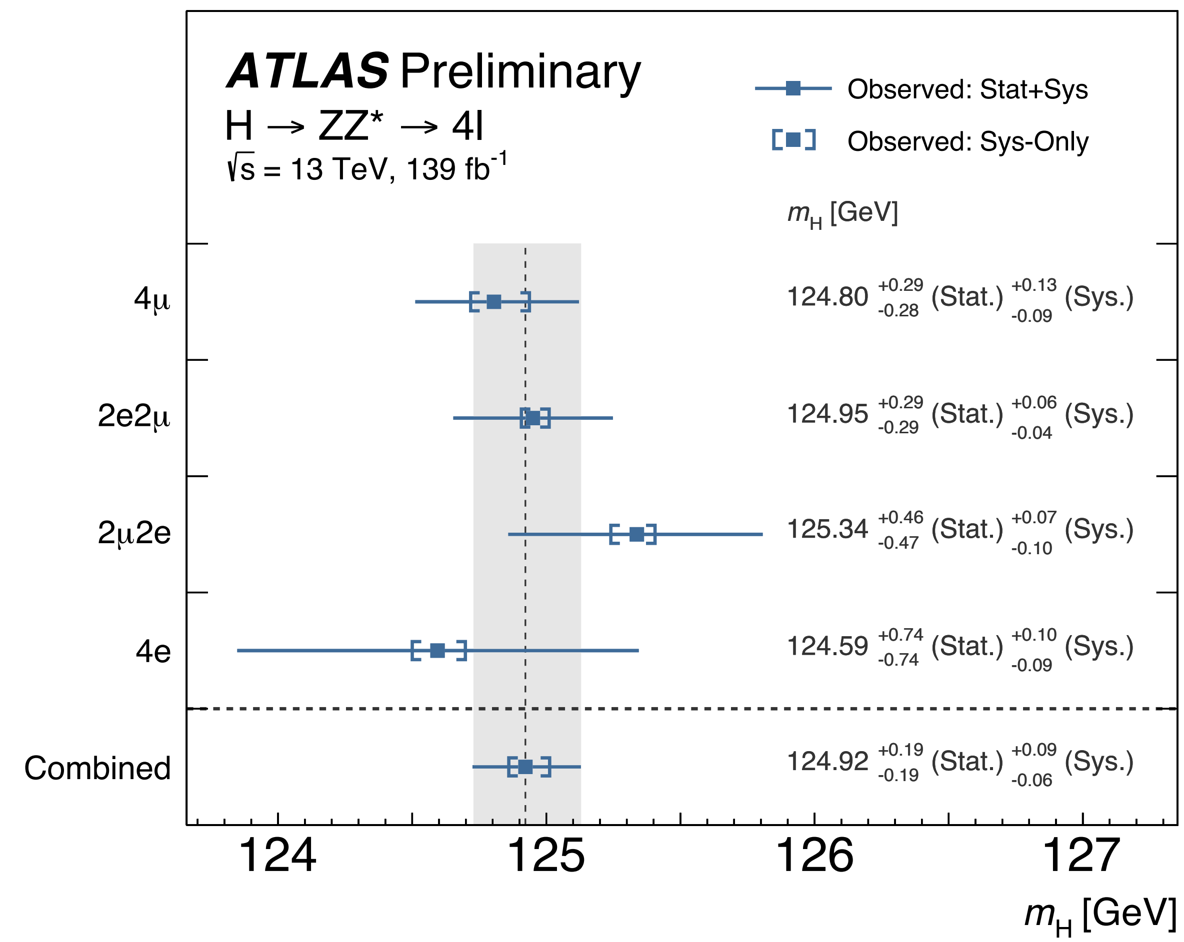

- ATLAS results: 200 MeV total, systematic uncertainty of ~70 MeV

Systematic Uncertainty	Impact (GeV)
Muon momentum scale	+0.08, −0.06
Electron energy scale	±0.02
Muon momentum resolution	±0.01
Muon sagitta bias correction	±0.01

$$m_H = 124.92^{+0.21}_{-0.20}\ \text{GeV}$$

Conclusion

- Higgs physics provide an excellent picture for
  - m_H one of the most precise measurements in the LHC scientific program.
  - High precision by ATLAS and CMS on m_H achieved by:

    (i) Deep understanding our detector at the per-mille level and

    (ii) Developing *smart* techniques for best usage of this understanding within the data analysis.
- After a decade of cracking the mass problem:

1. Measurement of m_H at the sub per mille precision level.
2. Clear understanding of our detectors performance on new resonance.

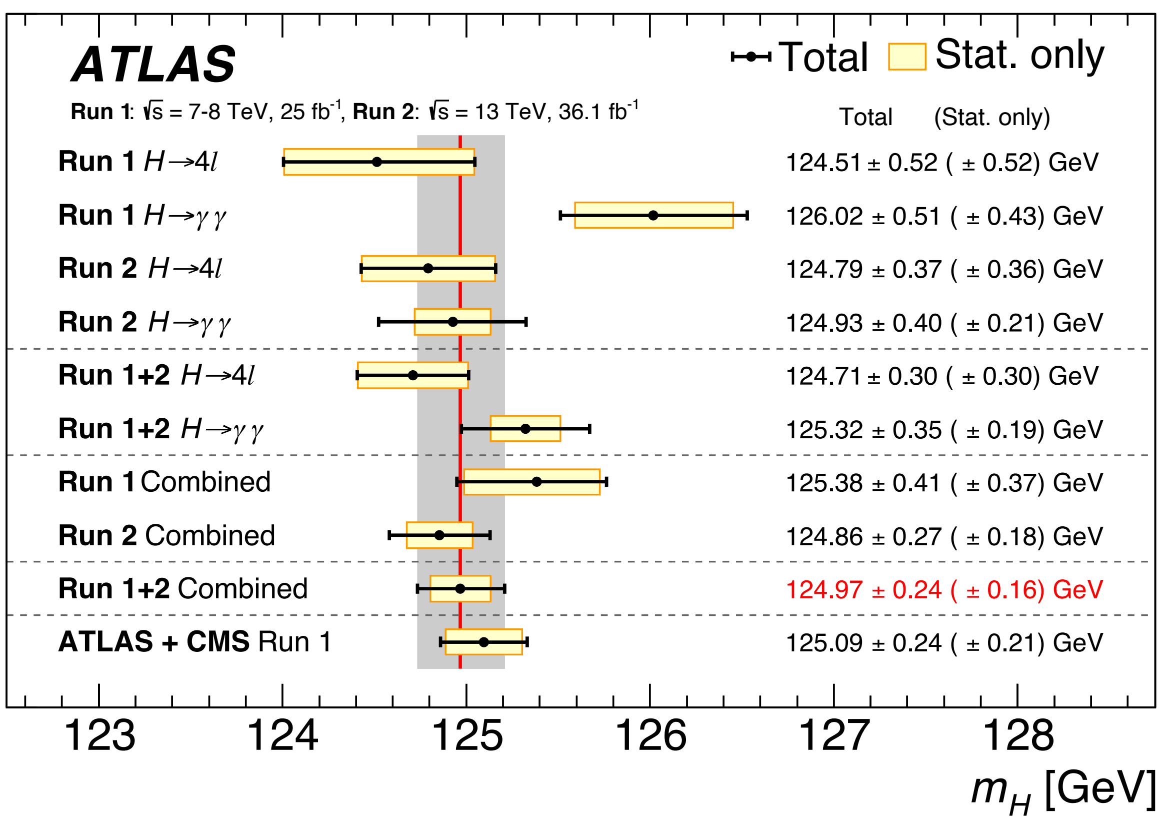

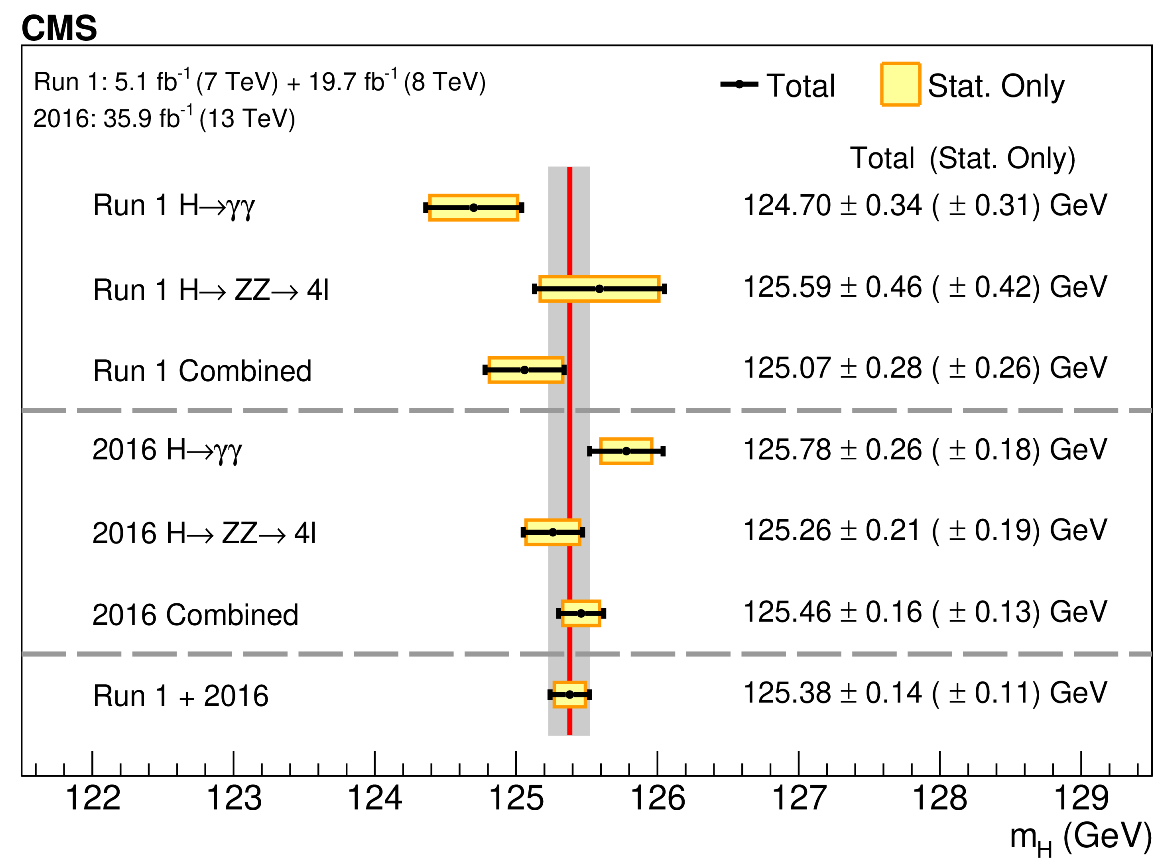

Additional material

Improve everywhere

- Three-prong approach to reduce uncertainty at analysis level:
  - (i) (~15%) from m_{12} constraint to m_Z with kinematic fit and m_Z constraints on alignment weak modes.
  - (i) (~2%) from kinematic discriminant selecting signal and background events
    - Boosted Decision Tree on $p_T(4\ell)$, $y(4\ell)$ (ATLAS) and $\log(|\mathscr{M}_H|^2/|\mathscr{M}_{ZZ*}|^2)$ (ATLAS and CMS).
  - (ii) (2-3% - 11%) from multivariate per-event resolution likelihood.
    - Neural network to solve uncertainty correlations induced by kinematic discriminant.

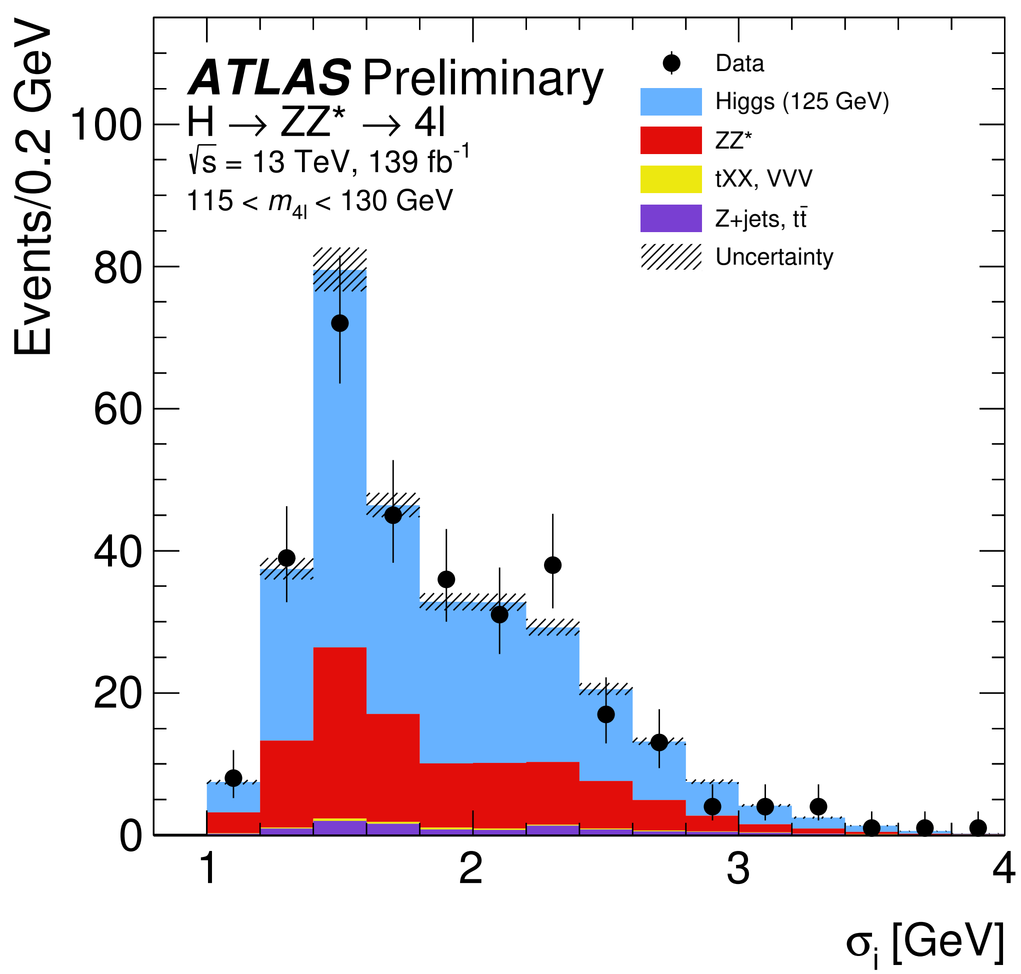

Neural network output of the event's uncertainty

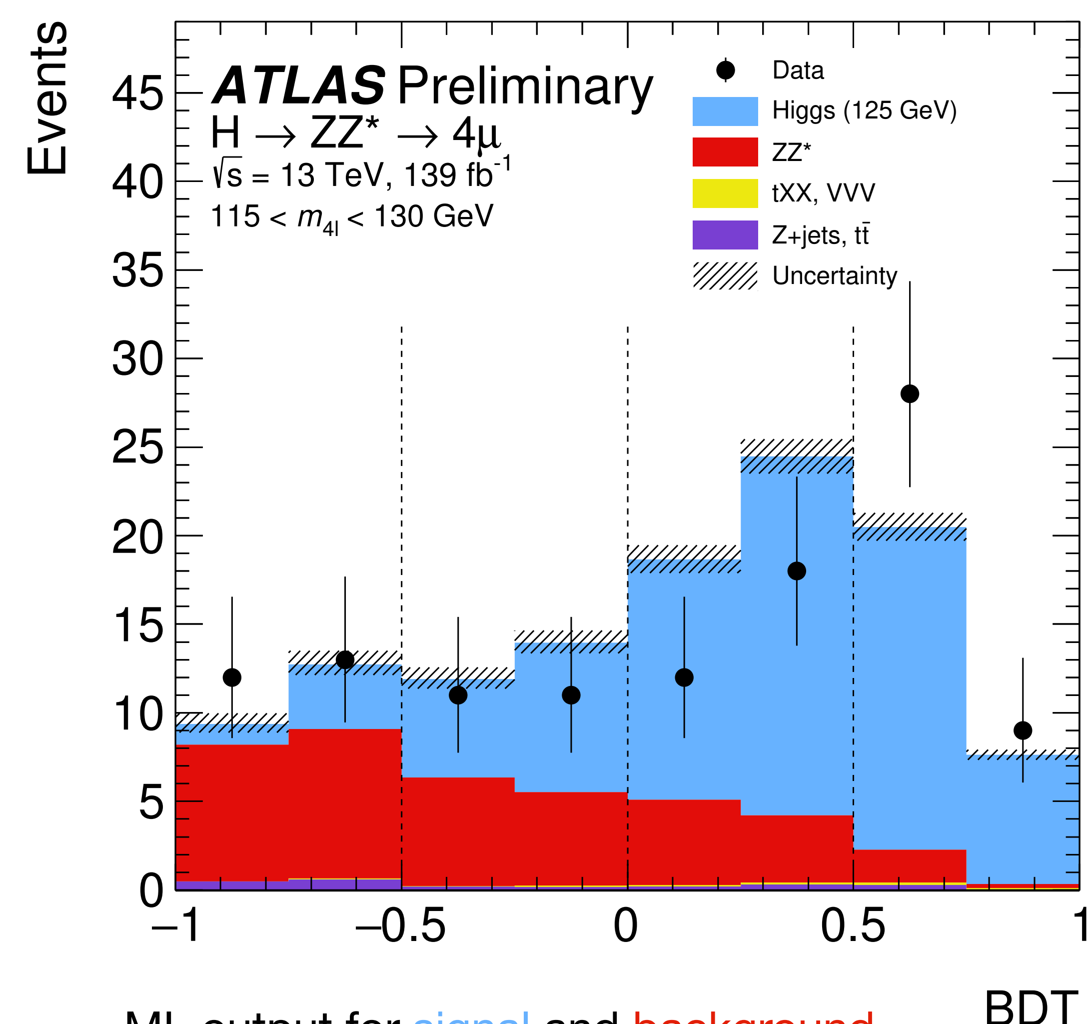

ML output for signal and background

- $H \to \gamma\gamma$ updated result at Run II. arXiv:1806.00242
  - Analytical function in kinematic and detector categories.
  - Reduction of uncertainty through categorisation of events as a function of resolution and signal significance.
- Expected statistical uncertainty of 0.21 GeV and 0.34 GeV systematic uncertainty

$$m_H^{\gamma\gamma} = 124.93 \pm 0.40\ (\pm 0.21\ \text{stat only})\ \text{GeV}$$

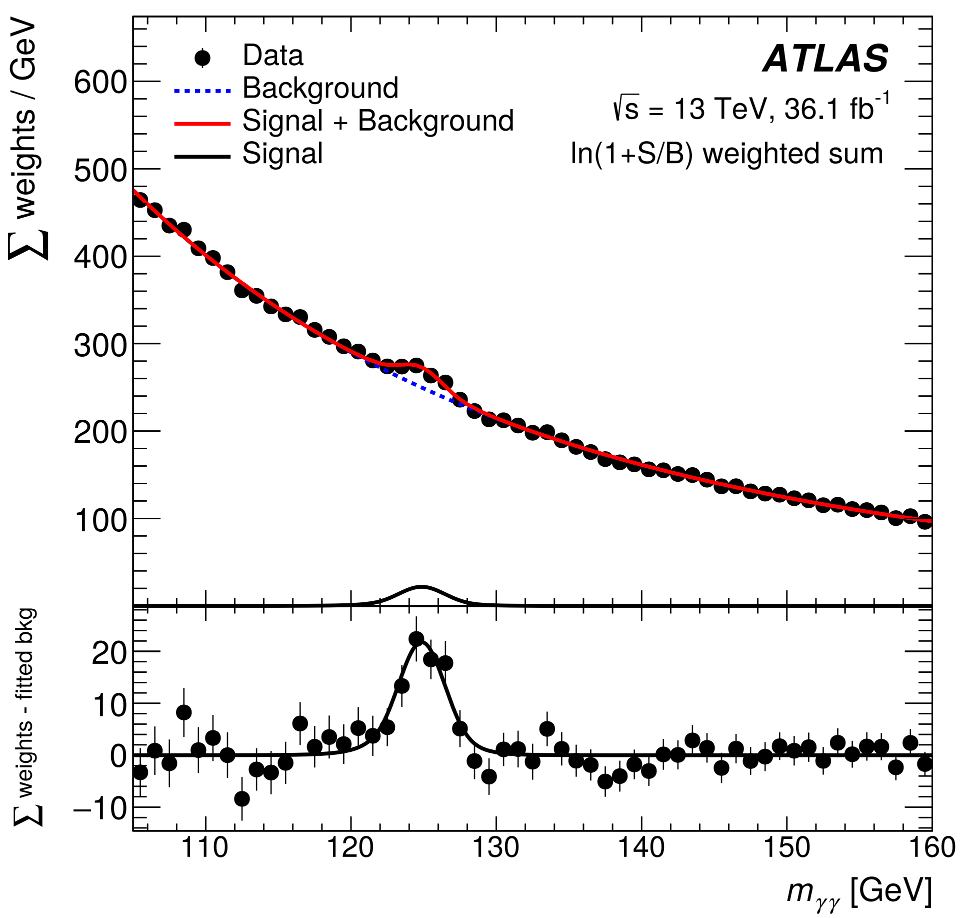

Source	Systematic uncertainty in m_H [MeV]
EM calorimeter response linearity	60
Non-ID material	55
EM calorimeter layer intercalibration	55
$Z \to ee$ calibration	45
ID material	45
Lateral shower shape	40
Muon momentum scale	20
Conversion reconstruction	20
$H \to \gamma\gamma$ background modelling	20
$H \to \gamma\gamma$ vertex reconstruction	15
e/γ energy resolution	15
All other systematic uncertainties	10

- $H \to \gamma\gamma$ updated result at Run II.

arXiv:1806.00242

  - Analytical function in kinematic and detector categories.
  - Reduction of uncertainty through categorisation of events as a function of resolution and signal significance.

- Expected statistical uncertainty of 0.21 GeV and 0.34 GeV systematic uncertainty

$$m_H^{\gamma\gamma} = 124.93 \pm 0.40\ (\pm 0.21\ \text{stat only})\ \text{GeV}$$

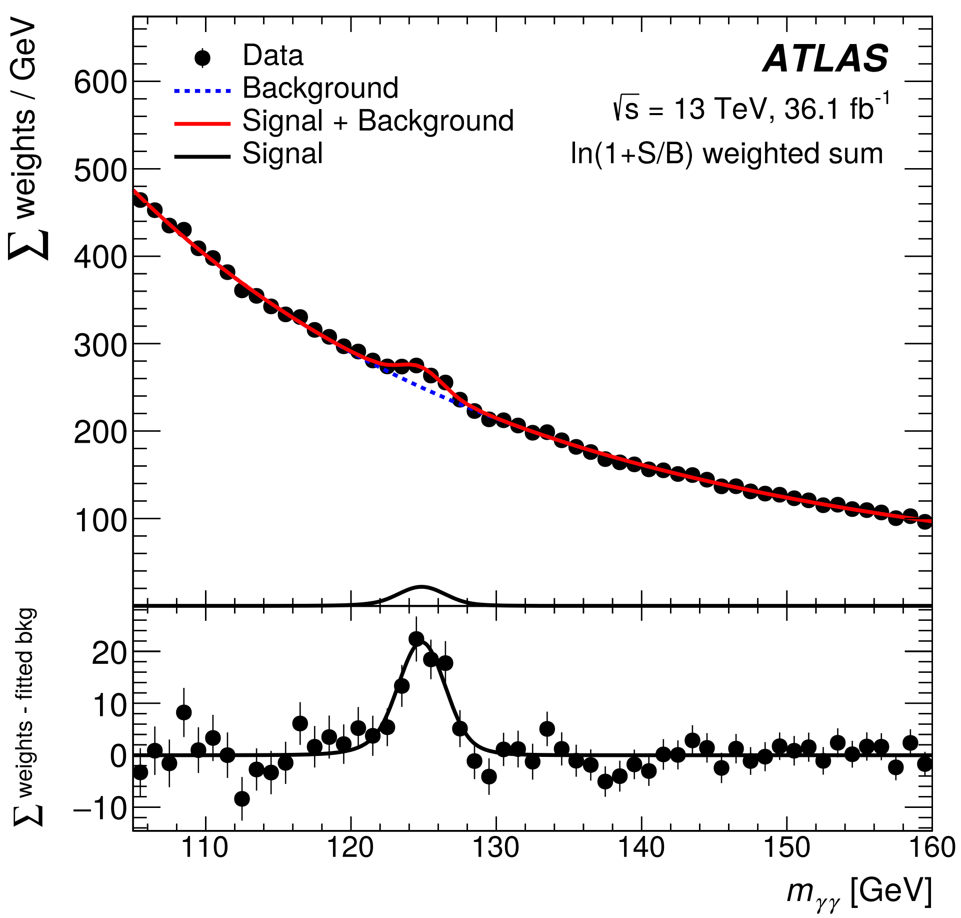

Source	Systematic uncertainty in m_H [MeV]
EM calorimeter response linearity	60
Non-ID material	55
EM calorimeter layer intercalibration	55
$Z \to ee$ calibration	45
ID material	45
Lateral shower shape	40
Muon momentum scale	20
Conversion reconstruction	20
$H \to \gamma\gamma$ background modelling	20
$H \to \gamma\gamma$ vertex reconstruction	15
e/γ energy resolution	15
All other systematic uncertainties	10

- Good energy calibration necessary for increased precision on m_H
  - Two step approach: i) material energy loss and ii) global calorimetric scale from $Z \to ee$ data
- Total scale uncertainty of at 40 GeV at the per-mille level.

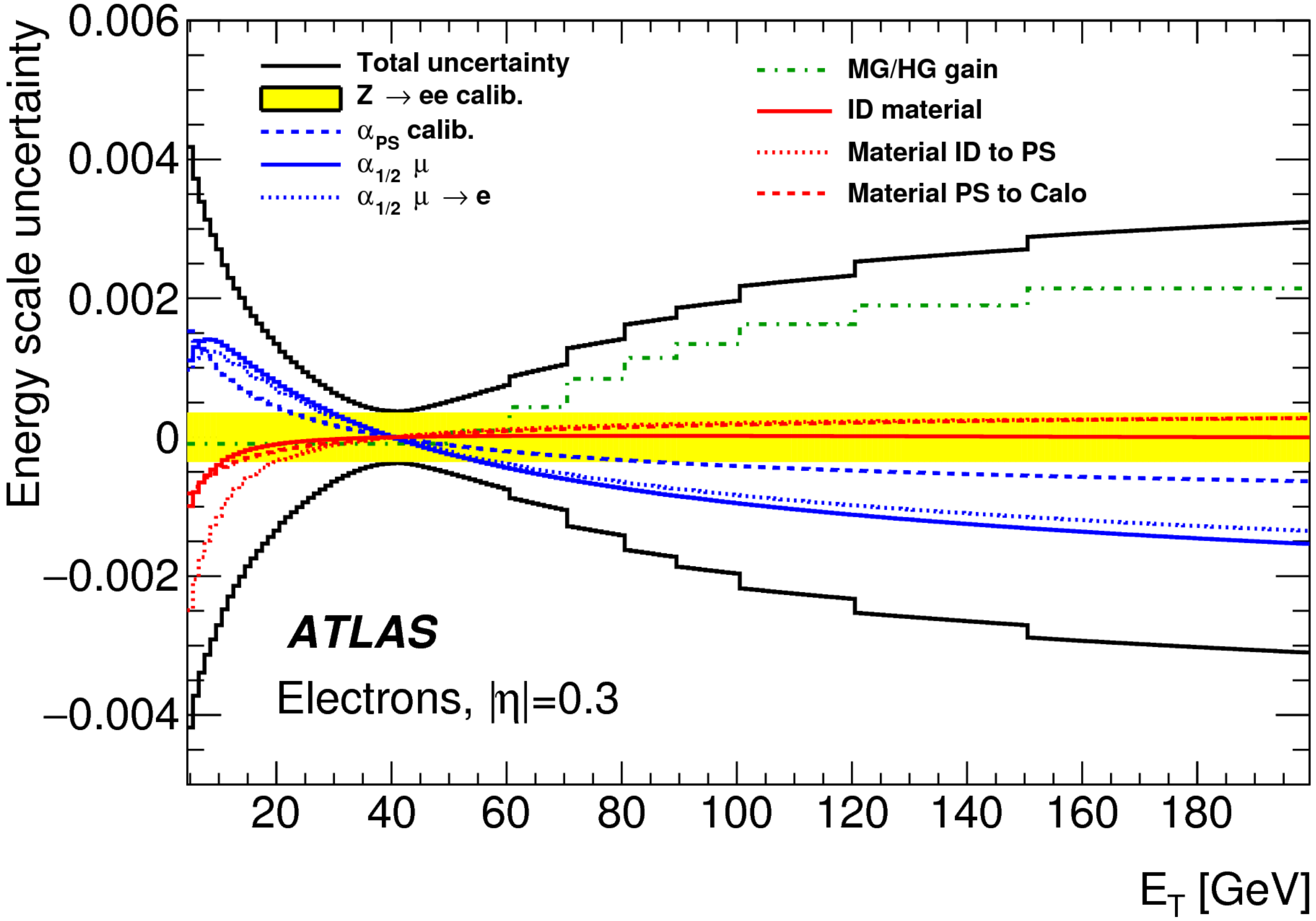

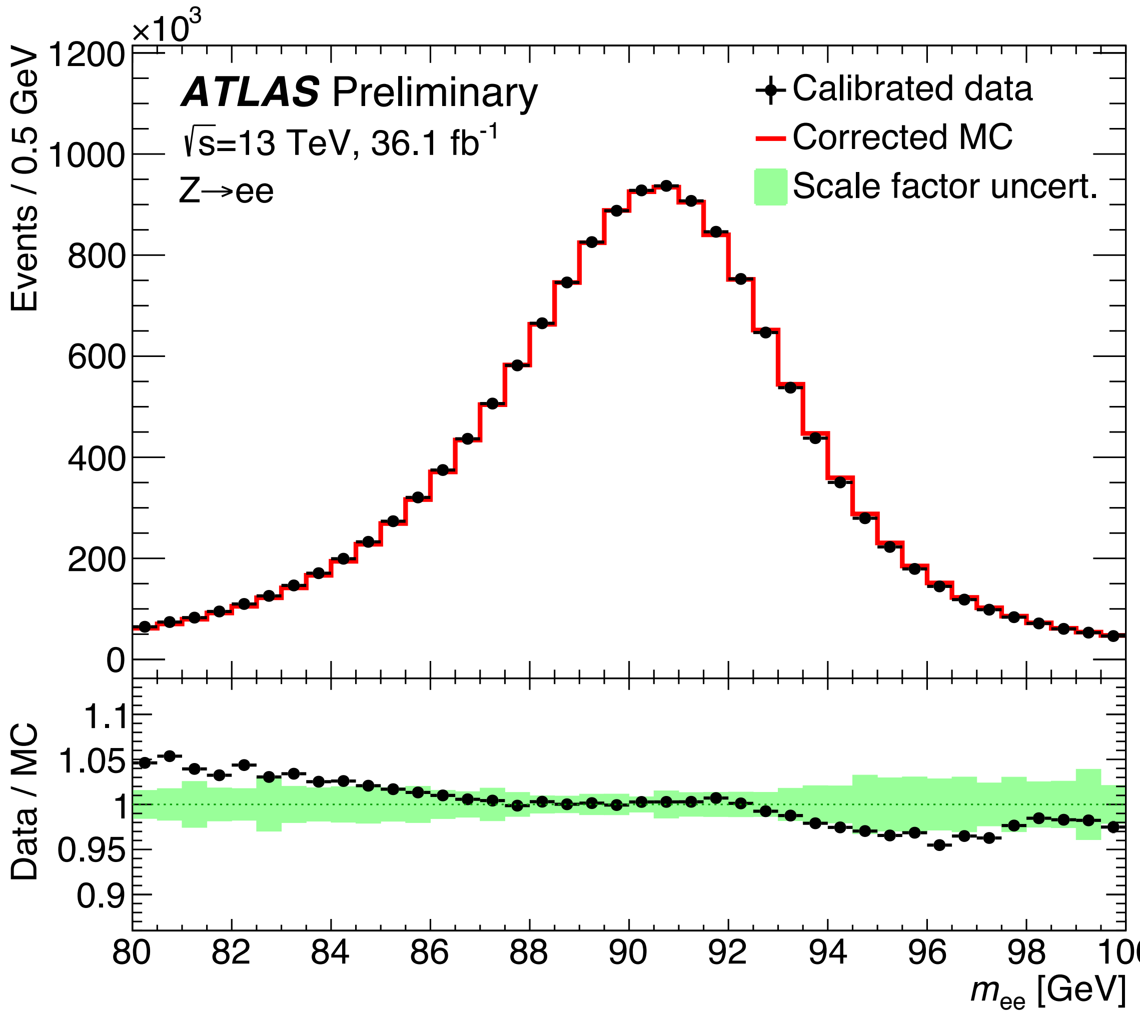

$E_T(e/\gamma)$ resolution

- Good energy calibration necessary for increased precision on m_H
  - Two step approach: i) material energy loss and ii) global calorimetric scale from $Z \to ee$ data
- Total scale uncertainty of at 40 GeV at the per-mille level.

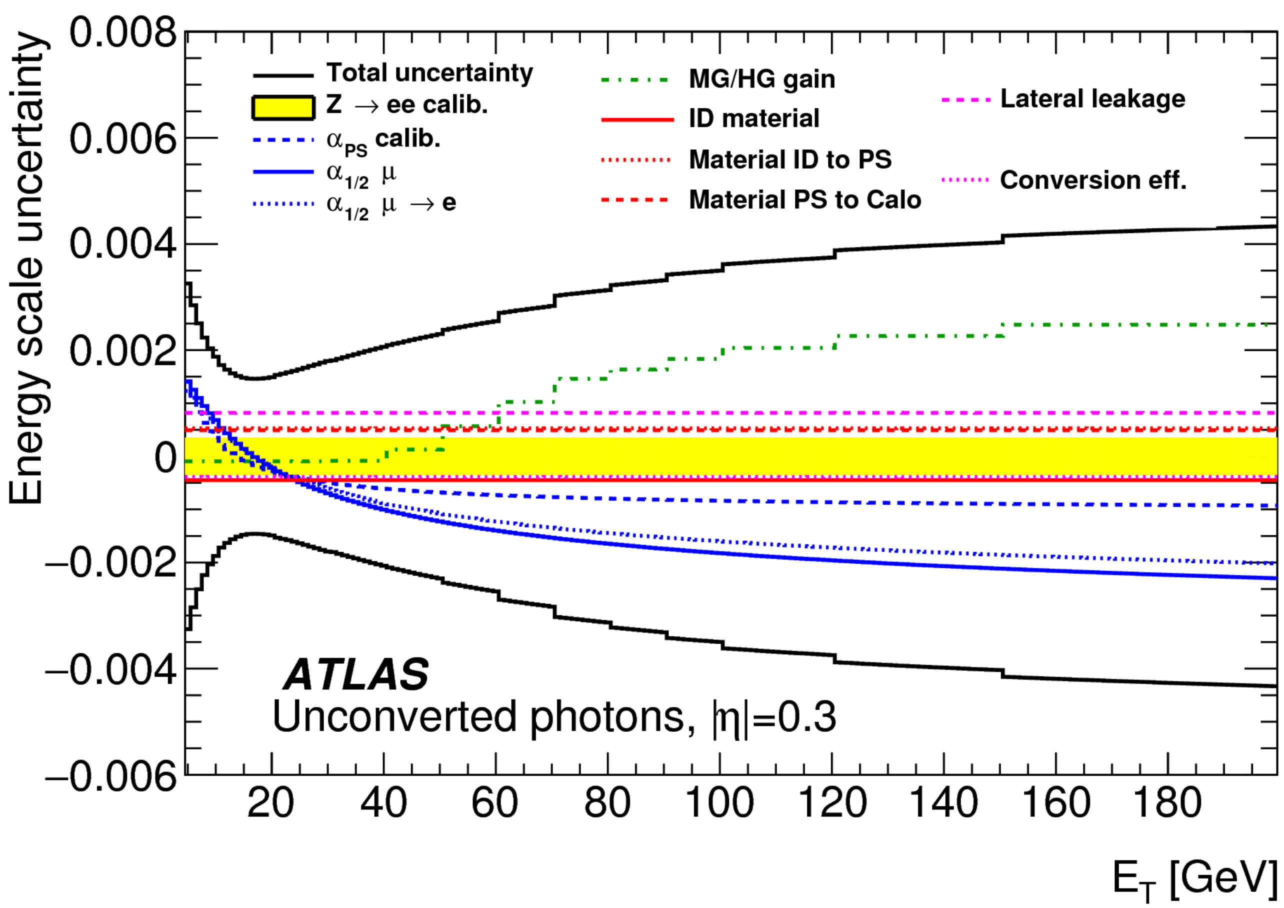

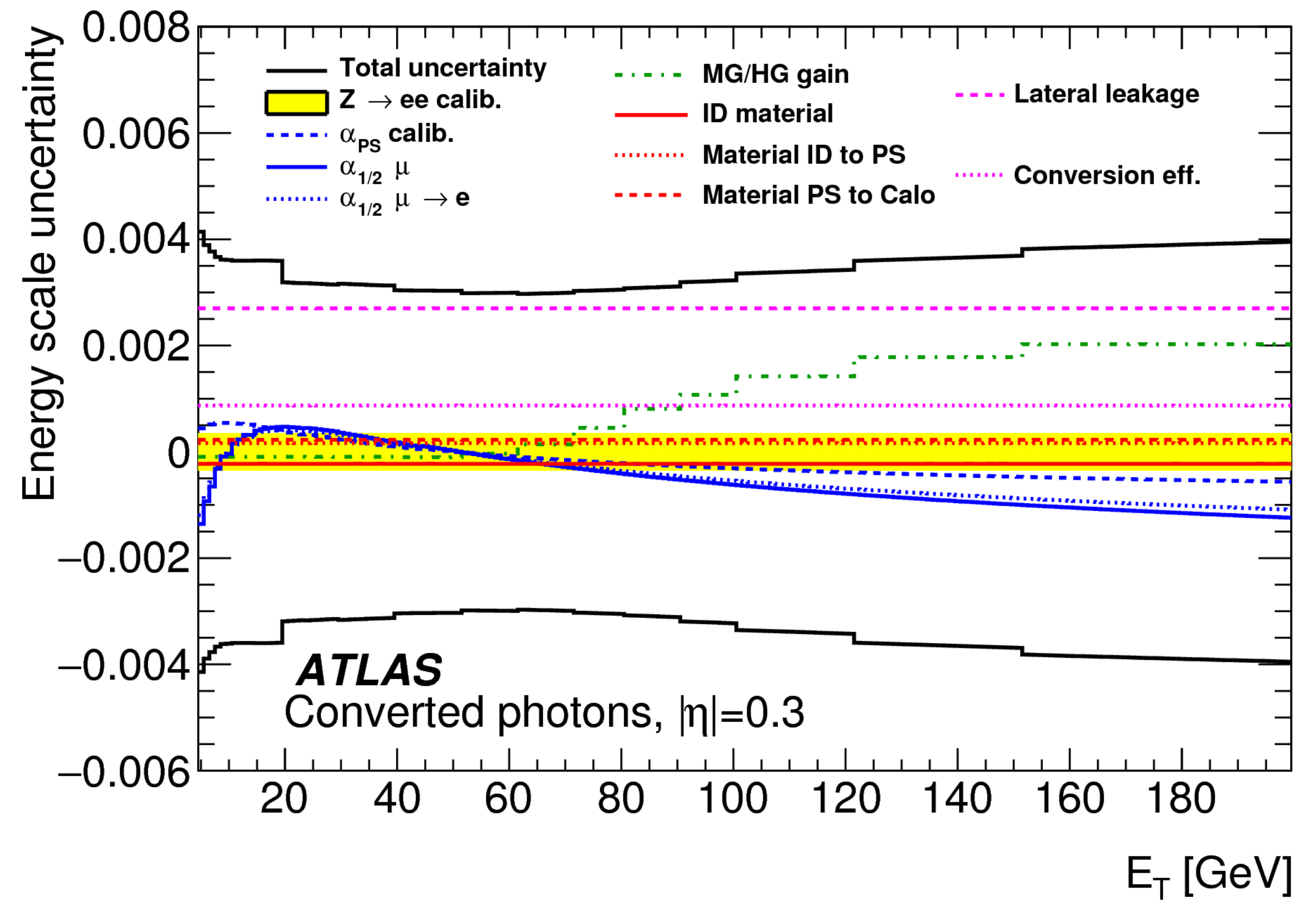

Run I status

- ATLAS run I precision on m_H of 0.33%
  - combined measurement from $H\to\gamma\gamma$ and $H\to ZZ^*\to 4\ell$.

Channel	Mass measurement [GeV]
$H\to\gamma\gamma$	$125.98 \pm 0.42\,(\text{stat}) \pm 0.28\,(\text{syst}) = 125.98 \pm 0.50$
$H\to ZZ^*\to 4\ell$	$124.51 \pm 0.52\,(\text{stat}) \pm 0.06\,(\text{syst}) = 124.51 \pm 0.52$
Combined	$125.36 \pm 0.37\,(\text{stat}) \pm 0.18\,(\text{syst}) = 125.36 \pm 0.41$

  - For both channels dominated by statistical uncertainty

- At Run2 aim in improving significantly on δm_H:
  - Expect 7 times more candidates, with 139 fb^{-1} at $\sqrt{s}$=13 TeV

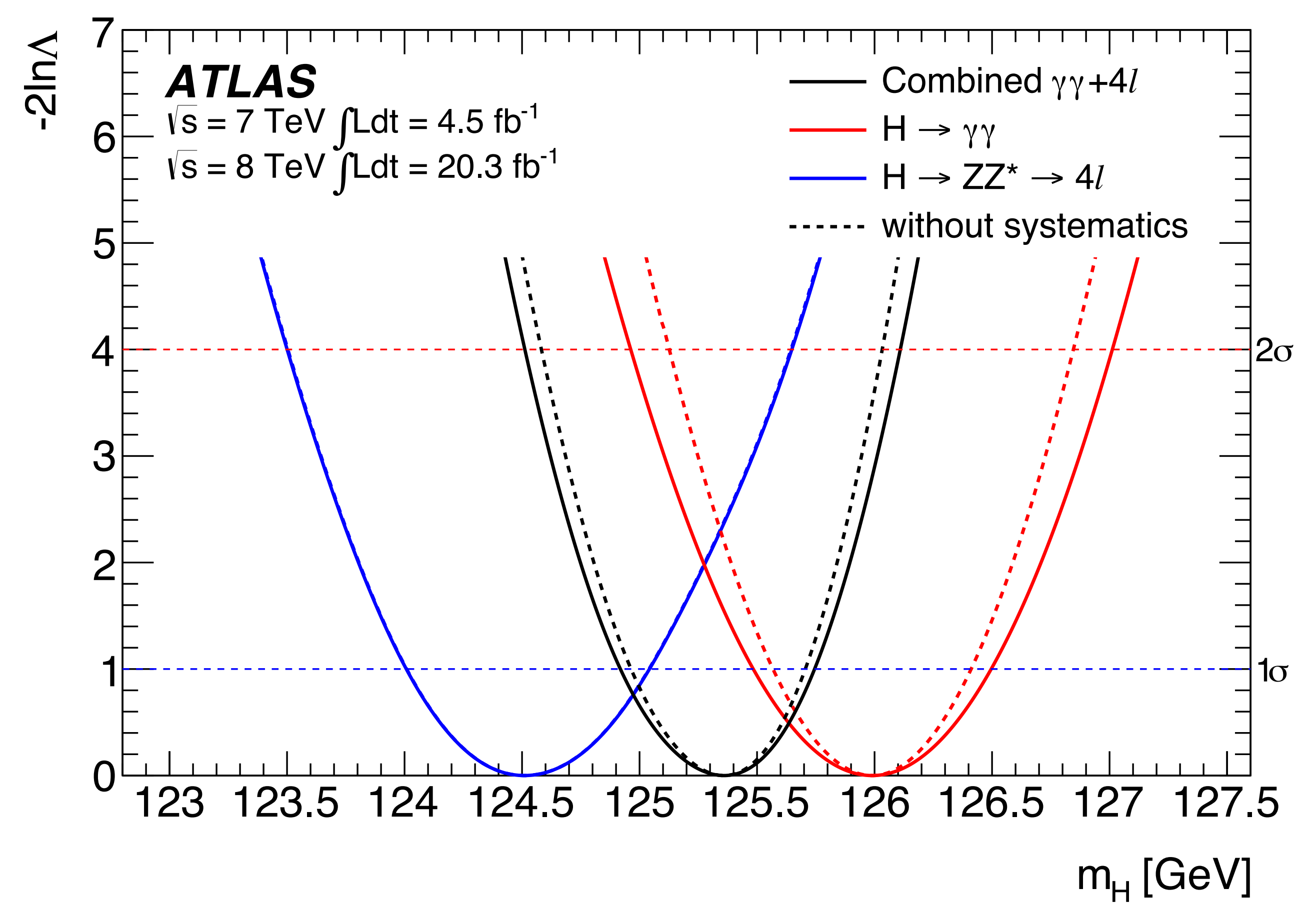

Run I Legacy

- Run-I featured *in primis* the discovery
  - First properties measurements
  - Programme largely limited by statistical accuracy.
- Properties:
  - ATLAS precision in m_H of 0.33%:
  - Couplings measured to 10% to 25% precision
  - $H \to \mathrm{inv.}$ constrained to < 30%
  - First studies of $J^{PC} = 0^{++}$, (indirect) width $\Gamma_H < 14.4$ MeV (15.2 MeV)

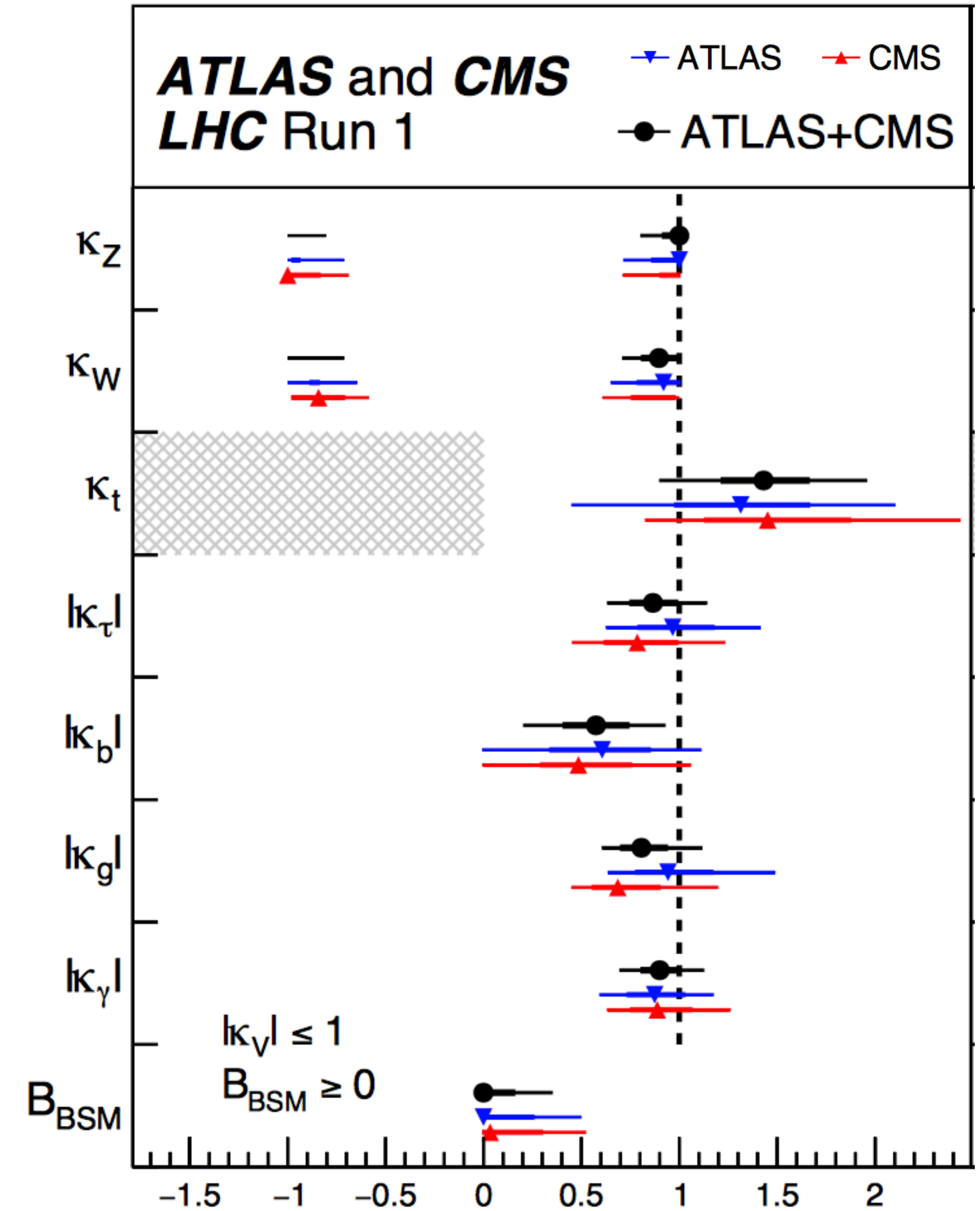

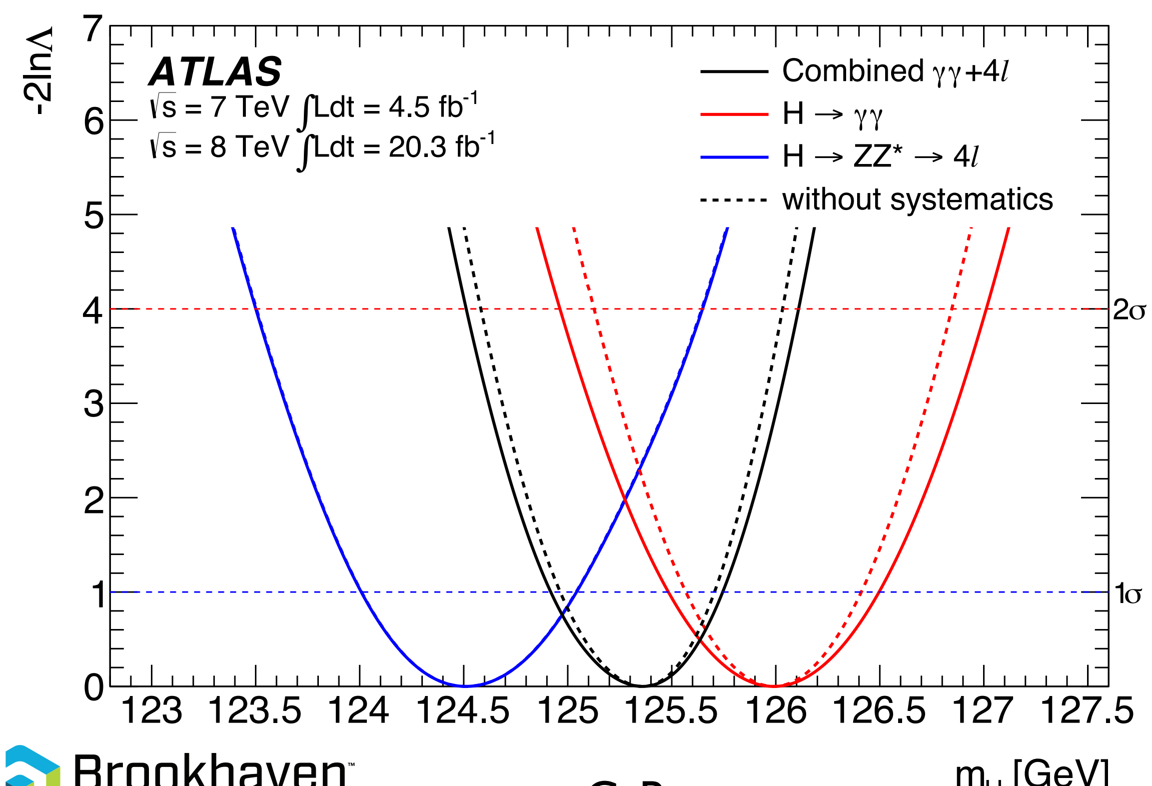

Channel	Mass measurement [GeV]
$H \to \gamma\gamma$	$125.98 \pm 0.42\,(\mathrm{stat}) \pm 0.28\,(\mathrm{syst}) = 125.98 \pm 0.50$
$H \to ZZ^* \to 4\ell$	$124.51 \pm 0.52\,(\mathrm{stat}) \pm 0.06\,(\mathrm{syst}) = 124.51 \pm 0.52$
Combined	$125.36 \pm 0.37\,(\mathrm{stat}) \pm 0.18\,(\mathrm{syst}) = 125.36 \pm 0.41$

arXiv:1806.00242

- $H \to \gamma\gamma$ updated result at Run II.
  - Analytical function in kinematic and detector categories.
  - Reduction of uncertainty through categorisation of events as a function of resolution and signal significance.
- Expected statistical uncertainty of 0.21 GeV and 0.34 GeV systematic uncertainty

$$m_H^{\gamma\gamma} = 124.93 \pm 0.40\ (\pm 0.21 \text{ stat only})\ \text{GeV}$$

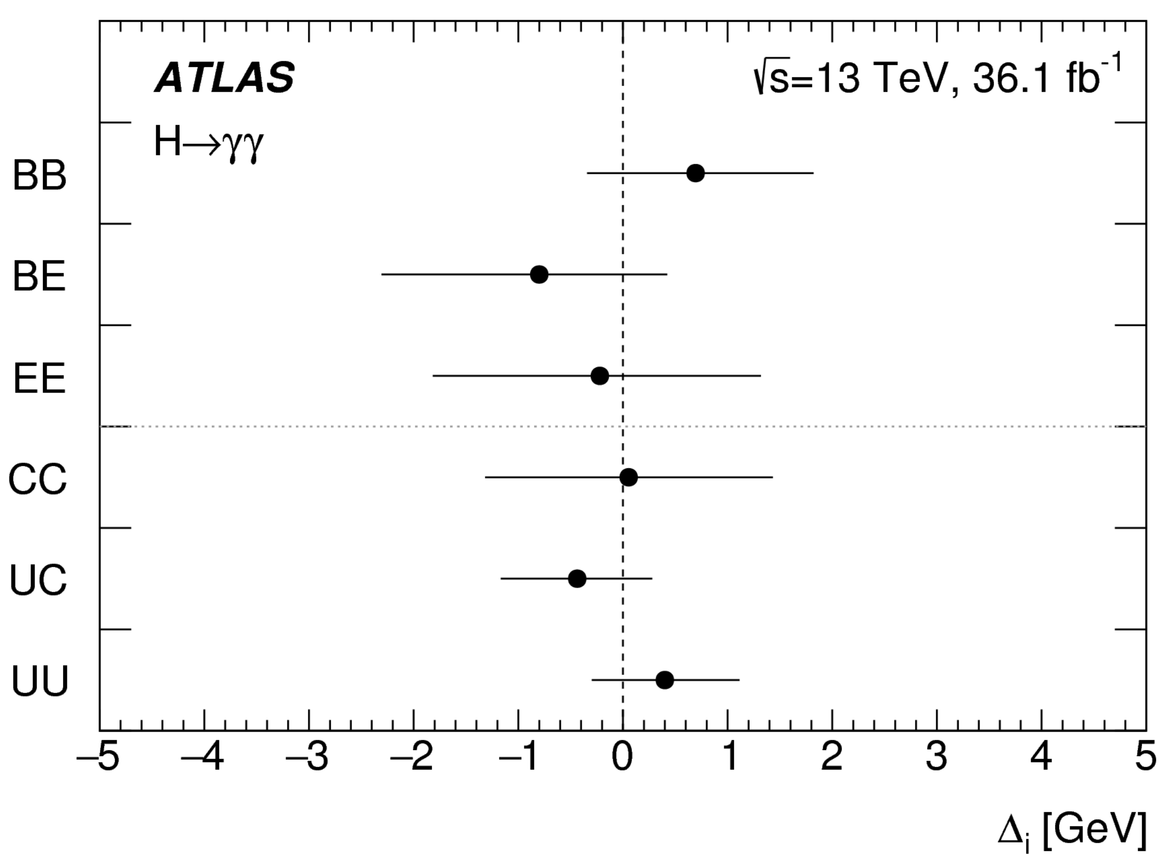

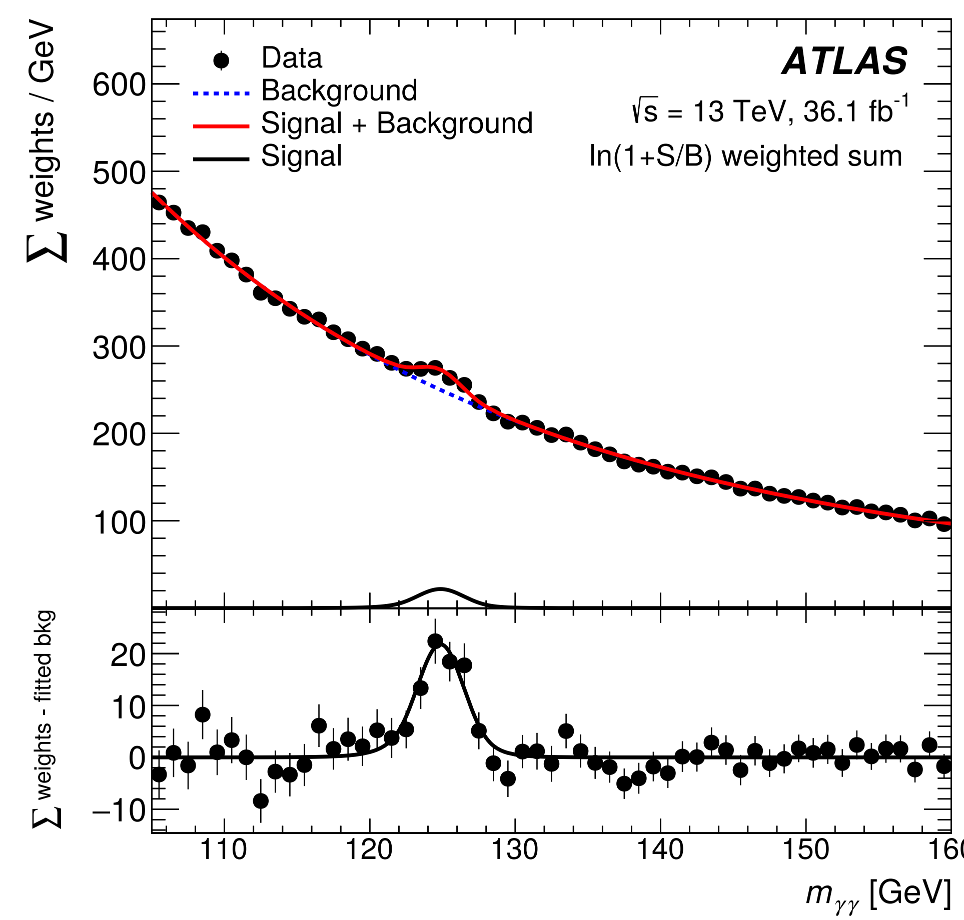

Object selection

- Electrons (e).
  - Isolated objects clustered from calorimeter energy deposits with associated ID track.
  - E_T > 7 GeV, $|\eta|$ < 2.47 and $|z_0 \sin(\vartheta)|$ < 0.5 mm

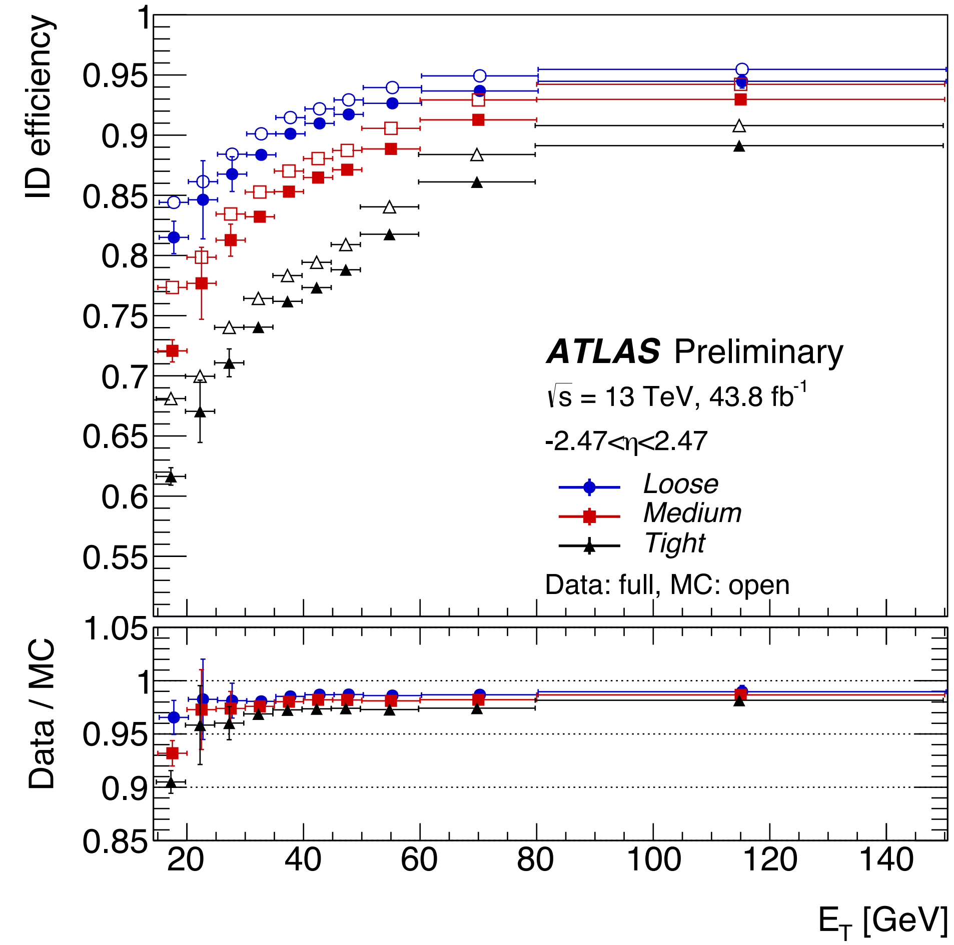

- Muons (μ).
  - Combined track fit of Inner Detector and Muon Spectrometer hits,
  - p_T > 5 GeV, $|\eta|$ < 2.7 $|z_0 \sin(\vartheta)|$ < 0.5 mm of "loose or medium quality"
  - Isolated objects

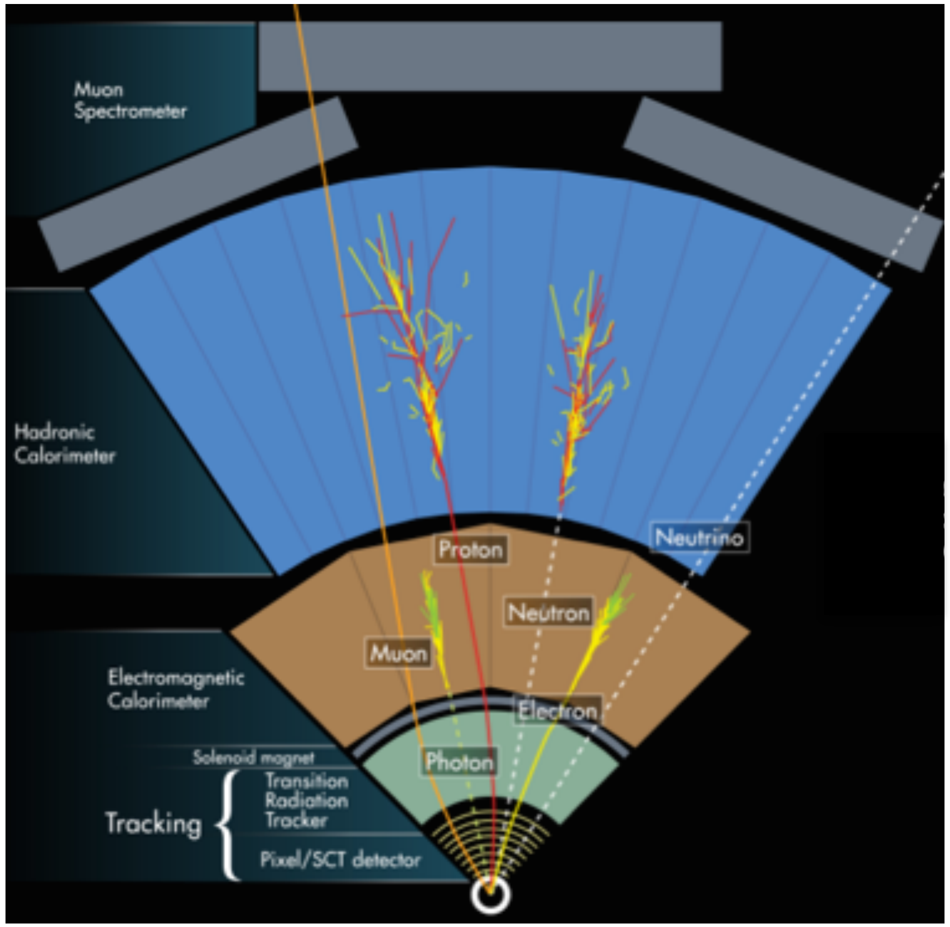

- Missing transverse energy (E_T^{miss}).
  - Inferred from transverse momentum imbalance

Object selection

- Electrons (e).
  - Isolated objects clustered from calorimeter energy deposits with associated ID track.
  - $E_T > 7$ GeV, $|\eta| < 2.47$ and $|z_0 \sin(\vartheta)| < 0.5$ mm

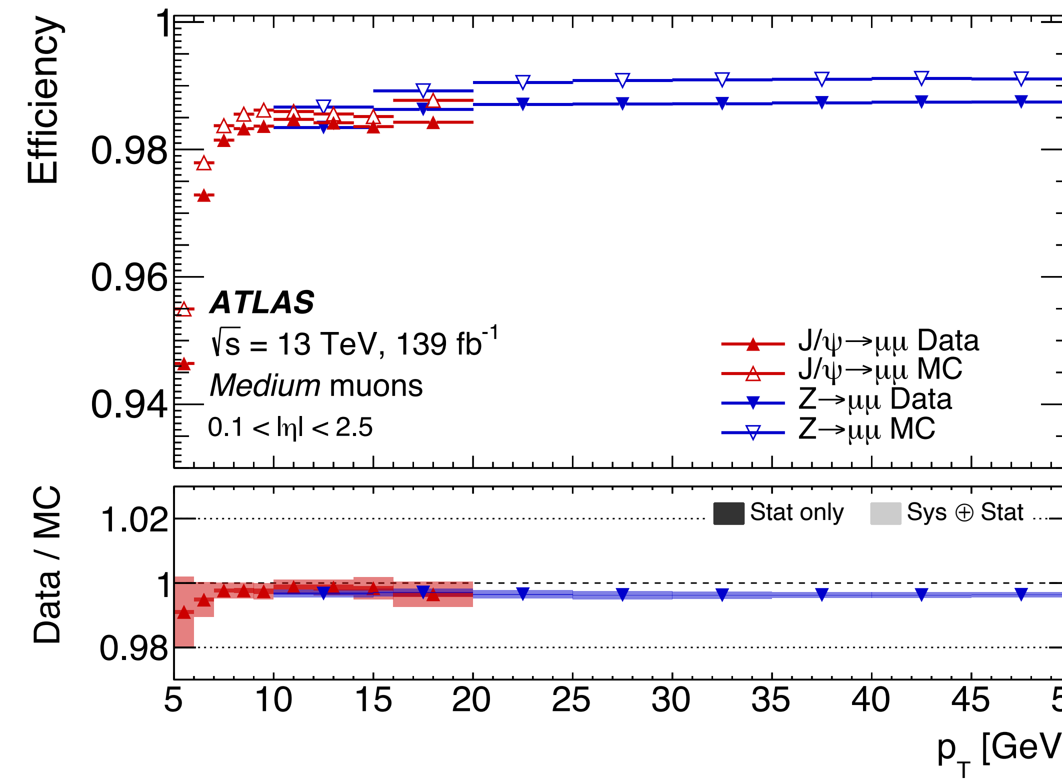

- Muons (μ).
  - Combined track fit of Inner Detector and Muon Spectrometer hits,
  - $p_T > 5$ GeV, $|\eta| < 2.7$ $|z_0 \sin(\vartheta)| < 0.5$ mm of "loose or medium quality"
  - Isolated objects

- Jets (j).
  - Energy deposit grouping with *infra*-red safe algorithm:
  - $p_T > 25$ GeV and $|\eta| < 4.5$
    - ✦ Clustering with anti-k_T, $R=0.4$

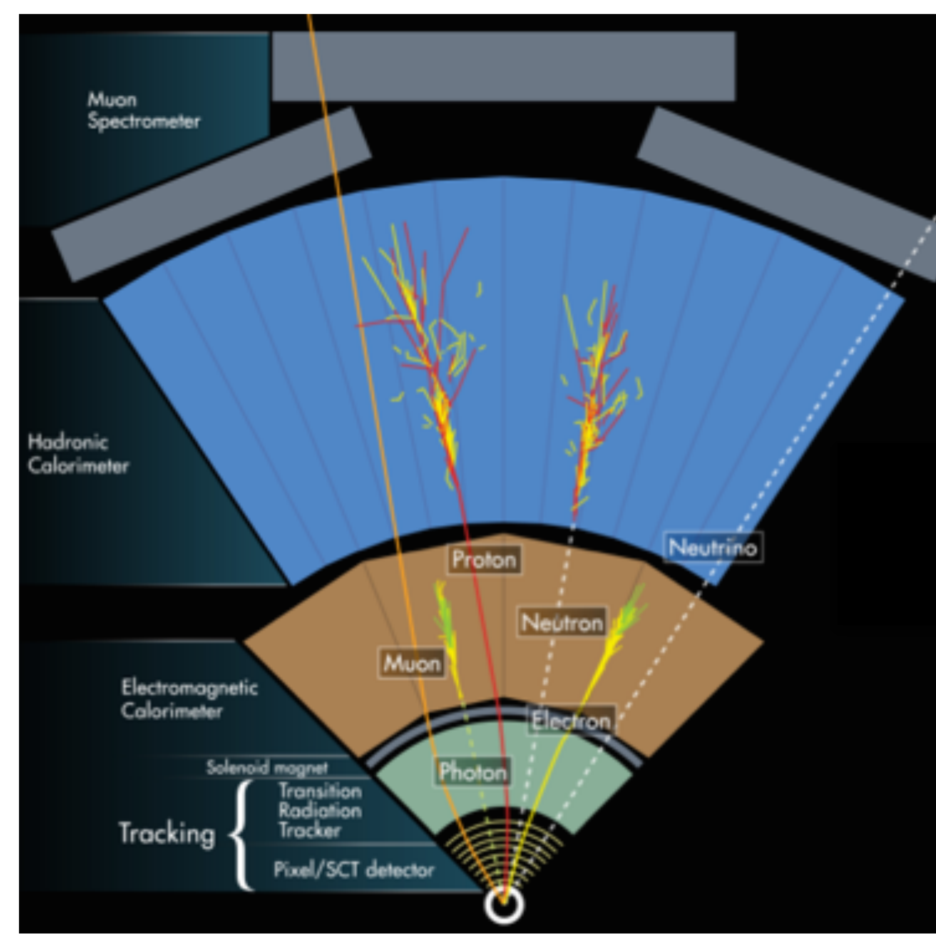

Object selection

- Electrons (e).
  - Isolated objects clustered from calorimeter energy deposits with associated ID track.
  - $E_T > 7$ GeV, $|\eta| < 2.47$ and $|z_0 \sin(\vartheta)| < 0.5$ mm

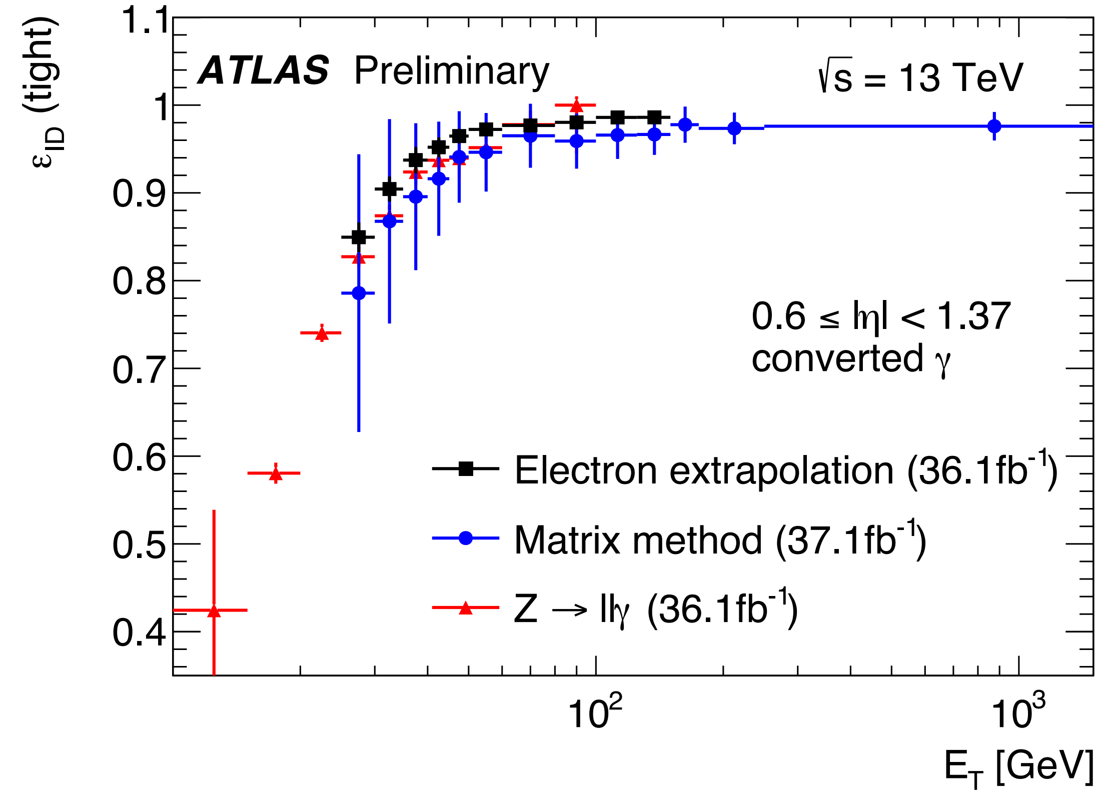

- Muons (μ).
  - Combined track fit of Inner Detector and Muon Spectrometer hits,
  - $p_T > 5$ GeV, $|\eta| < 2.7$ $|z_0 \sin(\vartheta)| < 0.5$ mm of "loose or medium quality"
  - Isolated objects

- Photons (γ).
  - Clustering of calorimeter energy deposits.
  - Identified with rectangular cuts on shower shapes.

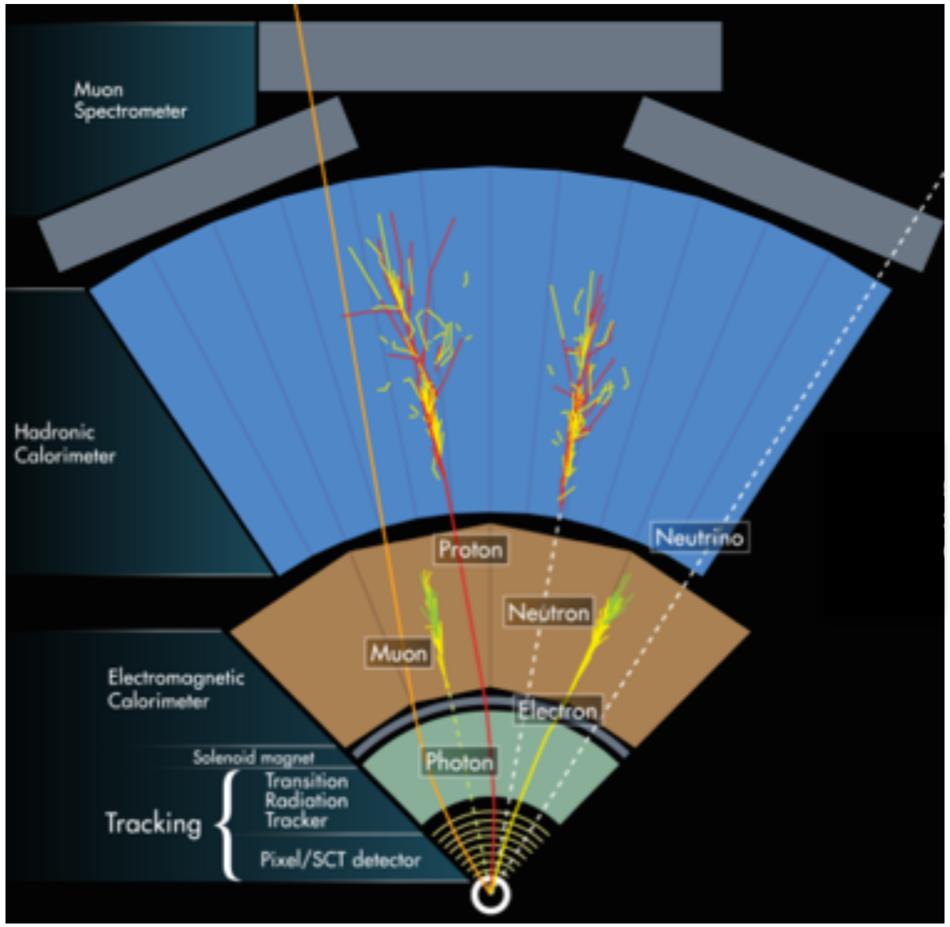

Object selection

- Electrons (e).
  - Isolated objects clustered from calorimeter energy deposits with associated ID track.
  - E_T > 7 GeV, $|\eta|$ < 2.47 and $|z_0 \sin(\vartheta)|$ < 0.5 mm

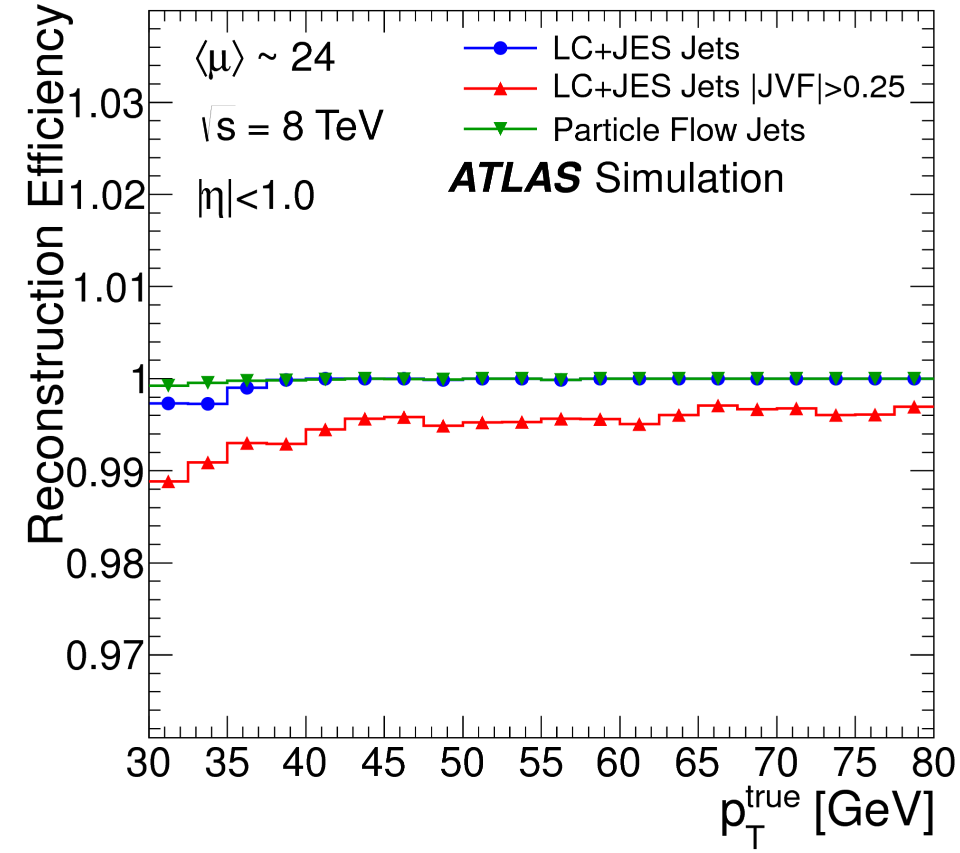

- Muons (μ).
  - Combined track fit of Inner Detector and Muon Spectrometer hits,
  - p_T > 5 GeV, $|\eta|$ < 2.7 $|z_0 \sin(\vartheta)|$ < 0.5 mm of "loose or medium quality"
  - Isolated objects

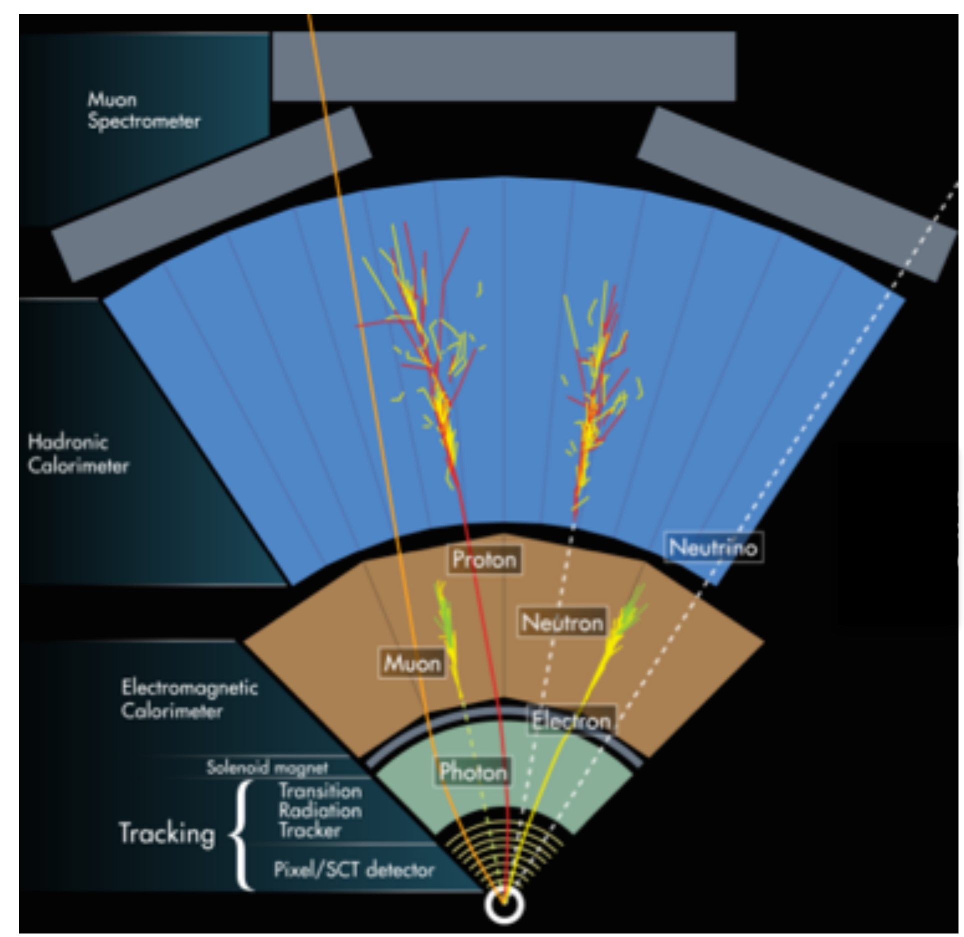

- Jets (j).
  - Energy deposit grouping with *infra*-red safe algorithm:
  - p_T > 25 GeV and $|\eta|$ < 4.5
    - ✦ Clustering with anti-k_{T}, R=0.4

Muon p_T resolution

- Resolution muon channels (4μ, 2e2μ and 4μ) crucial for m_H uncertainty:
  - Excellent momentum resolution of about 1% at about p_T 45 ~GeV.
- Momenta calibrated to J/ψ and Z samples in data
  - for residual mis modelling of E^{loss} in calorimeters, alignment precision etc.
  - Including corrections to data accounting for alignment weak modes.
  - Precision down to 0.5 per mille for |η|<1.0

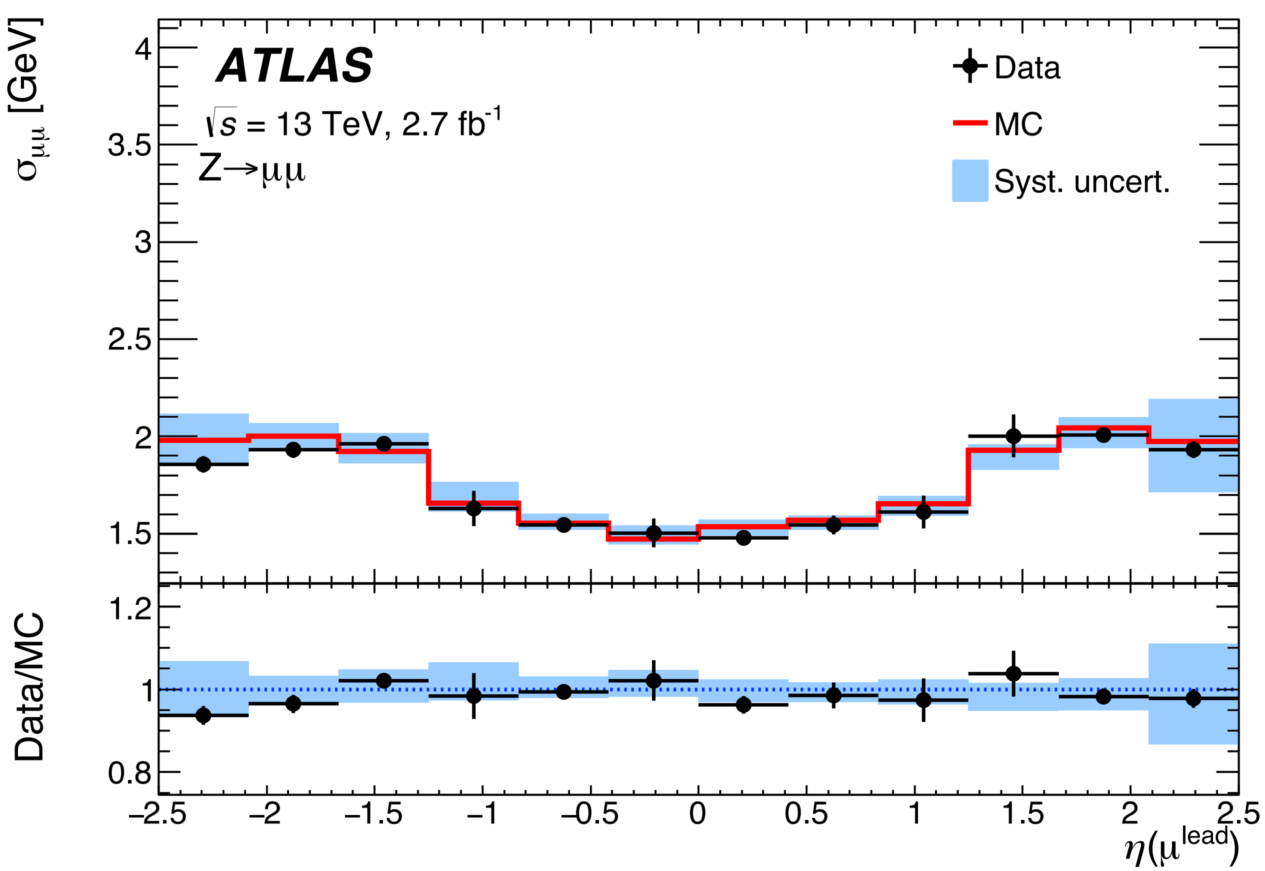

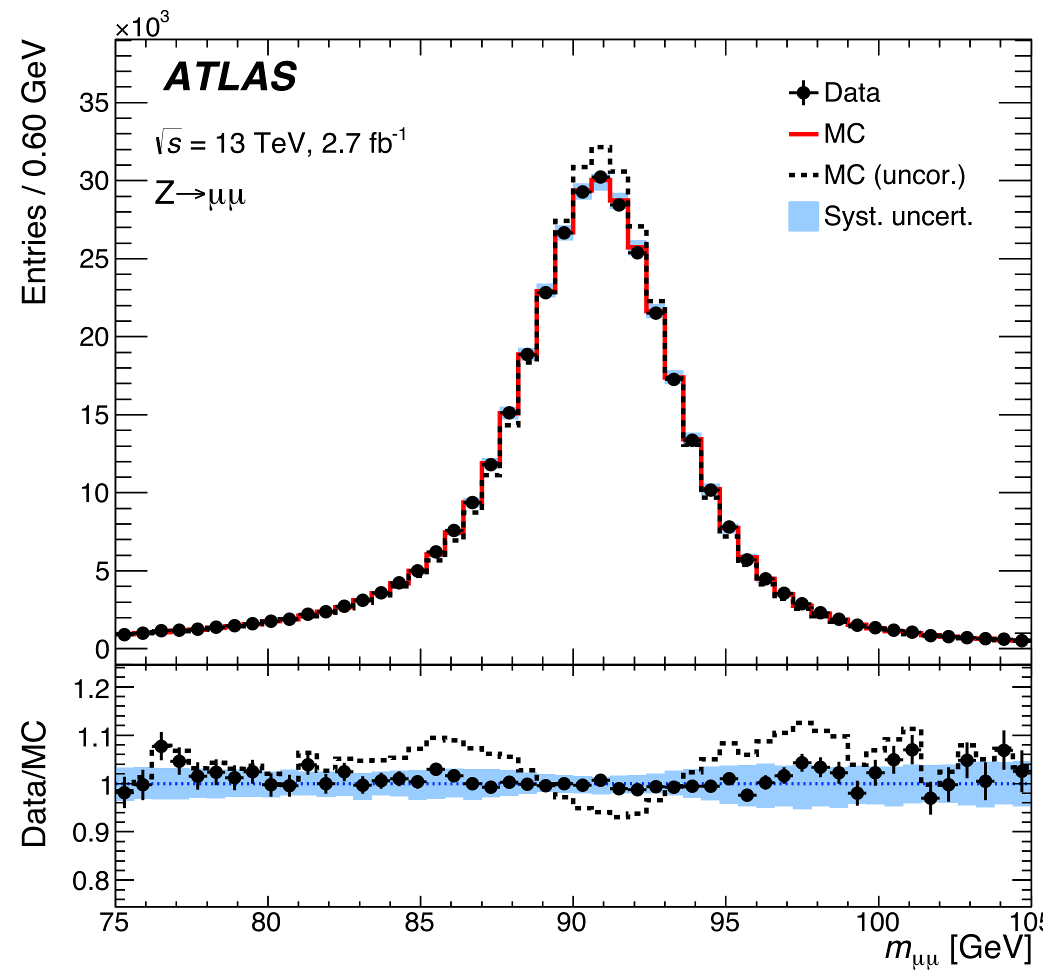

Muon p_T resolution

- Resolution muon channels (4μ, 2e2μ and 4μ) crucial for m_H uncertainty:
  - Excellent momentum resolution of about 1% at about p_T 45 ~GeV.
- Simulated momenta calibrated to J/ψ and Z samples in data
  - for residual mis modelling of E^{loss} in calorimeters, alignment precision etc.
  - Uncertainty of about 10% on the resolution and 0.5% on the momentum scale.

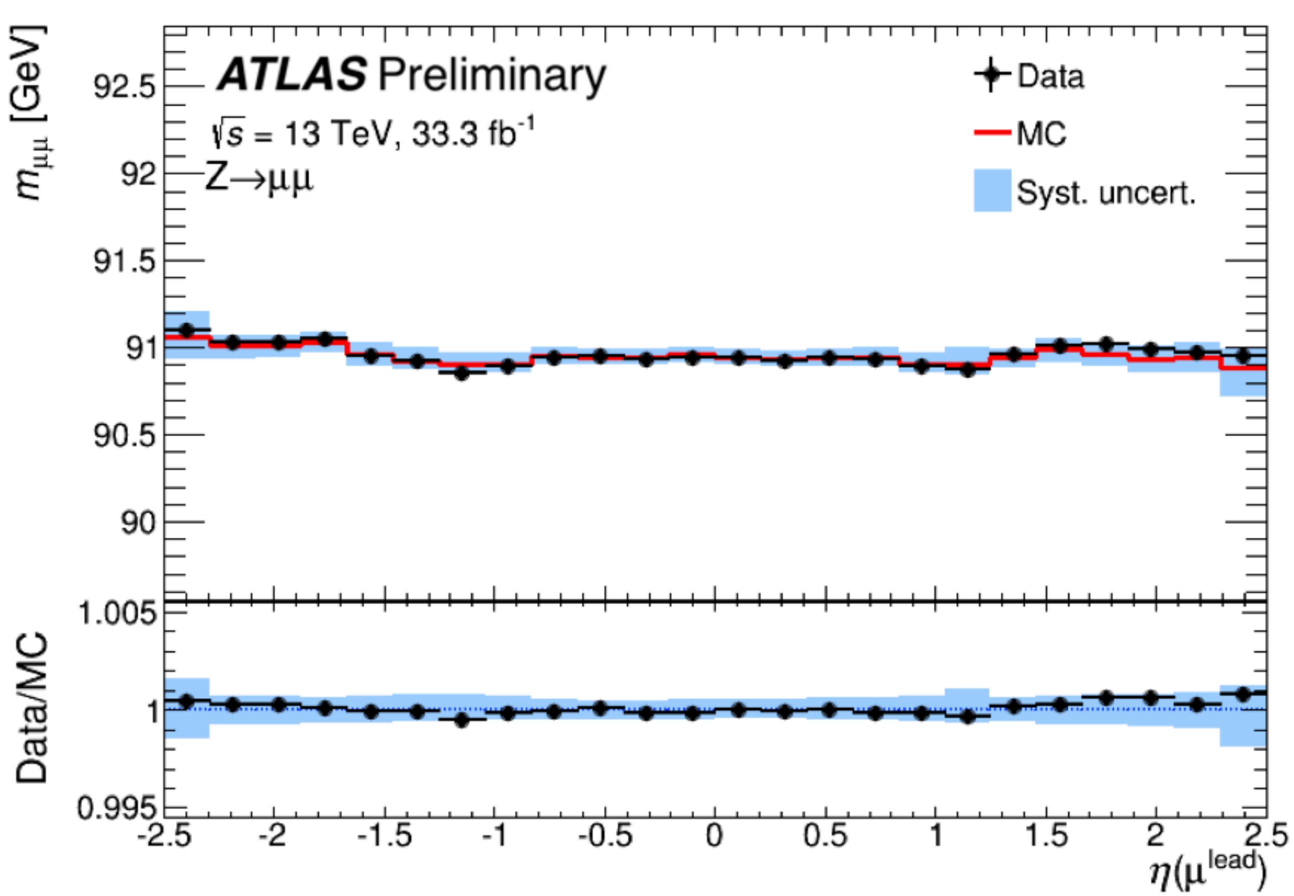

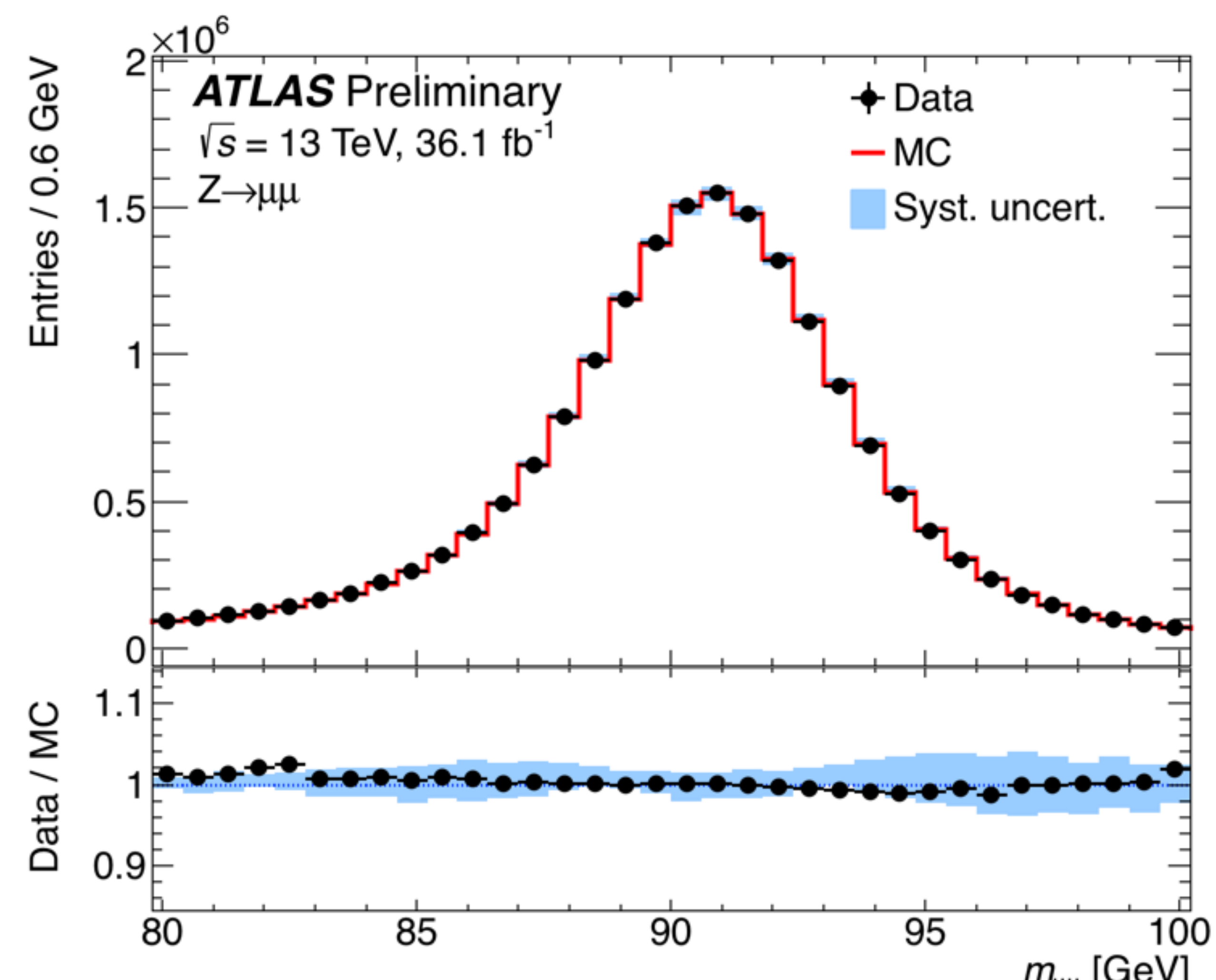

$E_T(e/\gamma)$ resolution

- Good energy calibration necessary for increased precision on m_H
  - Two step approach: i) material energy loss and ii) global calorimetric scale from $Z \to ee$ data
- Total scale uncertainty of at 40 GeV at the per-mille level.

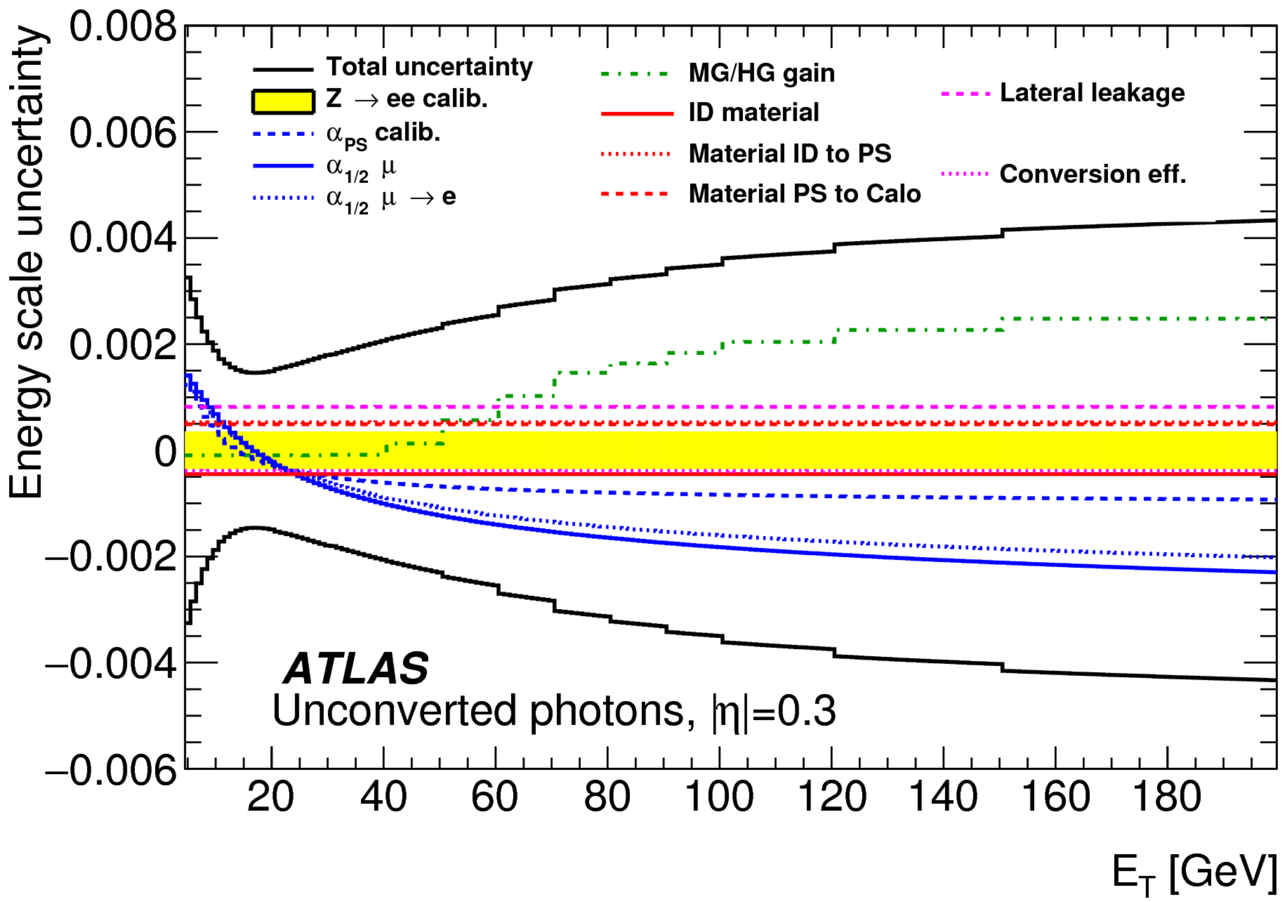

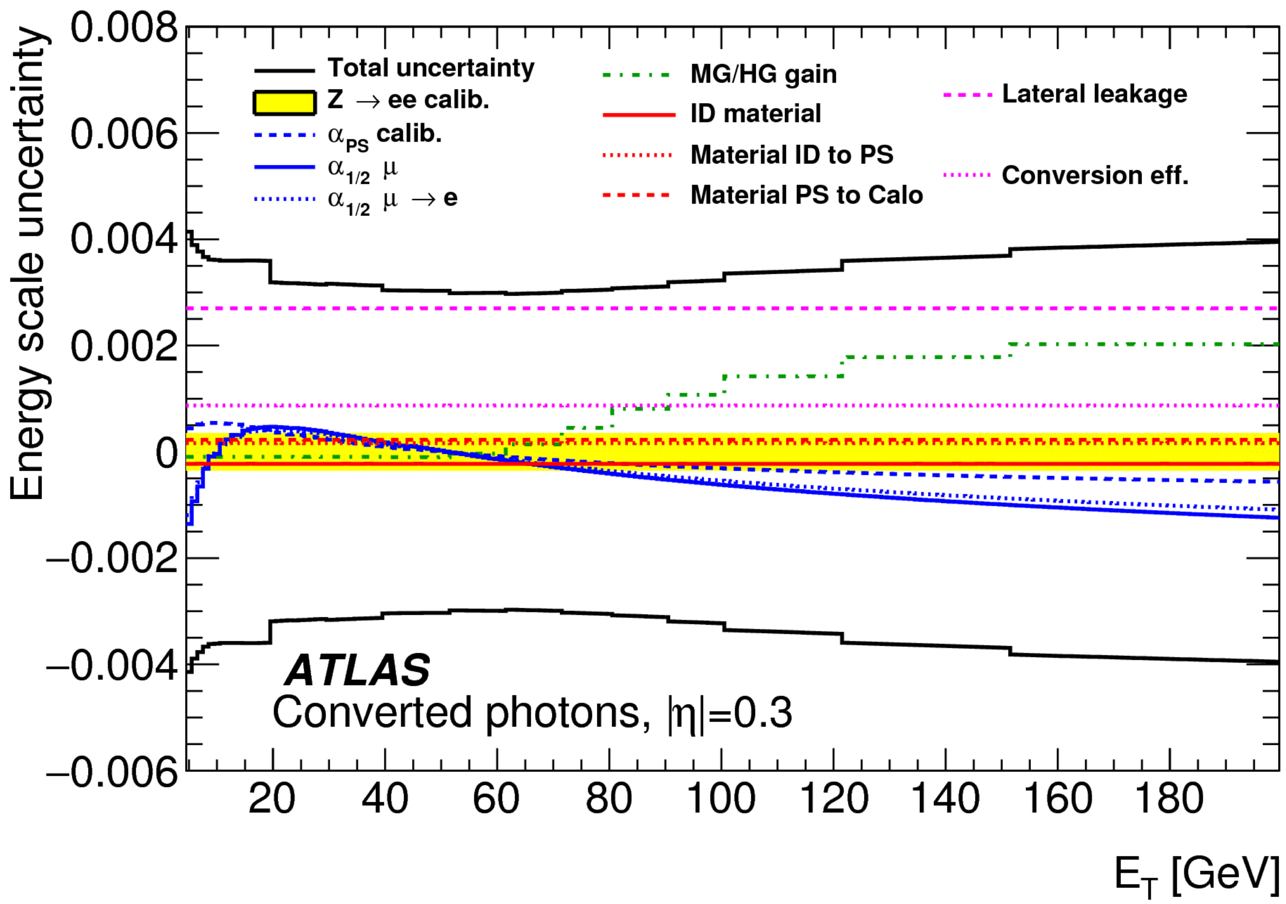

- $H \to \gamma\gamma$ updated result at Run II.

arXiv:1806.00242

  - Analytical function in kinematic and detector categories.
  - Reduction of uncertainty through categorisation of events as a function of resolution and signal significance.

- Expected statistical uncertainty of 0.21 GeV and 0.34 GeV systematic uncertainty

$$m_H^{\gamma\gamma} = 124.93 \pm 0.40\ (\pm 0.21 \text{ stat only})\ \text{GeV}$$

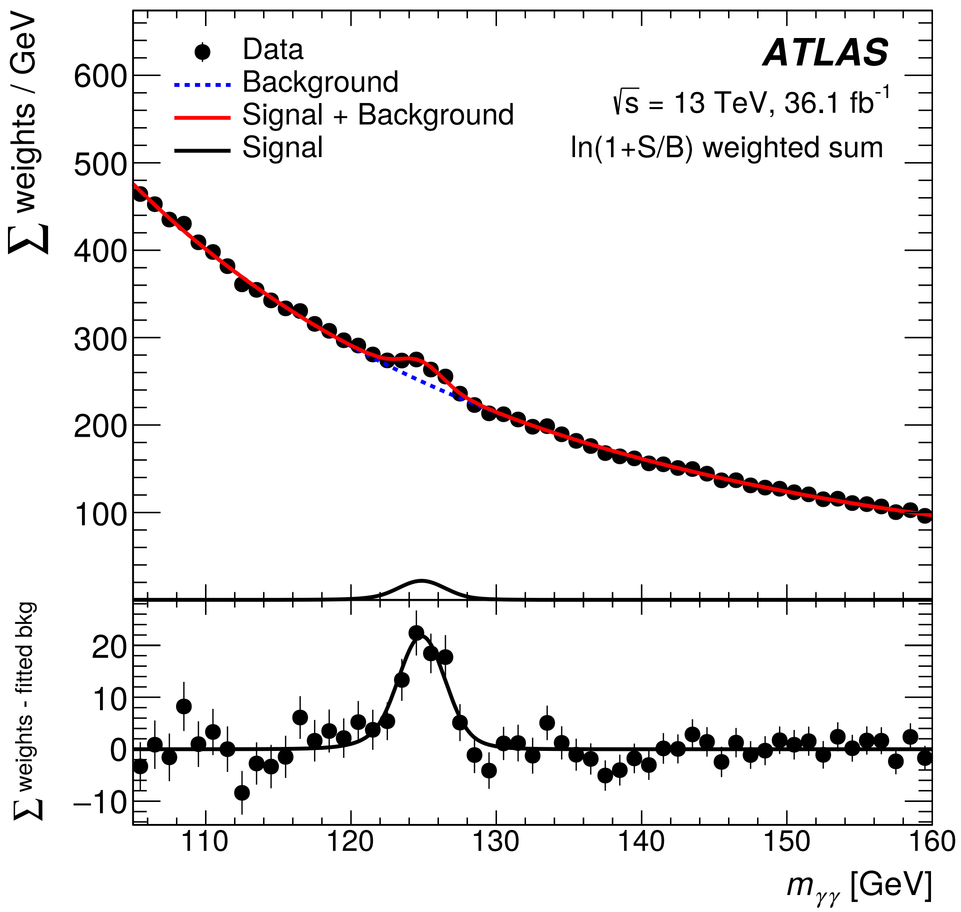

Source	Systematic uncertainty in m_H [MeV]
EM calorimeter response linearity	60
Non-ID material	55
EM calorimeter layer intercalibration	55
$Z \to ee$ calibration	45
ID material	45
Lateral shower shape	40
Muon momentum scale	20
Conversion reconstruction	20
$H \to \gamma\gamma$ background modelling	20
$H \to \gamma\gamma$ vertex reconstruction	15
e/γ energy resolution	15
All other systematic uncertainties	10

arXiv:1806.00242

- $H\to\gamma\gamma$ updated result at Run II.
  - Analytical function in kinematic and detector categories.
  - Reduction of uncertainty through categorisation of events as a function of resolution and signal significance.
- Expected statistical uncertainty of 0.21 GeV and 0.34 GeV systematic uncertainty

$$m_H^{\gamma\gamma} = 124.93 \pm 0.40 \ (\pm 0.21 \text{ stat only}) \text{ GeV}$$

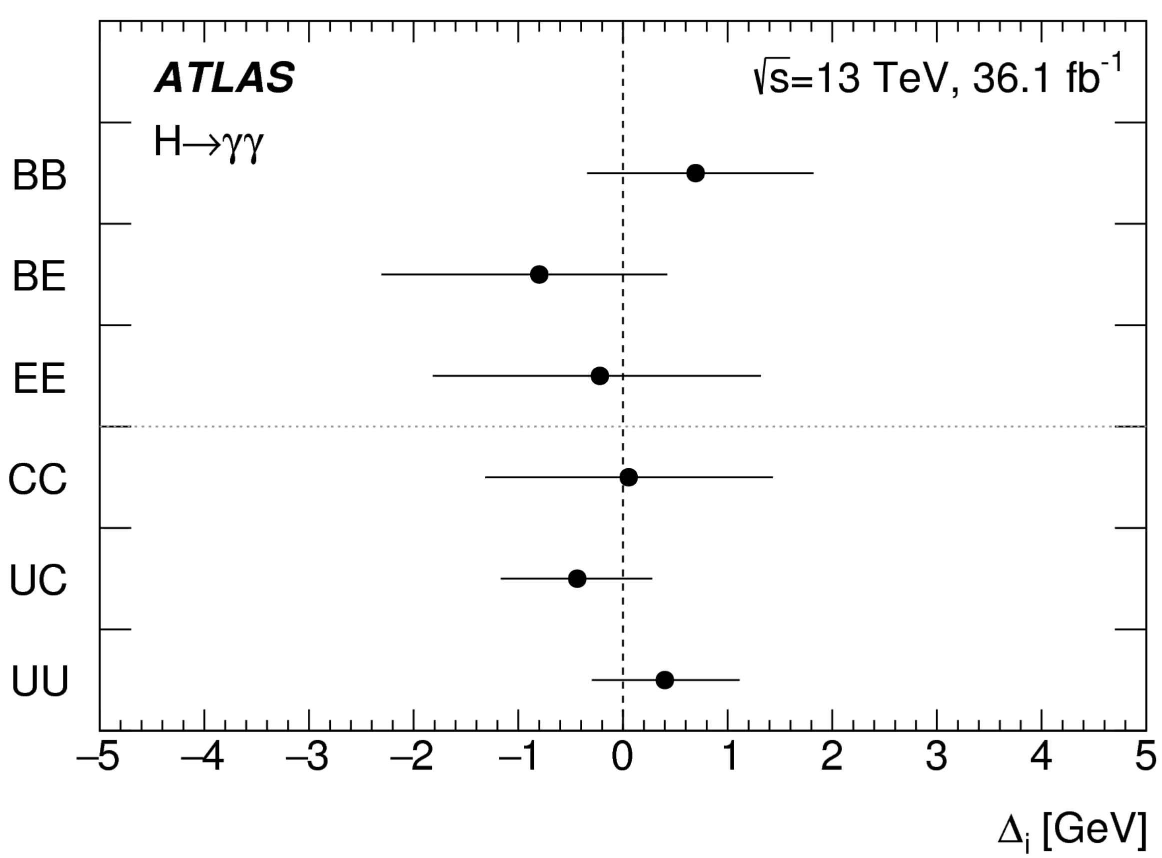

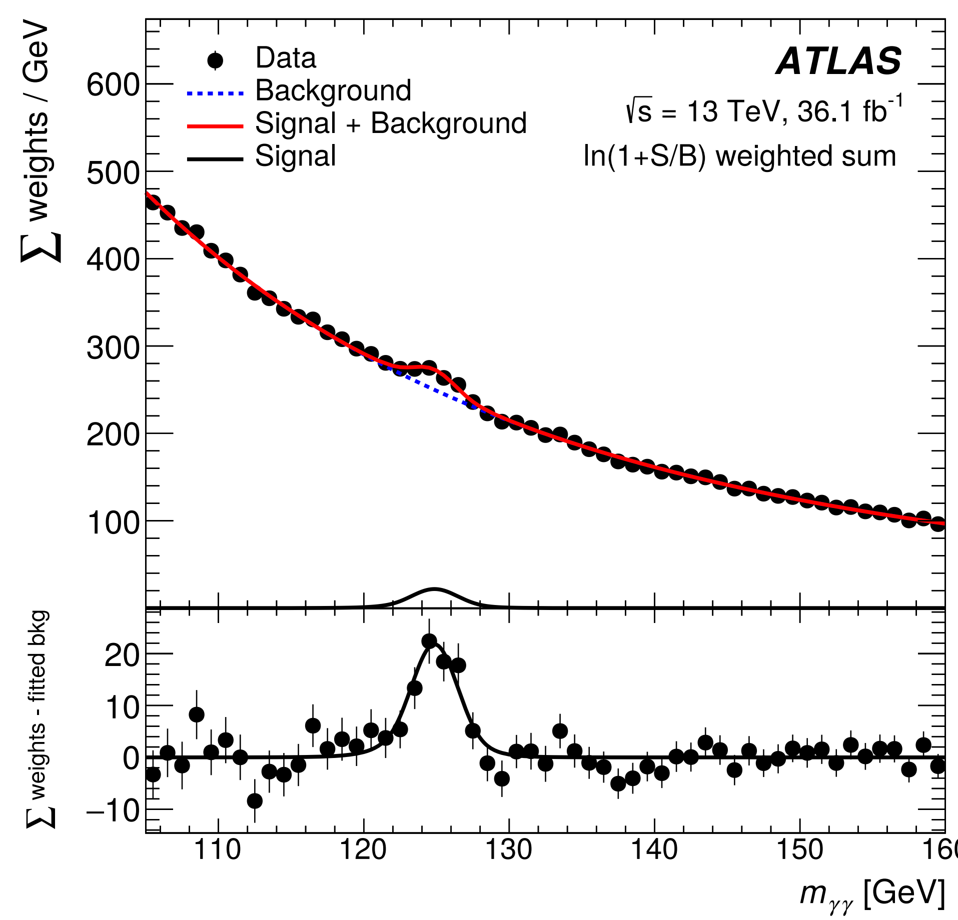

Run I status

- ATLAS run I precision on m_H of 0.33%
  - combined measurement from $H\rightarrow\gamma\gamma$ and $H\rightarrow ZZ^*\rightarrow 4\ell$.

Channel	Mass measurement [GeV]
$H\rightarrow\gamma\gamma$	$125.98 \pm 0.42\,(\text{stat}) \pm 0.28\,(\text{syst}) = 125.98 \pm 0.50$
$H\rightarrow ZZ^*\rightarrow 4\ell$	$124.51 \pm 0.52\,(\text{stat}) \pm 0.06\,(\text{syst}) = 124.51 \pm 0.52$
Combined	$125.36 \pm 0.37\,(\text{stat}) \pm 0.18\,(\text{syst}) = 125.36 \pm 0.41$

  - For both channels dominated by statistical uncertainty